IMPACTS OF SEA LEVEL RISE ON ARSENIC MOBILITY AND CYCLING IN CONTAMINATED COASTAL SOILS

by

Joshua J. LeMonte

A dissertation submitted to the Faculty of the University of Delaware in partial fulfillment of the requirements for the degree of Doctor of Philosophy in Environmental Soil Chemistry.

Spring 2016

IMPACTS OF SEA LEVEL RISE

ON ARSENIC MOBILITY AND CYCLING

IN CONTAMINATED COASTAL SOILS

by

Joshua J. LeMonte

Approved: _____

D. Janine Sherrier, Ph.D.
Chair of the Department of Plant & Soil Science

Approved: _____

Mark Rieger, Ph.D.
Dean of the College of Agriculture & Natural Resources

Approved: _____

Ann L. Ardis, Ph.D.
Senior Vice Provost for Graduate and Professional Education

I certify that I have read this dissertation and that in my opinion it meets the academic and professional standard required by the University as a dissertation for the degree of Doctor of Philosophy.

Signed: _____

Donald L. Sparks, Ph.D.
Professor in charge of dissertation

I certify that I have read this dissertation and that in my opinion it meets the academic and professional standard required by the University as a dissertation for the degree of Doctor of Philosophy.

Signed: _____

Amy L. Shober, Ph.D.
Member of dissertation committee

I certify that I have read this dissertation and that in my opinion it meets the academic and professional standard required by the University as a dissertation for the degree of Doctor of Philosophy.

Signed: _____

K. Ramesh Reddy, Ph.D.
Member of dissertation committee

I certify that I have read this dissertation and that in my opinion it meets the academic and professional standard required by the University as a dissertation for the degree of Doctor of Philosophy.

Signed: _____

Jörg Rinklebe, Ph.D.
Member of dissertation committee

I certify that I have read this dissertation and that in my opinion it meets the academic and professional standard required by the University as a dissertation for the degree of Doctor of Philosophy.

Signed: _____

Ryan Tappero, Ph.D.
Member of dissertation committee

ACKNOWLEDGMENTS

For Sloane Elizabeth & Zachary Scott

TABLE OF CONTENTS

LIST OF TABLES

LIST OF FIGURES

ABSTRACT

The impacts of sea level rise (SLR) on biogeochemical processes in contaminated soils and sediments along the world's coastlines remains poorly understood. Elevated levels of the carcinogen arsenic (As), from both geogenic and anthropogenic sources, are found along many coasts, most notably in south and southeast Asia, but also in the US, particularly along the Mid-Atlantic coast. In this work, a combination of laboratory and field techniques were used to ascertain the potential impacts of impending SLR on As mobility and cycling, and the current state of As mobility in a contaminated coastal zone of Delaware, USA. Advanced biogeochemical microcosm reactors were used to simulate inundation with natural sea and river waters on two historically As-contaminated Delaware coastal soils – a wetland soil and ditch sediment – across a wide range of redox potentials while monitoring chemical variables that are known to impact As mobility. Direct As speciation of the soils after reaction at different Eh values was obtained by bulk X-ray absorption near-edge structure (XANES) spectroscopy, μX-ray fluorescence (XRF) imaging, and μXANES spectroscopy. Reducing conditions led to As release and partial reduction of solid-phase As for both inundation scenarios and both soils. Sulfur speciation was also determined via XANES spectroscopy and showed evidence of sulfate reduction. Prolonged reducing conditions induced by SLR will drive the release of As from historically contaminated soils, but As release may be tempered when inundated by seawater as compared to river water for some soils (e.g. ditch sediment), possibly due to reduced microbial growth in high salinity conditions or

preferential sulfate reduction limiting reductive dissolution of As-bearing Fe oxides. However, other soils (e.g. wetland) may see ionic exchange driving pH shifts as a prominent factor driving As release in addition to Eh levels.

To assess the contaminant mobility at one of these former industrial sites along the Christina River, we conducted quantitative comparisons of hydrologic and biogeochemical dynamics across time scales ranging from hours to months, and throughout seasonal environmental variations. The use of synchrotron-based X-ray absorption spectroscopy as a geoforensic tool suggests that As from a neighboring Superfund site is likely contributing to recent accumulation of As at the site studied. Data were collected from pressure transducers in wells, multi-level redox sensors, and porewater samplers. Results indicate that groundwater surface interaction induced a tidally controlled redox gradient. In the tidally impacted variably saturated zone, redox potential varied between oxidizing and reducing conditions depending on the water table elevation. This strong correlation indicates that a rising water table may increase contaminant mobility. Porewater samples also confirm increasing arsenic (As) concentration during the rising tide.

Chapter 1

IMPENDING SEA LEVEL RISE AND ITS POTENTIAL IMPACT ON ARSENIC-CONTAMINATED COASTAL SOILS

1.1 Coastal Threat of Sea Level Rise

The climate is changing and, as a result, sea levels are rising. Sea level rise (SLR) is being driven by thermal expansion of the oceans and melting of land ice, such as glaciers, ice caps, and the ice sheets of Greenland and Antarctica.[1] Since about 1993, the global mean sea level has been increasing by 3 mm per year.[2] This level of SLR is nearly double that of the early 20th century rate (1.7 mm per year). Current model projections estimate that the global mean sea level will rise 0.8 m by 2100 with respect to 1990 levels.[2] The extent of SLR experienced by different regions of the world varies. For instance, the Mid-Atlantic coast of the United States is experiencing SLR rates higher than elsewhere in the world and twice as fast as earlier estimates due to the synergistic impact of coastal subsidence and SLR.[3] The rate of SLR varies annually, but in an upward trend. The composite interannual SLR of the Mid-Atlantic was 31.2 mm in 2009, ten times the global average.[4] The U.S. Climate Change Science Program's (CCSP) 2009 document, "Coastal Sensitivity to Sea Level Rise: A Focus on the Mid-Atlantic" recommends that states in this region need to prepare for rise in sea level of at least 1 m by 2100.[5] Additionally, SLR will contribute to increased severity of storm surge events, recession of the world's sandy beaches, and threaten low-lying islands.[1]

The very coasts that are threatened by SLR are the same coasts that much of the world's population calls home. It is estimated that 23% of the world's population lives within 100km of a coastline and below 100 m elevation (Figure 1).[6] In the US alone, 39% (more than 123 million people) of the nation's population lived in coastal shoreline

counties in 2010. Of this population, it is expected that SLR will directly impact 8.7 million people by 2050.[1]

Coasts are large population centers in part because they are also large industrial centers. In many places of the world, historic and current industrial activity has created a legacy of contamination of surrounding soil and groundwater. As the sea levels rise, a new two-fold problem is introduced: how will impending SLR impact low-lying coastal contaminated sites?

1.2 Delaware Case Study

Situated in the center of the mid-Atlantic coastal zone, Delaware is an ideal location to develop an understanding of the potential impacts of SLR on contaminated coastal soils. Delaware is the lowest lying state in the U.S., an average 18 m above sea level, with no part of the state more than 12.8 km from tidal waters, and all of the state is considered a coastal zone.[7] The eastern border of the state is a 90-mile coastline, with inland geography characteristic of piedmont and coastal plain. The Delaware Estuary is a large, brackish body of water adjacent to extensive marshlands.

Delaware is already experiencing a 0.3 m/century rate of SLR, and policymakers in the state are preparing for relative sea levels to rise by up to 1.5 m by 2100. In its Sea Level Rise Vulnerability Assessment, the state found that significant wildlife resources, industrial areas, evacuation routes, and wastewater facilities are subject to inundation in a 1.5 m SLR scenario.[8] In addition to the impacts of storm surges and SLR, the state is faced with subsidence of coastal areas at an estimated rate of 1.65 mm/yr, with higher rates in certain locations.[9] Expected SLR scenarios, coupled with the continued deterioration of aging coastal infrastructure - including century-old dikes, some of which protect industrial areas from daily tidal influx - increase the potential for inundation of hazardous waste sites. Delaware experiences storm surges throughout the entire length of its coastline as a result of nor'easters, hurricanes, and wind events. Hurricane Sandy

resulted in numerous records at tidal recording stations throughout the state with surges of 2-3 m.[10] Storm surges of 1 m are routinely recorded during nor'easters, which occur commonly throughout the winter and early spring.

In addition to being especially susceptible to SLR impacts, Delaware also has a long history of industrial activities and subsequent contamination – making Delaware an ideal location to investigate the two-fold issue of the impact of SLR on coastal contaminated sites. There are more than 700 contaminated sites comprising 60,088 acres of land (4% of the state) in Delaware. Among these sites are over 150 certified brownfields. Brownfields are sites that have been contaminated or have the stigma that they were contaminated and thereby the redevelopment and reuse of the land is complicated. In the U.S. over 5 million acres are classified as brownfields, a large portion of which are along the coasts (Fig. 2). There are more contaminated sites per square mile than all but three other counties in the U.S. in Delaware's northernmost county, New Castle. This same county is also home to more than 70% of the state's population. Brownfields make up 24% of the total acreage of Wilmington, Delaware's largest city.[7] Commonly found contaminants of this region include toxic metal(loid)s (As, Pb, Cr, etc.) and organics [polychlorinated biphenyls (PCBs), polycyclic aromatic hydrocarbons (PAHs)].[7]

Most of this contamination can be traced back to industrial activity during the 19th and 20th centuries. Industries in Wilmington included tanneries, foundries, ship builders, and railroad car construction. Wilmington was the second largest center for tannery processing on the east coast of the U.S. during the late 1800s and early 1900s. There were 128 tannery operations clustered in an area along the Christina River; these now constitute 53 brownfield sites.[7] Arsenic and chromium, once important chemicals in the tanning industry, remain at these sites as potentially hazardous contaminants.

In recent years as tanneries began to fade from existence, Wilmington has been home to management, research, chemical production, and ore processing.[11]

Unfortunately, these industries have also left behind a legacy of pollution, including metals and organics. The former tannery and industrial sites are now in use as both commercial and residential areas. Some sites have been remediated, some areas have been fenced off, and other areas are simply monitored but in use. These areas are disproportionately comprised of racial minorities and those below the poverty line. Sometimes these areas have unusually high levels of cancer, asthma, and other diseases that could be attributed to environmental pollution.[12]

Arsenic is a carcinogenic toxin deposited through former industry into soil and groundwater of these coastal communities. Arsenic stands to undergo changes in mobility and toxicity as SLR and increased storm surges inundate the soil. Understanding how As will behave under these altered conditions is an initiative of the Delaware Department of Natural Resource and Environmental Control (DNREC).

1.3 Arsenic in the Environment

Arsenic is a naturally occurring geogenic metalloid in the environment, commonly associated with sulfides and Al or Fe (hydr)oxides. Background levels of As in soils throughout the world average from 1-40 mg kg^{-1}, with large geographic variation.[13] However, As levels may be much higher than background values in the environment due to anthropogenic inputs including pesticides, mining, manufacturing, poultry litter, incineration, the burning of fossil fuels, and others. Most humans are chronically exposed to low levels of As through ingestion of food and water.[14] In regions near smelters or arid regions, people may be exposed to As through inhalation or ingestion of As-laden particulates.[15] This exposure is concerning, especially when As levels are elevated, because As is a carcinogenic toxin associated with skin, lung, bladder, and other internal organ cancers.[13]

Although remedial action plans instituted by regulatory agencies are often based solely on total metal(loid) concentration in soils, bulk concentration levels do not

adequately convey the fate, transport, bioavailbility, or toxicity of As. Speciation, or a determination of the redox state and binding environment, provides valuable information on As cycling, mobility, and toxicity. Speciation is determined by a multitude of environmental factors including oxidation-reduction, pH, time, types and amounts of sorbent phases, surrounding ions, and microbial community.

Toxicity and mobility of As in soils are primarily functions of redox state. The major redox states of As in the environment include arsenic-sulfides (As^{-1} to As^{II}), arsenite (As^{III}), and arsenate (As^{V}). It is generally thought that arsenite is the most mobile, and thus toxic of these As species. Arsenite and arsenate occur primarily as inorganic oxyanions in the natural environment and readily sorb to soil mineral oxides as inner-sphere complexes via bidentate binuclear surface complexes. Arsenite (As^{III}) is a weak acid and exists primarily in reducing conditions as H_3AsO_3 in the soil-water matrix. The arsenate (As^{V}) oxyanion is the dominant species under oxidizing conditions, commonly occurring as $HAsO_4^{2-}$ and $H_2AsO_4^{-}$. When conditions are oxic, arsenic can also occur in organic forms such as monomethylarsonic acid (MMA), dimethylarsinic acid (DMA), and trimethylarsine oxide (TMAO) through microbial biomethylation, although these are usually minor As components in the soil.[16] Despite organic forms of As being minor components in soils, they are usually more mobile than inorganic forms, following the pattern: methyl As(III) >> methyl As(V) > As(III) > As(V).[17] Toxicity of inorganic and organic forms of As in the soil are similar according to oxidation state, following the pattern: methyl As(III) > As(III) > As(V) > methyl As(V).[18]

Sorption behavior of As in soils varies with changing environmental conditions. Kinetics of As(V) sorption on mineral surfaces follows a typical biphasic pattern, where it is initially rapid followed by slower reactions.[19] How As(V) binds with surface OH groups depends on the surface loading.[20] Under high surface coverage, As(III) sorbs more strongly than As(V).[21]

Desorption and subsequent mobility of As in soils is determined by sorption complexes, total concentration, microbial activity, S chemistry, pH, and redox.[22] Microbes are able to either oxidize As(III) or reduce As(V). Microbial reduction of As(V) happens via dissimilatory reduction, where microbes utilize As(V) as the terminal electron receptor in anaerobic respiration or detoxification.[23,24] These microbial reduction pathways usually form as As(V) is desorbed from mineral surfaces and then biotically reduced.

Abiotic reduction of As is another important factor when assessing As mobility. Arsenic can be desorbed under reducing conditions by reductive dissolution of Fe and Mn (hydr)oxides.[22] Flooding can thus increase Fe(II) and As(III) concentrations in ground water and soil pore waters as an impact of reductive dissolution of Fe(III) (hydr)oxides and subsequent As(V) reduction.[25] It has also been shown that As(V) can be directly reduced to As(III) and desorbed.[26] The rate of sorbed As(V) reduction is slower than aqueous As(V).[27] Total concentrations of As in groundwater are strongly correlated with the presence of poorly soluble Fe (hydr)oxides that are strong sorbents of As(III) and As(V). If there is a proliferation of these Fe(III) minerals, they will act as strong sorbents of As and inhibit As mobilization until after sustained reducing conditions.[28] However, under long term flooding conditions (in excess of 1 week) in soils with high S content, aqueous As may decrease due to sulfide-iron precipitation and formation of As-mackinawite formations.[22,25] Manganese oxides are powerful oxidants in the environment that can impact As mobility and cycling by oxidizing As(III) to As(V) and thus altering mineral surface reaction sites.[29]

The use of X-ray absorption near-edge structure (XANES) spectroscopy has been used to demonstrate that reducing conditions can lead to As(V) reduction to As(III) on solid phase soil minerals.[30] The same XANES technique was used to determine that as aqueous As(III) encounters soil minerals, it preferentially binds to Fe(III) oxyhydroxides,

whereas aqueous As(V) will bind to Fe(III) oxyhydroxides, Al hydroxide, and aluminosilicates.[31]

1.4 Arsenic in the context of SLR and recent literature

Although trace metal(loid)s such as As are commonly found in floodplains and estuaries, research investigating the potential impacts of SLR on their biogeochemistry is limited. The changing hydrologic regime due to SLR, increased flooding and storm events are expected to impact biogeochemical processes including contaminant mobility and cycling.[28] Recent research has shown that seawater inundation can induce reductive dissolution of Fe(III) oxides, SO_4^{2-} reduction, and shift the speciation and mobility of As in certain soils through the aforementioned processes, including direct reduction of As(V) to As(III), and competitive desorption of anions by HCO_3^-.[32] Others found that inundation with water of increasing ionic strength can displace trace metals (e.g. Fe and Al) and protons sorbed onto soil particles in coastal lowland acid sulfate soils.[33] Following desorption, acidic trace metal cations may undergo hydrolysis and perpetuate desorption by creating more acidic conditions, despite the fact that the seawater's pH is above 8 and highly buffered. Increased concentrations of seawater with higher ionic strength can increase exchangeable trace metals in solution.

Although research has been conducted in areas with naturally occurring elevated levels of arsenic (coastal lowland acid sulfate soils), no research has been done specifically investigating the impacts of potential seawater inundation on anthropogenically As-contaminated coastal soils. It is expected that SLR, increased overtopping, and saltwater surges will infiltrate the subsurface, reduce oxygen levels in the soil profile, alter microbial communities, impact enzymes, and favor reducing conditions in formerly oxic soil zones. This promotes the dissolution of iron and manganese oxyhydroxides, which serve as crucial heavy metal sinks in soils. The high concentration of dissolved ions in saltwater, such as sodium and magnesium, are

exchanged for aluminum and hydrogen ions in the soil, causing acidification. This is known as the seasalt effect.[34] Acidic, reducing conditions create the ideal environment to mobilize metal(loid)s such as As, resulting in an immediate pulse of contaminated receding surge water.[33] The effects of storm surges are not just limited to the short term; even after flooding recedes, saltwater can remain trapped in soil pores. Long-term changes to groundwater chemistry have been noticed months after the original event, which can be explained by fundamental alterations to soil chemistry.[35,36]

It is not currently understood how SLR will impact mobilization of existing contaminants in coastal soils. To fill this knowledge gap we studied the mobilization of As from historically contaminated soils from the coastline of Delaware comparing river water and seawater inundation scenarios. The research herein seeks to answer the following questions:

1. How will flooding and newly introduced reducing zones in contaminated soils impact the speciation, cycling, and mobility of As?
2. What impact(s) will the introduction of salts via sea water inundation have on the speciation, mobility, and cycling of As in these reducing zones?
3. How are As speciation, cycling, and mobility currently being impacted by tidal fluctuations and hydrologic shifts in a coastal contaminated soil?
4. How does the existing As contamination in the coastal contaminated soils of Delaware migrate under current conditions?

We seek to answer these questions by inundating historically As contaminated soils from the coast of Delaware with river and seawater across carefully controlled across Eh zones. We analyzed As release coupled with solid and solution phase speciation under preset redox conditions for the first time, while monitoring controlling factors (e.g. pH, Fe, DOC, S). Additionally, samples were taken and instrumentation deployed in the field to validate the range of redox produced in the lab experiments and monitor on-going As dynamics in a coastal zone.

1.5 References Cited

(1) Church, J. a.; White, N. J.; Aarup, T.; Wilson, W. S.; Woodworth, P. L.; Domingues, C. M.; Hunter, J. R.; Lambeck, K. Understanding global sea levels: Past, present and future. *Sustain. Sci.* **2008**, *3*, 9–22.

(2) Church, J. a.; Clark, P. U.; Cazenave, a.; Gregory, J. M.; Jevrejeva, S.; Levermann, a.; Merrifield, M. a.; Milne, G. a.; Nerem, R. .; Nunn, P. D.; et al. Sea level change. *Clim. Chang. 2013 Phys. Sci. Basis. Contrib. Work. Gr. I to Fifth Assess. Rep. Intergov. Panel Clim. Chang.* **2013**, 1137–1216.

(3) Sallenger, A. H.; Doran, K. S.; Howd, P. a. Hotspot of accelerated sea-level rise on the Atlantic coast of North America. *Nat. Clim. Chang.* **2012**, *2*, 1–5.

(4) Goddard, P. B.; Yin, J.; Griffies, S. M.; Zhang, S. An extreme event of sea-level rise along the Northeast coast of North America in 2009–2010. *Nat. Commun.* **2015**, *6*, 6346.

(5) Titus, J. G. (Coordinating lead author); Anderson, K. E.; Cahoon, D. R.; Gesch, D. B.; Gill, S. K.; Gutierrez, B. T.; Thieler, E. R.; Williams, S. J. (lead authors). *Coastal Cycle Sensitivity to Sea-Level Rise : Focus on Mid-Atlantic Region*; Washington, D.C., USA, 2009.

(6) Small, C.; Nicholls, R. J. A global analysis of Human Settlement in Coastal Zones. *J. Coast. Res.* **2003**, *19*, 584–599.

(7) Carter, D.; Cervone, E. *Delaware Brownfield Inventory Selected Sites : South Wilmington*; 2005.

(8) Cooksey, S.; Carter, D.; Arndt, T.; Valencik, K.; Love, S.; Scarborough, R.; Wolanski, M.; Yetter, C. *Preparing for Tomorrow's High Tide, Sea Level Rise Vulnerability for the State of Delaware*; 2012.

(9) *Red Lion Dike Preliminary Design Report Delaware Bay Dikes Repair & Prevention Project New Castle, Delaware*; 2012.

(10) Survey, T. D. G. Stream and Tide Gage Data for Hurricane Sandy http://www.dgs.udel.edu/delaware-geology/stream-and-tide-gage-data-hurricane-sandy (accessed Jan 1, 2015).

(11) Hoffecker, C. E. *Portrait of an Industrial City, 1830-1910*; University Press of Virginia, 1974.

(12) Liu-Mares, W.; Mackinnon, J. a; Sherman, R.; Fleming, L. E.; Rocha-Lima, C.; Hu, J. J.; Lee, D. J. Pancreatic cancer clusters and arsenic-contaminated drinking water wells in Florida. *BMC Cancer* **2013**, *13*, 111.

(13) Mandal, B. K.; Suzuki, K. T. Arsenic round the world: A review. *Talanta* **2002**, *58*, 201–235.

(14) Basu, A.; Mahata, J.; Gupta, S.; Giri, A. K. Genetic toxicology of a paradoxical human carcinogen , arsenic : a review. *Mutat. Res.* **2001**, *488*, 171–194.

(15) Foster, A. L.; Brown Jr., G. E.; Tingle, T. N.; Parks, G. A. Quantitative arsenic speciation in mine tailings using X-ray absorption spectroscopy. *Am. Mineral.* **1998**, *83*, 553–568.

(16) Geiszinger, A.; Goessler, W.; Kosmus, W. Organoarsenic compounds in plants and soil on top of an ore vein. *Appl. Organomet. Chem.* **2002**, *16*, 245–249.

(17) Lafferty, B. J.; Loeppert, R. H. Methyl arsenic adsorption and desorption behavior on iron oxides. *Environ. Sci. Technol.* **2005**, *39*, 2120–2127.

(18) Petrick, J. S.; Ayala-Fierro, F.; Cullen, W. R.; Carter, D. E.; Vasken Aposhian, H. Monomethylarsonous acid (MMA(III)) is more toxic than arsenite in Chang human hepatocytes. *Toxicol. Appl. Pharmacol.* **2000**, *163*, 203–207.

(19) Zhang, H.; Selim, H. M. Modeling the Transport and Retention of Arsenic (V) in Soils. *Soil Sci. Soc. Am. J.* **2006**, *70*, 1677.

(20) Grossl, P. R.; Eick, M.; Sparks, D. L.; Goldberg, S.; Ainsworth, C. C. Kinetic Evaluation Using a Pressure-Jump Relaxation Technique. *Environ. Sci. Technol.* **1997**, *31*, 321–326.

(21) Manning, B. a.; Fendorf, S. E.; Goldberg, S. Surface structures and stability of arsenic(III) on goethite: Spectroscopic evidence for inner-sphere complexes. *Environ. Sci. Technol.* **1998**, *32*, 2383–2388.

(22) Du Laing, G.; Chapagain, S. K.; Dewispelaere, M.; Meers, E.; Kazama, F.; Tack, F. M. G.; Rinklebe, J.; Verloo, M. G. Presence and mobility of arsenic in estuarine wetland soils of the Scheldt estuary (Belgium). *J. Environ. Monit.* **2009**, *11*, 873–881.

(23) Ahmann, D.; Roberts, A. L.; Krumholz, L. R.; Morel, F. M. Microbe grows by reducing arsenic. *Nature*, 1994, *371*, 750.

(24) Langner, H. W.; Inskeep, W. P. Microbial reduction of arsenate in the presence of ferrihydrite. *Environ. Sci. Technol.* **2000**, *34*, 3131–3136.

(25) Burton, E. D.; Johnston, S. G.; Kocar, B. D. Arsenic Mobility during Flooding of Contaminated Soil: The Effect of Microbial Sulfate Reduction. *Environ. Sci. Technol.* **2014**, *48*, 13660–13667.

(26) Masscheleyn, P. H. Effect of Redox Potential and pH on Arsenic Speciation and Solubility in a Contaminated Soil. **1991**, 1414–1419.

(27) Zobrist, J.; Dowdle, P. R.; Davis, J. a.; Oremland, R. S. Mobilization of arsenite by dissimilatory reduction of adsorbed arsenate. *Environ. Sci. Technol.* **2000**, *34*, 4747–4753.

(28) Borch, T.; Kretzschmar, R.; Skappler, A.; Van Cappellen, P.; Ginder-Vogel, M.; Voegelin, A.; Campbell, K. Biogeochemical redox processes and their impact on contaminant dynamics. *Environ. Sci. Technol.* **2010**, *44*, 15–23.

(29) Manning, B. a; Fendorf, S. E.; Bostick, B.; Suarez, D. L. Arsenic(III) oxidation and arsenic(V) adsorption reactions on synthetic birnessite. *Environ. Sci. Technol.* **2002**, *36*, 976–981.

(30) Rochette, E. a.; Li, G. C.; Fendorf, S. E. Stability of Arsenate Minerals in Soil under Biotically Generated Reducing Conditions. *Soil Sci. Soc. Am. J.* **1998**, *62*, 1530.

(31) Manning, B. Arsenic Speciation in As(III)- and As(V)-Treated Soil Using XANES Spectroscopy. *Microchim. Acta* **2005**, *151*, 181–188.

(32) Johnston, S. G.; Keene, A. F.; Burton, E. D.; Bush, R. T.; Sullivan, L. a; McElnea, A.; Ahern, C. R.; Smith, C. D.; Powell, B.; Hocking, R. K. Arsenic mobilization in a seawater inundated acid sulfate soil. *Environ. Sci. Technol.* **2010**, *44*, 1968–1973.

(33) Wong, V. N. L.; Johnston, S. G.; Burton, E. D.; Bush, R. T.; Sullivan, L. a.; Slavich, P. G. Seawater causes rapid trace metal mobilisation in coastal lowland acid sulfate soils: Implications of sea level rise for water quality. *Geoderma* **2010**, *160*, 252–263.

(34) Wright, R. F.; Norton, S. A.; Brakke, D. F.; Frogner, T. Experimental verification of episodic acidification of freshwaters by sea salts. *Nature* **1988**, *334*, 422–424.

(35) Blood, A. E. R.; Anderson, P.; Smith, P. A.; Nybro, C.; Ginsberg, K. A.; Blood, E. R.; Carolina, S. Effects of Hurricane Hugo on Coastal Soil Solution Chemistry in South Carolina. *Biotropica* **1991**, *23*, 348–355.

(36) Steyer, G. D.; Perez, B. C.; Piazza, S.; Suir, G. Potential Consequences of Saltwater Intrusion Associated with Hurricanes Katrina and Rita. In *Science and the Storms-the USGS response to the hurricanes of 2005: US Geological Survey Circular 1306*; Farris, G. S.; Smith, G. J.; Crane, M. P.; Demas, C. R.; Robbins, L. L.; Lavoie, D. L., Eds.; 2007; pp. 137–146.

(37) Johnston, S. G.; Keene, A. F.; Bush, R. T.; Burton, E. D.; Sullivan, L. a.; Smith, D.; McElnea, A. E.; Martens, M. a.; Wilbraham, S. Contemporary pedogenesis of severely degraded tropical acid sulfate soils after introduction of regular tidal inundation. *Geoderma* **2009**, *149*, 335–346.

(38) Borch, T.; Kretzschmar, R.; Kappler, A.; Cappellen, P. Van; Ginder-Vogel, M.; Voegelin, A.; Campbell, K. Biogeochemical redox processes and their impact on contaminant dynamics. *Environ. Sci. Technol.* **2010**, *44*, 15–23.

(39) Tan, K. H. *Soil Sampling, Preparation, and Analysis*; Second.; Taylor & Francis Group: New York, 2005.

(40) Agency, U. S. E. P. *Method 3051a: Microwave Assisted Acid Digestion of Sediments, Sludges, Soils, and Oils*; Washington, D.C., USA, 1998.

(41) Loeppart, R. H.; Inskeep, W. P. Iron. In *Methods of Soil Analysis. Part 3. Chemical Methods*; Sparks, D. L., Ed.; Soil Science Society of America: Madison, WI, 1996; pp. 384–411.

(42) Yu, K.; Rinklebe, J. Advancement in soil microcosm apparatus for biogeochemical research. *Ecol. Eng.* **2011**, *37*, 2071–2075.

(43) Frohne, T.; Rinklebe, J.; Diaz-Bone, R. A.; Du Laing, G. Controlled variation of redox conditions in a floodplain soil: Impact on metal mobilization and biomethylation of arsenic and antimony. *Geoderma* **2011**, *160*, 414–424.

(44) Frohne, T.; Diaz-Bone, R. a.; Du Laing, G.; Rinklebe, J. Impact of systematic change of redox potential on the leaching of Ba, Cr, Sr, and V from a riverine soil into water. *J. Soils Sediments* **2015**, *15*, 623–633.

(45) Sparks, D. L. *Environmental Soil Chemistry*; Second.; Academic Press: New York, 2003.

(46) Landrot, G.; Tappero, R.; Webb, S. M.; Sparks, D. L. Arsenic and chromium speciation in an urban contaminated soil. *Chemosphere* **2012**, *88*, 1196–1201.

(47) Kunze, G. W.; Dixon, J. B. *Pretreatment for mineralogical analysis. in Methods of Soil Analysis, Part 1. Physical and Mineralogical Methods*; Klute, A., Ed.; 2nd ed.; American Society of Agronomy, Inc. and the Soil Science Society of America, Inc.: Madison, WI, 1986.

(48) Ogwada, R. A.; Sparks, D. L. Kinetics of Ion Exchange on Clay Minerals and Soil: I. Evaluation of Methods 1. *Soil Sci. Soc. Am. J.* **1986**, *50*, 1158–1162.

(49) Bar-Tal, A.; Sparks, D. L.; Pesek, J. D.; Feigenbaum, S. Analyses of Adsorption Kinetics Using a Stirred-Flow Chamber: I. Theory and Critical Tests. *Soil Sci. Soc. Am. J.* **1990**, *54*, 1273–1278.

(50) O'Day, P. A.; Carroll, S. A.; Randall, S.; Martinelli, R. E.; Anderson, S. L.; Jelinski, J.; Knezovich, J. P. Metal Speciation and Bioavailability in Contaminated Estuary Sediments, Alameda Naval Air Station, California. *Environ. Sci. Technol.* **2000**, *34*, 3665–3673.

(51) Lafferty, B. J.; Ginder-vogel, M.; Sparks, D. L. Arsenite Oxidation by a Poorly Stirred-Flow Experiments. *Environ. Sci. Technol.* **2010**, *44*, 8460–8466.

(52) Wielinga, B.; Mizuba, M. M.; Hansel, C. M.; Fendorf, S. Iron promoted reduction of chromate by dissimilatory iron-reducing bacteria. *Environ. Sci. Technol.* **2001**, *35*, 522–527.

(53) Lafferty, B. J.; Ginder-Vogel, M.; Sparks, D. L. Arsenite oxidation by a poorly crystalline manganese-oxide 1. Stirred-flow experiments. *Environ. Sci. Technol.* **2010**, *44*, 8460–8466.

1.6 Figures

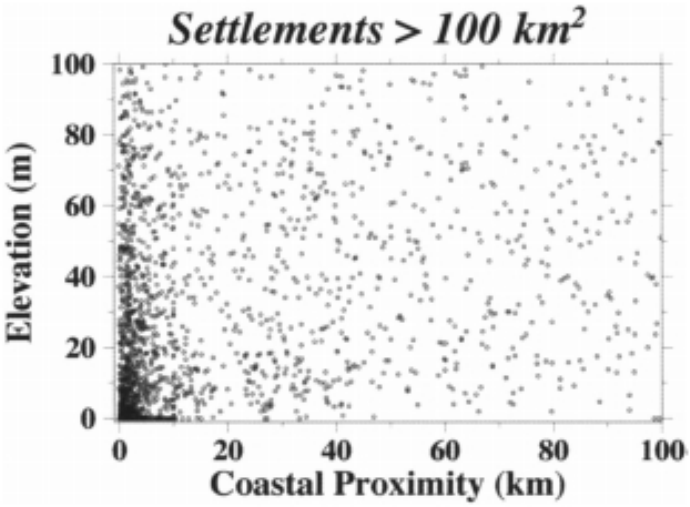

Figure 1.1: Settlements of the world within 100 km^2 of a coast and below 100 m elevation. Adapted from [6]

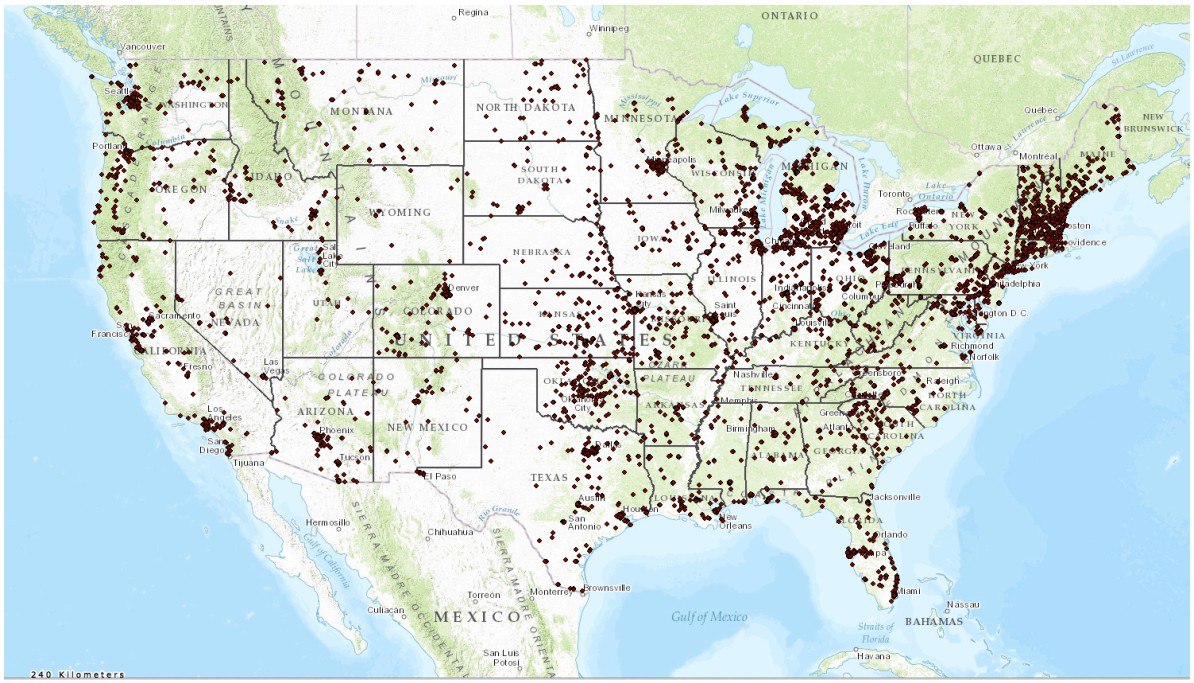

Figure 1.2: Brownfield locations in the United States. Source: http://superfund.ciesin.columbia.edu/sfmapper/mapviewer.jsf?width=873&height=517

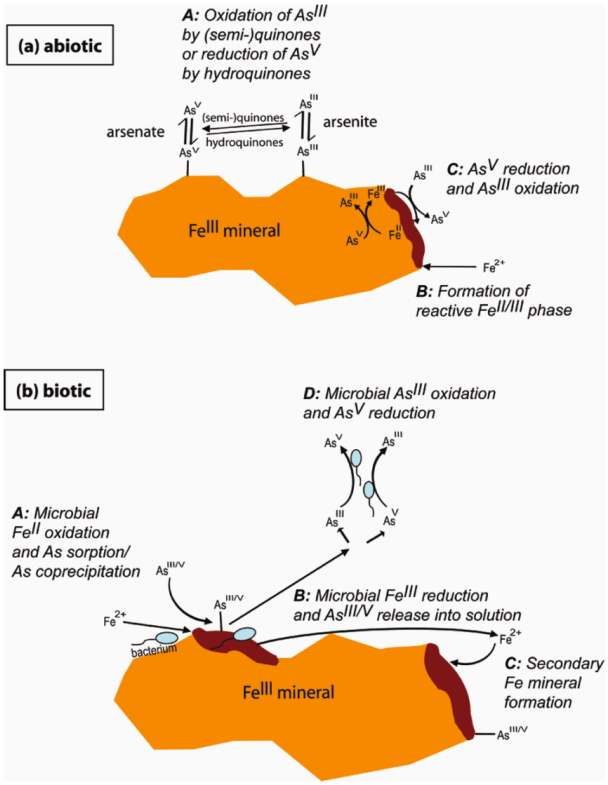

Figure 1.3: Conceptual model showing selected (a) abiotic and (b) biotic mechanisms of As redox chemistry, adapted from [28]

Chapter 2

SEA LEVEL RISE INDUCED ARSENIC RELEASE FROM HISTORICALLY CONTAMINATED COASTAL SOILS

2.1 ABSTRACT

The impacts of sea level rise (SLR) on biogeochemical processes in contaminated soils and sediments along the world's coastlines remains poorly understood. Elevated levels of the carcinogen arsenic (As), from both geogenic and anthropogenic sources, are found along many coasts, most notably in south and southeast Asia, but also in the US, particularly along the Mid-Atlantic coast. In this study, advanced biogeochemical microcosm reactors were used to simulate inundation with natural sea and river waters on a historically As-contaminated coastal soil across an Eh range of -300 mV to +200 mV. Eh values below +100 mV led to considerable As and Fe release into solution for both inundation scenarios. Arsenic release was strongly correlated to Eh, pH, Fe^{II}, DOC, and alkalinity in solution. Arsenic release into solution was lower in the seawater treatments than the river water. Direct As speciation of the soils after reaction at different Eh values was obtained by bulk X-ray absorption near-edge structure (XANES) spectroscopy, μX-ray fluorescence (XRF) imaging, and μXANES spectroscopy. Reducing conditions led to partial reduction of solid-phase As for both inundation scenarios, with more As reduction occurring when inundated with river water than with seawater. Sulfur speciation was also determined via XANES spectroscopy and showed evidence of sulfate reduction. Prolonged reducing conditions induced by SLR will drive the release of As from historically

contaminated soils, but As release may be tempered when inundated by seawater as compared to river water, possibly due to reduced microbial growth in high salinity conditions or preferential sulfate reduction limiting reductive dissolution of As-bearing Fe oxides.

2.2 INTRODUCTION

Earth's climate is changing. As a result, frequency and intensity of storm surges are increasing and sea levels are rising.[1] Sea level rise is driven by thermal expansion of oceans and melting of land ice, such as glaciers, ice caps, and the ice sheets of Greenland and Antarctica.[1] It is estimated that the global mean sea level will rise by 0.8 m over the next century and impact the 25% of the world's population that inhabits the coastal zone.[2,3] Increased storm surges and flooding have garnered the bulk of research and media attention associated with SLR due to the physical and economic threats posed to coastal regions. However, chemical and mineralogical changes in the subsurface that result from saltwater inundation and prolonged flooding, and their effects on contaminant fate and transport, remain poorly understood.[4,5]

Climate change induced shifts in the hydrologic regime are expected to impact biogeochemical processes including contaminant mobility and cycling.[6] These changes will alter soil redox conditions and introduce newly formed reducing zones and salinity in areas that have long remained oxic or less brackish and thus threaten to release redox sensitive elements (e.g., arsenic) to groundwater. Elevated levels of As are found along coastlines throughout the world from both geogenic and anthropogenic sources. In south and southeast Asia, tens of millions of people have been chronically poisoned by As-contaminated groundwater.[7] Within the United

States, As has been detected in nearly 20% of public groundwater supplies, and more than a third of the USEPA's superfund sites on the National Priorities List have excessive levels of arsenic.[8] Parts of the world are experiencing faster rates of SLR than the global average.[9,10] The Atlantic coastlines are particularly susceptible to near-future SLR, including the Mid-Atlantic coast of the U.S. where SLR rates are higher than elsewhere in the world due to the combination of SLR and coastal subsidence.[9,11] It has been recommended that states in this region prepare for SLR of at least 1 m by 2100.[12] Situated in the center of the Mid-Atlantic, Delaware is expecting at least 1 m of SLR, likely impacting many coastal As-contaminated sites.

The fate and transport of As in soils and sediments is intimately tied to environmental conditions (e.g., Eh, pH, carbon sources, ionic competition) as well as the biogeochemical redox cycling of other soil constituents such as Fe, Al, and Mn (oxyhydr)oxides (referred to as "oxides" hereafter), and S and C.[6,7,13] Anaerobic conditions can lead to reduction of surface bound As^{V} to the more weakly sorbed As^{III}, and thus increase mobility.[14] Reducing conditions also promote reductive dissolution of [As-bearing] Fe(III) oxides and favor dissimilatory metal reducing bacteria (DMRB). Dissimilatory reduction of Fe(III) hydroxides is the suspected primary driver of As release under reducing conditions in soils and sediments. Dissimilatory SO_4^{2-} reduction can be energetically favorable in high SO_4^{2-} systems and thus impact As mobility through preferential dissimilatory SO_4^{2-} reduction and subsequent preservation of As-bearing Fe oxides.[15]

While much research has been conducted on As cycling, our current understanding of how SLR will impact the mobilization of As in contaminated soils is limited. Using historically As contaminated soils from the coast of Delaware, we seek

to understand how inundation with seawater and river water impacts As mobilization and cycling across defined Eh zones. It is not currently understood how SLR will impact mobilization of existing contaminants in coastal soils. To fill this knowledge gap we studied the mobilization of As from historically contaminated soils from the coastline of Delaware comparing river water and seawater inundation scenarios. We analyzed As release coupled with solid and solution phase speciation under preset redox conditions for the first time, while monitoring controlling factors (e.g. pH, Fe, DOC, S).

2.3 EXPERIMENTAL

2.3.1 Soil Sampling and Characterization.

The city of Wilmington, DE has a long history of industrial activities including leather tanning, chemical production, and ore processing.[16] Each of these industries has contributed to the widespread As contamination currently found along the banks of the tidally influenced Christina River that flows through Wilmington. A site with elevated levels of As was selected in Wilmington that falls within the state of Delaware's 1m SLR scenario. The soil was sampled from 10 distinct areas along the banks of a tidal basin that was constructed as part of a remediation effort for an adjacent USEPA superfund site.

The soil was sampled from 0-20 cm from 10 random locations at the site and combined into one composite sample.[17] The composited sample was homogenized, air-dried, ground to pass through a 2 mm sieve, and stored at 4°C in the dark until experiments were conducted. Soil pH_{water}, texture, and organic matter were measured using standard methods. Particle size was determined by laser diffraction (Beckman

Coulter LS 13 320). Total metal content of the homogenized soil samples was determined by microwave-acid digestion (US EPA 1995 Method 3051), followed by analysis via inductively coupled plasma atomic emission spectrometry (ICP-AES, Thermo Elemental Intrepid II XSP Duo View).[18] Total ("free") iron oxide content was determined using the citrate-bicarbonate-dithionite method.[19] Poorly crystalline ("active") iron oxide content was determined using the acid ammonium oxalate in darkness method.[19] Soil mineralogy was determined via X-ray diffraction (Bruker D8 Discover).

2.3.2 Microcosm Experimental Set-up.

An advanced automated biogeochemical microcosm (MC) system was used to simulate oxidizing and reducing conditions. This system has been used successfully by others; a detailed description can be found therein.[20–22] Soils were mixed, in triplicate, with water from the Christina River in Wilmington, DE, USA or seawater from the Atlantic Ocean collected at Cape Henlopen State Park in Sussex County, DE, USA. A soil:solution ratio of 1:8 was used for optimum slurry mixing conditions in each MC.[21,22] The rate of mixing was set to minimize sedimentation on the bottom of the vessel, while avoiding over-mixing which could change the behavior of the soil particles, particularly surface area.[23] Mixing of the MC ensured a homogenous system so that the soil/solution ratio remained constant for the extent of the experiment.

At the initiation of each MC trial, an additional 10 g of "fresh" (moist) soil collected from the respective field location was added to each MC as a microbial inoculant. Additionally, 10 g of dried and ground reed (*Phragmites australis*) collected at the site was used as a slow-release C source for microorganisms. Two 10 g doses of glucose were also added to each MC to prime the system for reaching low redox

potentials by ensuring a C-limited system did not exist. Minimum Eh levels were obtained through microbial reduction and flushing the MC with N_2 gas.

After reaching a stable Eh minimum, the Eh was sequentially raised in 100 +/- 20 mV increments by injecting O_2 gas into the reactor then regulating at the target Eh using O_2 (to increase Eh) or N_2 (to decrease Eh). Each targeted Eh window was maintained for 72 h and then a slurry sample was taken. A total of six distinct Eh levels (-300 to +200 mV) were set and sampled for each replicate.

Measurements of Eh, pH, and temperature of the microcosms were logged every 10 minutes for the entirety of the incubation. Mean Eh values during the 6h prior to sampling was previously determined to give the best correlation coefficients between Eh/pH and metal(loid)s in solution within the MC system and therefore will be presented in this study.[22]

Slurry samples were sealed at sampling and immediately centrifuged at 2400 rpm for 10 min. Once centrifuged, samples were moved into an anaerobic glove box and the supernatant was filtered through a 0.45um Millipore nylon membrane (Whatman, Inc). While under the 95% O_2/5% H_2 atmosphere, aqueous subsamples were prepared for total elemental analyses. Subsamples analyzed via ICP mass spectrometry (ICP-MS) for total metal content in solution were acidified to 2% trace metal grade HNO_3 (Agilent Technologies, 7700 ICP-MS). To determine As speciation in supernatant solution, samples were stored at -20 C in the dark until immediately before analysis by high performance liquid chromatography ICP-MS (HPLC-ICP-MS) using a 10mM NH_4NO_3 and 10 mM $(NH_4)_3PO_4$, pH 9.4 eluent solution and a Hamilton PRP-X100 column. Total organic carbon (TOC) was determined by high temperature catalytic oxidation (Vario TOC cube, Elementar Americas, Mt. Laurel,

NJ) Immediately following MC sampling, centrifugation and filtering, the unstable species in solution were analyzed within 2 h. Iron(II) was determined by the phenanthroline method (Hach, Loveland, CO), sulfide was determined by the US EPA methylene blue method (Hach), ammonium was determined by the high range salicylate method (Hach), and alkalinity was determined by the bromcresol green-methyl red indicator method using the Hach digital titrator.

2.3.3 Bulk X-ray Absorption Spectroscopy.

Samples from each defined redox window, from -300 mV to +200 mV in 100 mV increments, were selected from both the freshwater and seawater trials for As K-edge X-ray absorption spectroscopy (XAS) analysis. Following centrifugation and decanting, samples were dried under a 95%N_2/5%H_2 atmosphere and the dried soils were mounted onto 1 mm thick aluminum between layers of 25 ¦ m thick Kapton tape. Analyses were performed at beamline 4-3 at the Stanford Synchrotron Radiation Lightsource (SSRL). The beamline is equipped with a Si (111) monochromator for energy selection and was detuned 30-40% for harmonic rejection. Energy calibration was performed by assigning the absorption edge of Au foil to the L_3 edge energy of 11,919 eV. Gold foil was monitored between the second and third ion chamber for each scan and was used to correct drift. X-rays were measured in fluorescence mode using a Lytle detector. Fitting was performed with the refined manual linear combination fitting tool available from beamline 10.3.2 at the Advanced Light Source (ALS; https://sites.google.com/a/lbl.gov/als-beamline1032).

2.3.4 Micro X-ray fluorescence (μXRF) mapping and μXANES spectroscopy.

Samples from the most extreme redox windows (-300 mV and +200 mV) were selected from both the freshwater and seawater trials. These samples were dried under 95%N_2/5%H_2 atmosphere and resin-embedded (EPOTEK 301_2FL). A thin section was then prepared and mounted onto a quartz slide at low temperature and low O_2 (Spectrum Petrographics method X26A). Samples were transported to the beamline under inert atmosphere, where they were kept until analysis. To determine elemental hot spots and colocation patterns, fine-scale μXRF mapping and μXANES spectroscopy were performed at SSRL beamline 2-3 following a previously described protocol. The beamline was equipped with KB focusing mirrors providing a spot size of 2x2 μm. Elemental maps were generated using a single-element Si drift Vortex detector; the sample was continuously rastered across the X-ray beam using a 5 μm pixel size and dwell time of 50 ms per pixel. Windowed counts of each element were isolated from the full X-ray fluorescence spectra and normalized to the intensity of the incident X-ray beam (I0). Energy was selected using a Si (111) double crystal monochromator and calibrated by assigning the whiteline position of Na_3AsO_4 standard to 11.874 keV.

Based on μXANES spectra of six As standards, representing the potential chemical species within the reacted sediments, a 1.5 mm x 1.5 mm (2.25 mm^2) region of the thin section was mapped at 11.867, 11.870, 11.873, 11.877, and 11.881 keV incident energy. Using the SMAK routine[24], principal component analysis (PCA) was performed on dead time corrected maps to determine optimal locations for μXANES spectral analysis. Least squares fitting of normalized μXANES spectra was optimized at ±20 eV from E0 in Athena.[25] Normalized μXANES spectra of the As standards

corresponding to the five incident energies were used to fit the multiple energy μXRF maps in a non-negative linear least squares routine in SMAK.[26]

2.4 RESULTS AND DISCUSSION

2.4.1 Characterization of the soil and natural waters.

The soil used in the MC was a loam with a mean particle size of 737.1 μm (s.d. 641.6 μm) and pH = 5.9. Prior to MC trials, the total As concentration in the soil was 1.3 g kg^{-1} and the total Fe concentration was 9.7 wt %, 17% of which were "free" Fe oxides (Table 1). Arsenic speciation in the soil collected and preserved for XANES analysis was primarily As^{III} (data not shown). The river water had a pH of 7.2 and an EC of 0.7 mmhos cm^{-1}. Total Fe and As in the natural river water were below detection (< 0.1 mg L^{-1}). The DOC was 4.4 mg L^{-1} and the S was 7.8 mg L^{-1}. The seawater had a pH of 7.8 and an EC of 45.6 mmhos cm^{-1}. Total Fe and As in the natural seawater were < 0.1 mg L^{-1}. The DOC was 5.5 mg L^{-1} and the S was 788.7 mg L^{-1}.

2.4.2 Microcosm solution dynamics.

Inundation of the soil with both waters led to decreased Eh and increased pH, as has been reported by others (Fig. 1).[21,27,28] The actual Eh values for river water ranged from -375 – +198 mV, while seawater values ranged from -369 – +196 mV (Table 1).

Arsenic concentrations in solution (i.e., As release) increased as Eh decreased in both the river water and seawater trials (Fig. 2). While dissolved As was measured across all Eh windows, a noted increase occurred at Eh values below +100 mV. This increase of As corresponds to the reported value at which reductive dissolution of Fe

oxides begins.[29] Arsenic release was higher in river water than in seawater microcosms, with river water releasing approximately twice as much As than seawater (Fig. 2). This difference could be attributed to a salinity impact on the microbial community, as the microbial inoculant for the microcosm reactions was from a freshwater system.. If this is the case, it suggests that a fast shift from fresh water to seawater, such as from storm surges and subsequent flooding, will limit the microbial activity in the inundated soils. However, with a slow shift from fresh water to more saline, as in the case of SLR, it is plausible that the microbial community may have time to adjust and the more halophytic anaerobes will play a larger role, thus impacting As mobilization under saline conditions brought on by SLR. It is expected that some of the As in solution can be attributed to methylation, because As is subject to biomethylation (i.e. addition of CH_3 through biological activity) under oxic as well as anoxic conditions, and can increase solubility.[30,31]

Similar to dissolved As, Fe(II) in solution also increased under reducing conditions, with the lowest recorded levels of Fe(II) present at the highest Eh levels. A similar trend was displayed in total solution Fe. The apparent critical point of reductive Fe-oxide dissolution for both inundation scenarios is near +100 mV. The reacted soil was high in Fe content with concentrations nearly 10 wt. % total Fe, and 1.6 wt. % free Fe oxides. Both the river water and seawater trials reached maximum concentrations of Fe(II) in solution of approximately 1000 mg L^{-1} under the most reducing conditions (below -200 mV), at which time As in solution was also at its peak. Though both inundation scenarios demonstrated significant correlations between As and Fe(II), a stronger relationship was observed in the freshwater ($r^2 = 0.82$ for river water, $r^2 = 0.38$ for seawater; Fig. 2).

Arsenic release was correlated with a number of other measured factors, including pH, total Fe, alkalinity, and DOC (Fig. 2). Despite the seawater having a higher initial pH prior to inundation, when reacted with the soil (soil pH = 5.9), the MC pH dropped lower than that found in the river water microcosms, and remained lower throughout the experiment (Fig. 1). Maximum pH levels for the seawater trials were approximately 1 pH unit below the freshwater trials, likely due to the "sea salt effect" (where cation exchange processes cause acidification following seasalt-rich inundation) and the hydrolysis of exchangeable metal cations (e.g., Al) in the soil.[32,33,34]

The correlations of As and alkalinity were significant for both river water and seawater, though the correlation was stronger with the river water (r^2 = 0.82 and 0.59, respectively). The alkalinity concentrations for the river water reached up to 5000 mg L^{-1} at -225 mV, while the seawater alkalinity concentrations' maximum was at 3500 mg L^{-1} at -187 mV.

In an effort to ensure that this experiment was not C limited, glucose and *P. australis* were added and thus led to the high concentrations of DOC in solution. Concentrations of DOC in both waters were similar in concentration, ranging from approximately 1600 mg L^{-1} at the onset of the experiment, and under the most reducing conditions, to 800 mg L^{-1} at the conclusion, and most oxidizing conditions of the experiment. The decrease in DOC in solution with increasing Eh levels may be attributed to increased microbial C consumption under more oxidizing conditions, or simply the microbial utilization of DOC over the course of the experiment.[28,35] Arsenic was positively correlated with DOC in solution. The highest concentrations of As were present under the same conditions that the highest concentrations of DOC were

observed, suggesting more available C can stimulate microbially driven reductive release of As from As-bearing oxides. The DOC-As correlation was stronger when inundated with river water ($r^2 = 0.69$) than with seawater ($r^2 = 0.38$).

While As cycling is normally strongly impacted by the S cycle in reduced soils and sediments, As in solution was not correlated to sulfide (S^{2-}) or sulfate in solution for either inundation scenario. Additionally, there was no pattern of S^{2-} or SO_4^{2-} in solution across Eh and pH values. Sulfide was below the method detection limit (1 mg L^{-1}) for both waters for the duration of the experiment. Despite this, it is likely that S^{2-} was formed under the reducing conditions through the reduction of SO_4^{2-}. Any S^{2-} that was formed would have rapidly been utilized through the formation Fe-S, As-S, or Fe-As-S precipitates in the high As^{III} and Fe^{II} solution,[15] resulting in the low S^{2-} in solution throughout the duration of the experiment. Thioarsenic species can be found in environmental samples that have high levels of solution As and S, but likely were not significant in this system because of the high levels of Fe that would sequester As and S by coprecipitation.[36]

Total SO_4^{2-} in the seawater system was ten times that of the freshwater system, with levels reaching nearly 70 mg L^{-1} at Eh levels greater than 100 mV (cross link). It has previously been suggested that elevated SO_4^{2-} in solution can competitively inhibit dissimilatory reduction of As^{V} and Fe^{III} due to preferential dissimilatory reduction of SO_4^{2-} at pH > 5.0, represented as:[15,37]

$$CH_3COOH + SO_4^{2-} \rightarrow 2HCO_3^- + H_2S$$

Preferential SO_4^{2-} reduction may preserve occluded As^{V} and result in decreased As release, which is a possible explanation for the decreased As in solution in the seawater inundation scenario as compared to the river water. This is a

thermodynamic possibility if the Gibbs free energy (ΔG^0) of dissimilatory sulfate or Fe reduction are equally favorable, as can be the case depending on which Fe oxide is being reduced.[38] It has been shown that following intrusion by water with high salinity, mineralization of organic C can shift rapidly from iron reduction to sulfate reduction.[39] This shift would act to preserve As bearing Fe oxide minerals and thereby decrease As release.

Seawater contained ten times more Cl^- in solution than river water, with no pattern of release corresponding to As in solution or Eh.

2.4.3 Solid phase As speciation changes via bulk XANES.

Arsenic speciation, as determined by bulk XANES, showed considerable As reduction at the lowest reductive potential for both inundation scenarios, which agrees with the solution data. Both scenarios produced partial reduction of As^V to As^{III}, with As^V present under even the most anoxic conditions (Fig. 4). In fact, mixed oxidation states were present at all Eh zones, which demonstrates the heterogeneity within the soil. Additionally, authigenic As-S complexes formed in both water treatments. The extent of the As reduction was more pronounced in the freshwater as compared to the seawater under the most reducing conditions, with the linear combination fitting (LCF) results showing up to 79% As^{III} contribution due to the river water treatment and a maximum of 66% As^{III} ascribed to the seawater treatment (Table 2). As the systems incrementally moved from reducing to oxidizing, As was incrementally oxidized and the proportion of As^{III} decreased by a total of 18% in the river water systems, and 9% in the seawater systems. Arsenic solid phase speciation was similar (60% As^{III}, 40% As^V) at the most oxic Eh zone (+200±20 mV) (Table 2).

Seawater trials led to more As^V across the entire Eh range (Fig. 4, Table 2). As mentioned earlier, with As in solution high levels of SO_4^{2-} can lead to less dissimilatory reduction of iron-oxyhydroxysulfate minerals.[15] The solid phase speciation shows less reduction of As in the high SO_4^{2-} seawater than the river water, which further suggests that there was indeed preferential dissimilatory SO_4^{2-} reduction rather than dissimilatory Fe (hydr)oxide reduction.

2.4.4 Solid phase As speciation changes via μXRF and μXANES.

Arsenic speciation, as determined by μXANES, showed the same pattern found in the bulk XANES analyses, but provides additional insights into the heterogeneity that leads to the mixed oxidation state results shown in the bulk XANES data. Multi-energy μXRF mapping of the most reduced and oxic samples from each inundation scenario suggests very little, if any, As oxidation states that are not some kind of As(III)/As(V) mixture. It is possible that this is a limitation of the method, and perhaps the use of a nanoprobe beamline would enable detection of distinct oxidation states. Tri-color RGB μXRF maps used to determine elemental colocation of As, Fe, and S indicate a stronger correlation between As and Fe in the solid phase with the seawater (Figure 5). These maps also show signs of deflocculation in the seawater with visibly smaller particle sizes present in the maps, probably due to the sodicity of the seawater.

The mean of all 10 points measured by μXANES at each Eh zone was similar to that measured by bulk XANES at the same Eh zones, which indicates that the microprobe data adequately represent the same heterogeneity present in the bulk XANES (Table 3). There were three to five phases of mixed oxidation states at each Eh zone (Fig. 5). Similar to the bulk XANES, the more oxic Eh zones were on

average mostly As^{V}. However, some spots (river water 184 mV spot A and seawater 183 mV spot A) were comprised of approximately 70% As^{III} under these oxidizing conditions. This demonstrates further the heterogeneity of the samples and possible influence of microsites on the overall As release.

A similar, but inverse, phenomenon was found in the most reducing zones. The solid phase where river water was used showed 4 components of mixed oxidation state from the principle component analysis (PCA), ranging from 69-85% As^{III}, coupled with some As-S precipitation at -324 mV. The largest contribution from As^{V} at this Eh zone was 32% (river water -324 mV, spot D). However, for the seawater microcosms at the lowest Eh zone (-254 mV), 3 oxidation state mixed PCA components were identified and none of the μXANES indicated less than 28% contribution by As^{V} (seawater -254 mV spot A). The maximum contribution of As^{V} for the reducing seawater microcosms reached up to 59% (seawater -254 spot C).

These results further demonstrate the decreased As reduction in the seawater inundations as compared to the river water inundations. The reduction of As^{V} under reducing conditions in soil can be a direct enzymatic process, or can result from the dissimilatory reductive dissolution of As-bearing Fe (hydr)oxides such as ferrihydrite, goethite, lepidocrocite, magnetite, or hematite. The energy requisite for reducing these Fe^{III} minerals, their reactivity, surface area, and As sorption capacity are unique for each Fe oxide.[40] While under some environmental conditions dissimilatory reductive of Fe oxides is energetically favorable compared to dissimilatory SO_4^{2-} reduction, it is possible that preferential SO_4^{2-} reduction would occur in the presence of more crystalline Fe oxides with increased Gibbs free energy. Because reductive dissolution of Fe oxides is a primary driver of As release from soils, it is therefore reasonable to

assume As^{V} reduction and release is limited in the seawater inundations as compared to the river water by . reduced microbial activity.

2.4.5 Solid phase S speciation changes via bulk XANES spectroscopy.

Sulfur speciation, as determined by bulk XANES spectroscopy, showed considerable variation in S speciation between the inundation scenarios (Fig. 6). The feature in the S XANES spectra that indicates oxidized forms of S, such as sulfate, between 2480-2485 eV, decreased in the solid phase of both the sea and river water. In the river water, the pyrite (S^{1-}) contribution increased under reducing conditions, which suggests the formation of Fe-As-S coprecipitates under reducing conditions and is in agreement with the solid phase As speciation. In the river water trial, pyrite contribution increased by ~13% and organic sulfides (S^{2-}) decreased by ~16% with decreasing Eh levels. The sulfoxide (S^{0}) contribution increased in reducing Eh zones and did not contribute at the most oxic conditions for the river water. Sulfate ester (S^{6+}) only contributed to the S speciation at the highest Eh zone (+184 mV).

The percentage of pyrite contribution remained the same (approx. 30%) across Eh levels in the seawater. The contribution of organic sulfides to the S speciation increased by ~5 wt% in the solid phase with seawater whereas sulfate ester decreased by ~9 wt % with decreasing Eh levels. The contribution of sulfoxide species slightly increased (by 2.5%) with decreased Eh. This decrease in the oxidized sulfate ester species, paired with increases in the more reduced sulfoxide and organic sulfide species, is evidence of sulfate reduction in the seawater solids.

2.4.6 Implications for Sea Level Rise.

The compounding issues of SLR and its impacts on the cycling of contaminants in coastal soils is of merit and calls for field- and lab-based observations to understand the risks posed to these soils and surrounding communities. Climate change induced seawater inundation, short and/or long term flooding, and salinification will alter the biogeochemistry of these sensitive sites. Newly flooded areas will see formerly oxic zones turn more reducing and thereby change the ability of the soils and sediments to sequester contaminants. Our findings show that introducing reducing conditions can lead to As release from soils through reductive dissolution of As-bearing mineral oxides in both river water and seawater inundations scenarios. Additionally, short-term inundation with seawater can lead to less As release than inundation with freshwater. Accordingly, the threat of SLR stands to impact release of As from contaminated coastal soils primarily by changing the redox conditions and subsurface mineralogy. Future work should include abiotic controls to further understand the mechanisms of As release, a microbial inoculant from a brackish or seawater soil or sediment to determine how similar experimental conditions impact As cycling with a microbial community adept to salinity.

2.5 References Cited

(1) Church, J. a.; White, N. J.; Aarup, T.; Wilson, W. S.; Woodworth, P. L.; Domingues, C. M.; Hunter, J. R.; Lambeck, K. Understanding global sea levels: Past, present and future. *Sustain. Sci.* **2008**, *3*, 9–22.

(2) Church, J. a.; Clark, P. U.; Cazenave, a.; Gregory, J. M.; Jevrejeva, S.; Levermann, a.; Merrifield, M. a.; Milne, G. a.; Nerem, R. .; Nunn, P. D.; et al. Sea level change. *Clim. Chang. 2013 Phys. Sci. Basis. Contrib. Work. Gr. I to Fifth Assess. Rep. Intergov. Panel Clim. Chang.* **2013**, 1137–1216.

(3) Small, C.; Nicholls, R. J. A global analysis of Human Settlement in Coastal Zones. *J. Coast. Res.* **2003**, *19*, 584–599.

(4) Nicholls, R. J.; Tol, R. S. J. Impacts and responses to sea-level rise: a global analysis of the SRES scenarios over the twenty-first century. *Philos. Trans. A. Math. Phys. Eng. Sci.* **2006**, *364*, 1073–1095.

(5) Hinkel, J.; Jaeger, C.; Nicholls, R. J.; Lowe, J.; Renn, O.; Peijun, S. Sea-level rise scenarios and coastal risk management. *Nat. Clim. Chang.* **2015**, *5*, 188–190.

(6) Borch, T.; Kretzschmar, R.; Skappler, A.; Van Cappellen, P.; Ginder-Vogel, M.; Voegelin, A.; Campbell, K. Biogeochemical redox processes and their impact on contaminant dynamics. *Environ. Sci. Technol.* **2010**, *44*, 15–23.

(7) Stuckey, J. W.; Schaefer, M. V.; Kocar, B. D.; Dittmar, J.; Pacheco, J. L.; Benner, S. G.; Fendorf, S. Peat formation concentrates arsenic within sediment deposits of the Mekong Delta. *Geochim. Cosmochim. Acta* **2015**, *149*, 190–205.

(8) DeLemos, J. L.; Bostick, B. C.; Renshaw, C. E.; Stürup, S.; Feng, X. Landfill-stimulated iron reduction and arsenic release at the Coakley Superfund Site (NH). *Environ. Sci. Technol.* **2006**.

(9) Krasting, J. P.; Dunne, J. P.; Stouffer, R. J.; Hallberg, R. W. Enhanced Atlantic sea-level rise relative to the Pacific under high carbon emission rates. *Nat. Geosci.* **2016**, 0–5.

(10) Rietbroek, R.; Brunnabend, S.-E.; Kusche, J.; Schröter, J.; Dahle, C. Revisiting the contemporary sea-level budget on global and regional scales. *Proc. Natl. Acad. Sci.* **2016**, 201519132.

(11) Sallenger, A. H.; Doran, K. S.; Howd, P. a. Hotspot of accelerated sea-level rise on the Atlantic coast of North America. *Nat. Clim. Chang.* **2012**, *2*, 1–5.

(12) Titus, J. G. (Coordinating lead author); Anderson, K. E.; Cahoon, D. R.; Gesch, D. B.; Gill, S. K.; Gutierrez, B. T.; Thieler, E. R.; Williams, S. J. (lead authors). *Coastal Cycle Sensitivity to Sea-Level Rise : Focus on Mid-Atlantic Region*; Washington, D.C., USA, 2009.

(13) Kocar, B. D.; Herbel, M. J.; Tufano, K. J.; Fendorf, S. Contrasting effects of dissimilatory iron (III) and arsenic (V) reduction on arsenic retention and transport. *Environ. Sci. Technol.* **2006**, *40*, 6715–6721.

(14) Charlet, L.; Morin, G.; Rose, Jã©.; Wang, Y.; Auffan, Mã©.; Burnol, A.; Fernandez-Martinez, A. Reactivity at (nano)particle-water interfaces, redox processes, and arsenic transport in the environment. *Comptes Rendus Geosci.* **2011**, *343*, 123–139.

(15) Burton, E. D.; Johnston, S. G.; Kraal, P.; Bush, R. T.; Claff, S. Sulfate availability drives divergent evolution of arsenic speciation during microbially mediated reductive transformation of schwertmannite. *Environ. Sci. Technol.* **2013**, *47*, 2221–2229.

(16) Landrot, G.; Tappero, R.; Webb, S. M.; Sparks, D. L. Arsenic and chromium speciation in an urban contaminated soil. *Chemosphere* **2012**, *88*, 1196–1201.

(17) Tan, K. H. *Soil Sampling, Preparation, and Analysis*; Second.; Taylor & Francis Group: New York, 2005.

(18) Agency, U. S. E. P. *Method 3051a: Microwave Assisted Acid Digestion of Sediments, Sludges, Soils, and Oils*; Washington, D.C., USA, 1998.

(19) Loeppart, R. H.; Inskeep, W. P. Iron. In *Methods of Soil Analysis. Part 3. Chemical Methods*; Sparks, D. L., Ed.; Soil Science Society of America: Madison, WI, 1996; pp. 384–411.

(20) Yu, K.; Rinklebe, J. Advancement in soil microcosm apparatus for biogeochemical research. *Ecol. Eng.* **2011**, *37*, 2071–2075.

(21) Frohne, T.; Rinklebe, J.; Diaz-Bone, R. A.; Du Laing, G. Controlled variation of redox conditions in a floodplain soil: Impact on metal mobilization and biomethylation of arsenic and antimony. *Geoderma* **2011**, *160*, 414–424.

(22) Frohne, T.; Diaz-Bone, R. a.; Du Laing, G.; Rinklebe, J. Impact of systematic change of redox potential on the leaching of Ba, Cr, Sr, and V from a riverine soil into water. *J. Soils Sediments* **2015**, *15*, 623–633.

(23) Sparks, D. L. *Environmental Soil Chemistry*; Second.; Academic Press: New York, 2003.

(24) Webb, S. M. The microanalysis toolkit: X-ray fluorescence image processing software. In *10th International Conference on X-ray Microscopy*; McNulty, I.; Eyberger, C.; Lai, B., Eds.; 2011; pp. 196–199.

(25) Ravel, B. A THENA U ser ’ s G uide. **2009**.

(26) Mayhew, L. E.; Webb, S. M.; Templeton, a. S. Microscale imaging and identification of fe speciation and distribution during fluid-mineral reactions under highly reducing conditions. *Environ. Sci. Technol.* **2011**, *45*, 4468–4474.

(27) Frohne, T.; Rinklebe, J.; Diaz-Bone, R. a. Contamination of Floodplain Soils along the Wupper River, Germany, with As, Co, Cu, Ni, Sb, and Zn and the Impact of Pre-definite Redox Variations on the Mobility of These Elements. *Soil Sediment Contam. An Int. J.* **2014**, *23*, 779–799.

(28) Shaheen, S. M.; Rinklebe, J.; Frohne, T.; White, J. R.; DeLaune, R. D. Redox effects on release kinetics of arsenic, cadmium, cobalt, and vanadium in Wax Lake Deltaic freshwater marsh soils. *Chemosphere* **2015**, 1–9.

(29) Reddy, R.; Delaune, R. D. *Biogeochemistry of Wetlands: Science and Applications*; CRC Press: Boca Raton, FL, 2008.

(30) Bentley, R.; Chasteen, T. G. Microbial Methylation of Metalloids : Arsenic , Antimony , and Bismuth Microbial Methylation of Metalloids : Arsenic , Antimony , and Bismuth. *Microbiol. Mol. Biol. Rev.* **2002**, *66*, 250–271.

(31) Thayer, J. S. Biological methylation of less-studied elements. *Appl. Organomet. Chem.* **2002**, *16*, 677–691.

(32) Wright, R. F.; Norton, S. A.; Brakke, D. F.; Frogner, T. Experimental verification of episodic acidification of freshwaters by sea salts. *Nature* **1988**, *334*, 422–424.

(33) Wong, V. N. L.; Johnston, S. G.; Burton, E. D.; Bush, R. T.; Sullivan, L. a.; Slavich, P. G. Seawater causes rapid trace metal mobilisation in coastal lowland acid sulfate soils: Implications of sea level rise for water quality. *Geoderma* **2010**, *160*, 252–263.

(34) Dixit, S.; Hering, J. G. Comparison of arsenic(V) and arsenic(III) sorption onto iron oxide minerals: Implications for arsenic mobility. *Environ. Sci. Technol.* **2003**, *37*, 4182–4189.

(35) Yu, K.; Böhme, F.; Rinklebe, J.; Neue, H.-U.; DeLaune, R. D. Major Biogeochemical Processes in Soils-A Microcosm Incubation from Reducing to Oxidizing Conditions. *Soil Sci. Soc. Am. J.* **2007**, *71*, 1406.

(36) Stucker, V. K.; Silverman, D. R.; Williams, K. H.; Sharp, J. O.; Ranville, J. F. Thioarsenic species associated with increased arsenic release during biostimulated subsurface sulfate reduction. *Environ. Sci. Technol.* **2014**, *48*, 13367–13375.

(37) Blodau, C. A review of acidity generation and consumption in acidic coal mine lakes and their watersheds. *Sci. Total Environ.* **2006**, *369*, 307–332.

(38) Bethke, C. M.; Sanford, R. A.; Kirk, M. F.; Jin, Q.; Flynn, T. M. The thermodynamic ladder in geomicrobiology. *Am. J. Sci.* **2011**, *311*, 183–210.

(39) Weston, N. B.; Dixon, R. E.; Joye, S. B. Ramifications of increased salinity in tidal freshwater sediments: Geochemistry and microbial pathways of organic matter mineralization. *J. Geophys. Res.* **2006**, *111*, G01009.

(40) Pedersen, H.; Postma, D.; Jakobsen, R. Release of arsenic associated with the reduction and transformation of iron oxides. *Geochim. Cosmochim. Acta* **2006**, *70*, 4116–4129.

2.6 TABLES AND FIGURES

Table 2.1: Soil and water characterization

Soil Name	Depth (cm)	Texture	Mean Particle Size (um)	pH	Free Fe Oxides	As	Cr	Pb	Total Fe	Mn	S	Al
					---------- mg kg^{-1} ----------							
Ditch Sediment	0-20	Loam	737	5.9	16,493	13,296	62	360	97,057	558	4157	16,265

Water Type	pH	EC	DOC	Ca	Mg	Na	As	Cr	Pb	Total Fe	Mn	S	Al
		(mmhos/cm)	---------- mg kg^{-1} ----------										
River	7.2	0.7	4157	16,265	1091	7153	bd*	bd	bd	bd	bd	789	bd
Sea	7.8	45.6	5.5	24	9.4	42.4	bd	bd	bd	bd	bd	7.8	bd

*bd indicates values that were below the detection limit of 0.1 mg kg^{-1}

Table 2.2: Arsenic bulk XANES spectroscopy linear combination fit results.

Sea water					
Eh_{6h} (mV)	As^{2+} **	As^{3+} (%)	As^{5+}	del-E (eV)	NSS *
183	0	57	43	0.40	1.06E-03
169	0	57	43	0.30	9.95E-04
125	7	56	37	-0.13	1.03E-03
120	6	56	38	0.28	8.80E-04
10	7	59	34	-0.11	9.86E-04
-25	7	59	34	0.31	8.29E-04
-94	9	63	28	-0.25	9.24E-04
-127	9	61	30	0.36	7.83E-04
-187	9	62	29	-0.43	9.50E-04
-188	9	61	30	0.25	8.01E-04
-240	8	60	32	0.20	8.35E-04
-254	8	66	26	-0.58	8.89E-04

River water					
Eh_{6h} (mV)	As^{2+}	As^{3+} (%)	As^{5+}	del-E (eV)	NSS
185	0	60	40	0.22	1.10E-03
184	0	63	37	-0.81	1.13E-03
108	8	60	32	0.38	8.49E-04
81	8	64	28	-0.56	9.71E-04
13	10	67	23	0.46	8.26E-04
-19	11	68	21	-0.62	8.86E-04
-117	12	71	17	0.22	7.45E-04
-118	11	69	20	-0.69	8.29E-04
-214	11	73	17	-0.50	8.02E-04
-225	11	75	14	-0.04	7.31E-04
-314	10	76	13	-0.20	8.02E-04
-318	10	79	11	0.13	7.12E-04
-324	10	78	12	-0.35	7.09E-04
-348	10	78	12	-0.23	7.52E-04

*NSS = normalized sum of squares residual of the fit, determined by $NSS = \Sigma(y - y_{fit})^2)/\Sigma(y^2)$
**The standard used for linear combination fitting that is represented by As^{2+} was realgar. The standards used for As^{3+} and As^{5+} were sodium arsenite and sodium arsenate, respectively.

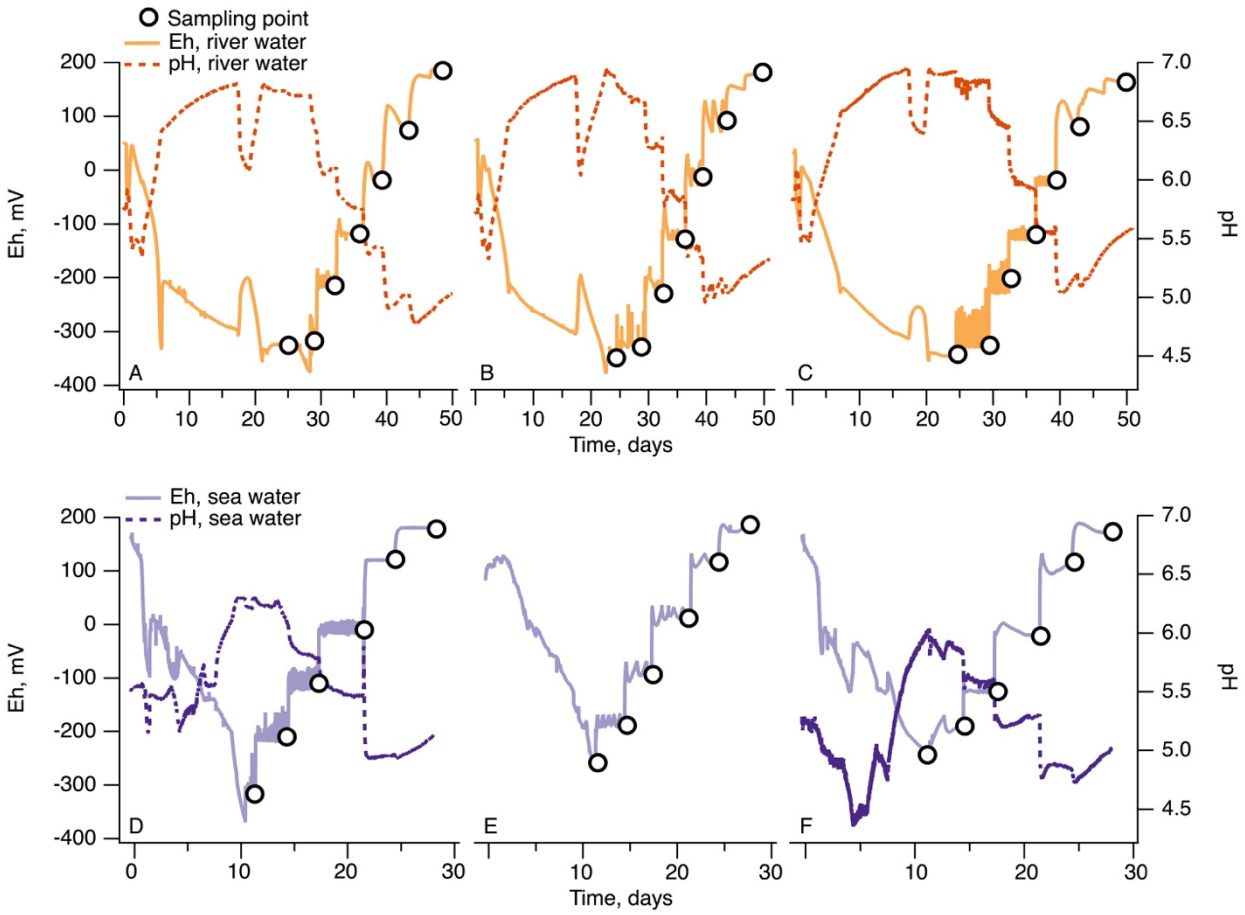

Figure 2.1: Detailed rendering of redox potential (Eh) and pH relationship for the duration of the trial, including all replicates. River water and seawater are represented by subfigures A-C and D-F, respectively.

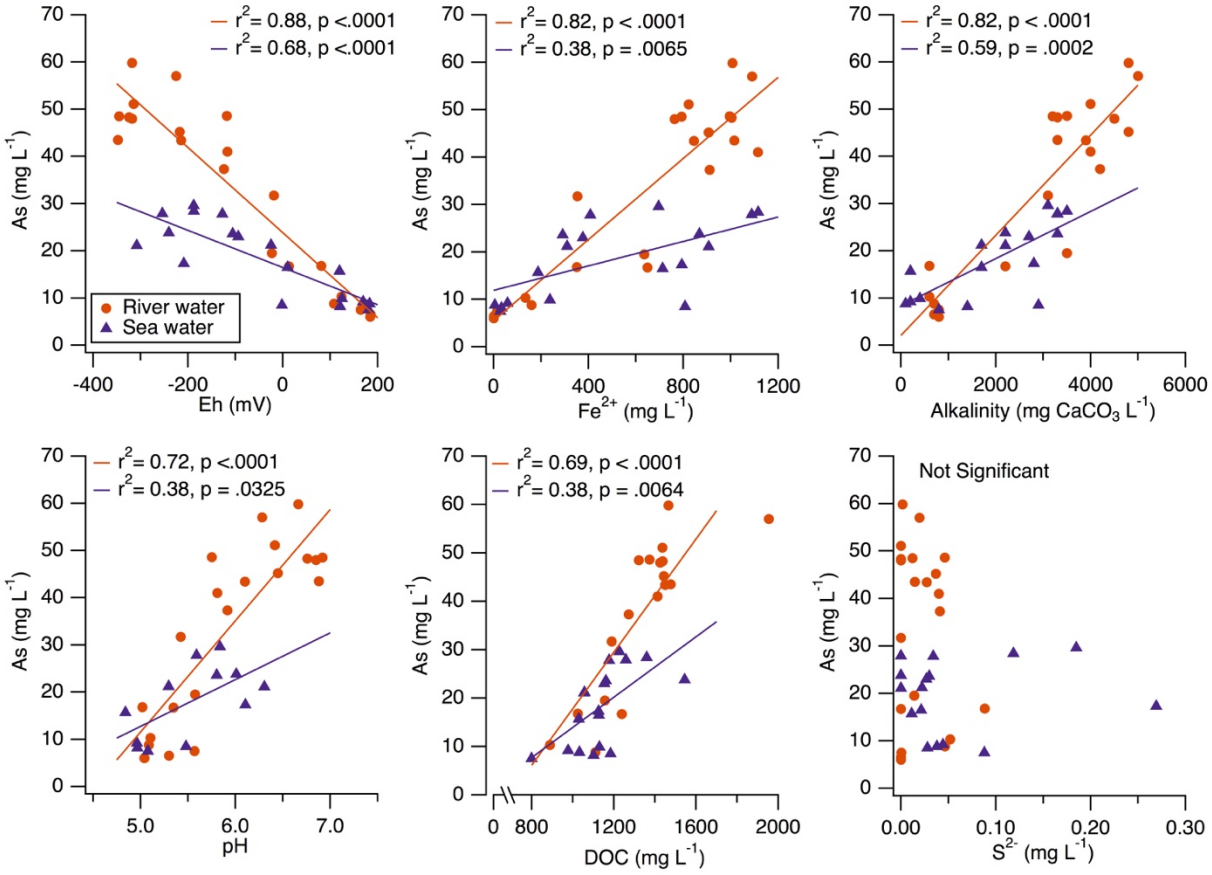

Figure 2.2: Arsenic in solution as regressed to significantly linked factors. For all bivariate linear regression analyses, n = 20, p value given by analysis of variance.

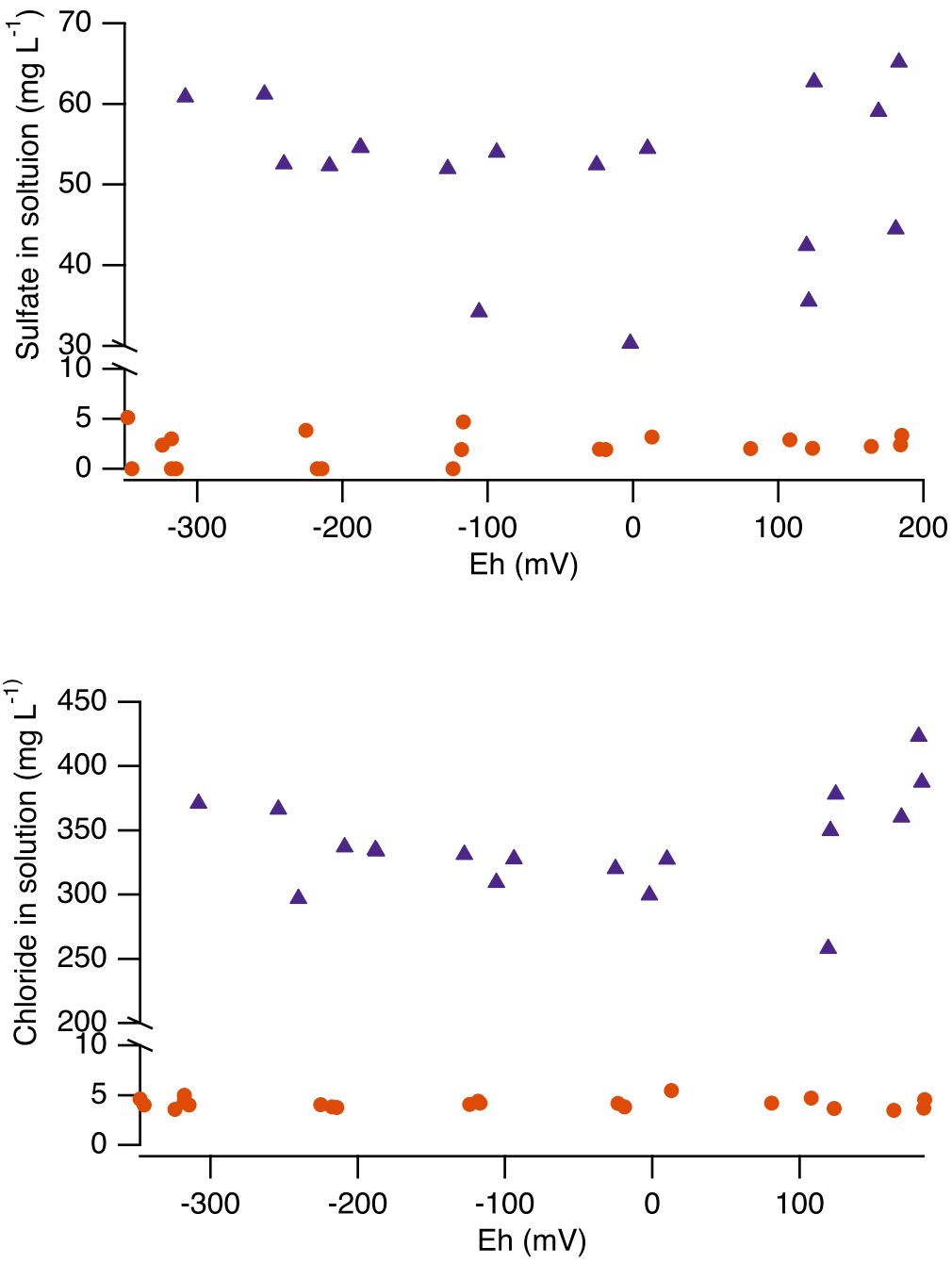

Figure 2.3: Sulfate (top) and chloride (bottom) in solution as a factor of Eh for both sea water (purple triangles) and river water (orange circles) inundation scenarios.

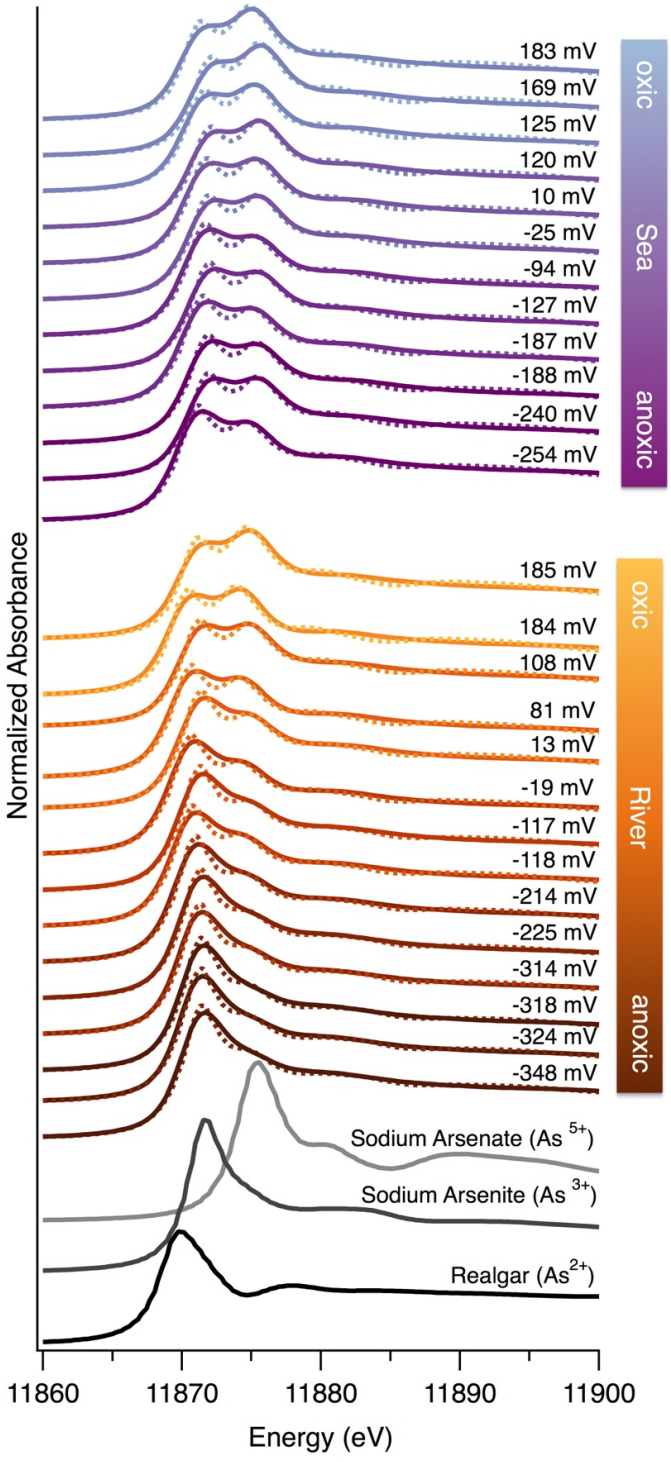

Figure 2.4: Arsenic XANES for sea water and river water inundations scenarios across designated Eh windows following 72 h equilibration time at that Eh. Data are represented by the solid lines and fits obtained by linear combination fitting are dotted lines.

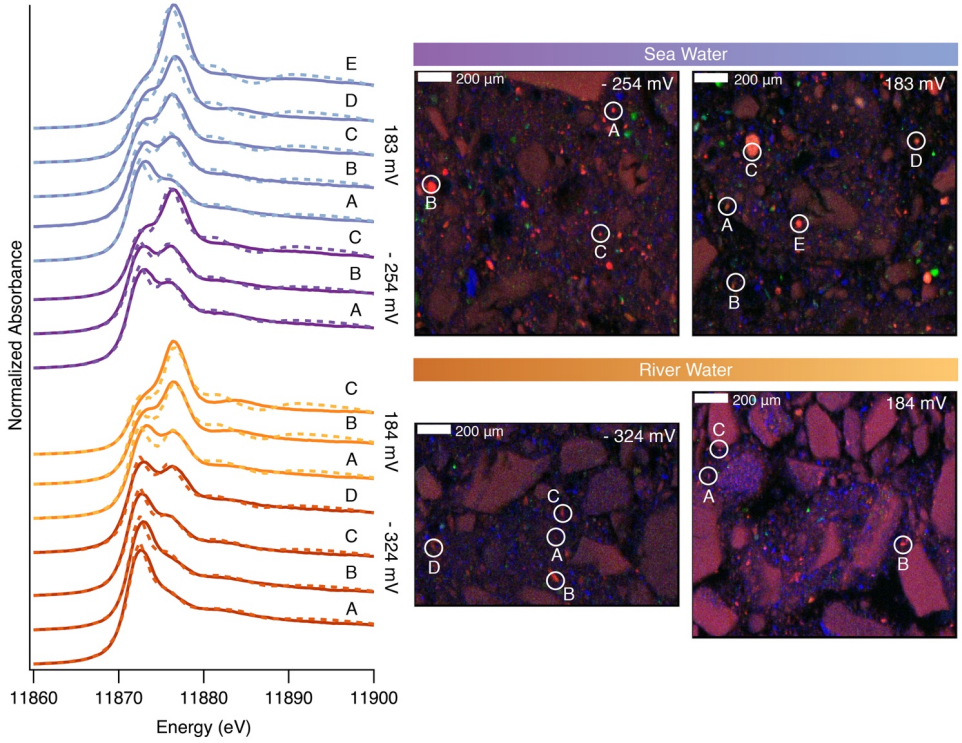

Figure 2.5: Solid phase As speciation changes via μXRF and μXANES spectrosocpy. River water spectra are expressed in orange and sea water are purple, with the darker shades indicating lower Eh values. Data are represented by the solid lines and fits obtained by linear combination fitting are dotted lines. In the tri-color RBG maps red represents As, blue represents Fe, and green represents S.

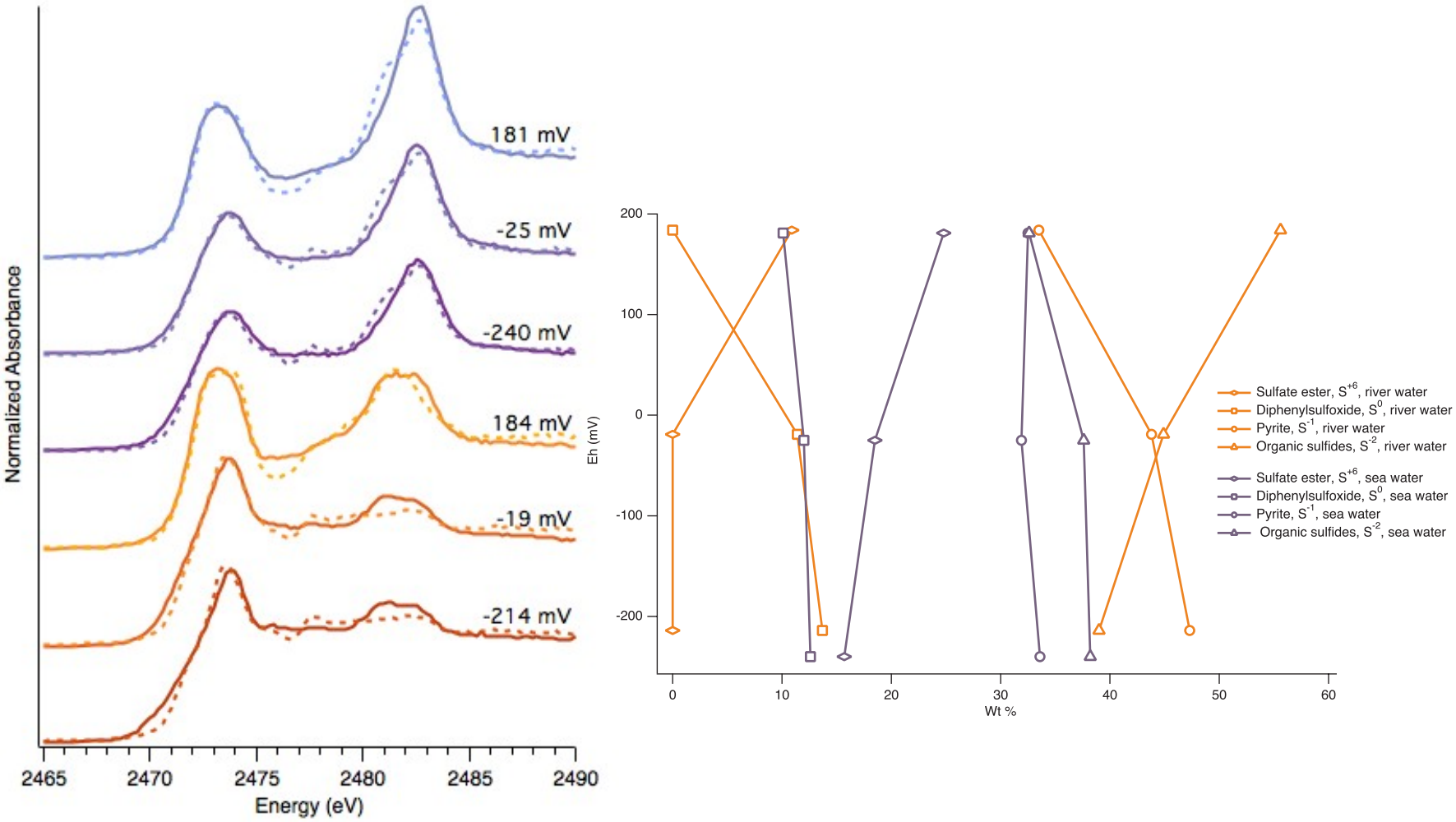

Figure 2.6: Solid phase S speciation changes via bulk XANES. River water spectra are expressed in orange and sea water are purple, with the darker shades indicating lower Eh values. Data are represented by the solid lines and fits obtained by linear combination fitting are dotted lines. Linear combination fitting was performed using sulfate ester, pyrite, diphenylsulfoxide, and organic sulfides (methionine, cystine, and diphenyldisulfide).

Chapter 3

POTENTIAL IMPACTS OF SEA LEVEL RISE ON ARSENIC MOBILITY AND CYCLING FROM A CONTAMINATED WETLAND SOIL

3.1 Introduction

Sea levels are rising as a result of thermal expansion of oceans and melting of land ice due to a changing climate.[1] It is estimated that the global mean sea level will rise by 0.8 m compared to 1990 sea levels by the year 2100.[2] However, some parts of the world are experiencing faster rates of SLR than the global average. Observed rates of SLR in the Mid-Atlantic coast of the U.S. are higher than elsewhere in the world and faster than early estimates due to the combination of SLR and coastal subsidence.[3] It has been recommended that states in this region prepare for SLR of at least 1 m by 2100.[4]

Sea level rise is estimated to directly impact more than 8.5 million people in the U.S. This number stands to increase over time as approximately 40% of the U.S. population lives in coastal counties.[1] In addition to being home to a large population, many coasts throughout the world have long been centers for industrial activity. Industries have left a wide spread legacy of contaminated coastal soils and groundwater. The hydrologic changes due to SLR and increased storm surges from a changing climate will impact existing contamination along the coasts as formerly aerobic zones turn anaerobic and salinity is introduced by encroaching seawater.

Thus, metal(loid)s formerly sorbed to soil minerals may become mobile and more toxic through competitive ionic exchange, ligand exchange, and changes in redox potential. Arsenic deposited into soils and groundwater through industrial activity is one of the contaminants that may be released into the environment. Exposure to elevated levels of As through anthropogenic inputs can lead to skin, lung, bladder, and other

internal organ cancers.[5] Toxicity and mobility of As in the environment are primarily functions of redox state. The major redox states of As in the environment include arsenic-sulfides (As^{-1} to As^{II}), arsenite (As^{III}), and arsenate (As^{V}). It is generally thought that arsenite is the most mobile, and thereby most toxic, of these As species.

Arsenic is commonly associated with Al, Fe or Mn (hydr)oxides and sulfides in soils and sediments. Seawater inundation of coastal soils and sediments has been shown to cause a significant shift in redox and lead to reductive dissolution of Fe^{3+}, SO_4^{2-} reduction, followed by precipitation of S-Fe minerals in certain soils.[6] Redox transitions initiated by seawater inundation can also lead to the reductive dissolution of As-bearing Fe minerals and their subsequent mobilization, or direct reduction of As(V) to As(III).[7,8]

There is no work to our knowledge that has been done to investigate the potential impacts of SLR on contaminants in urban coastal soils and sediments within the U.S. The above referenced work was performed with coastal lowland acid sulfate soils in Australia.[9,7,10,6] It is important to understand the geochemical cycling of As in soils and sediments near densely populated urban areas with a history of contamination following inundation with seawater. This work seeks to determine how introducing redox transitions and salinity will impact the solid and aqueous phase speciation and distribution of As by mimicking field conditions with advanced automated biogeochemical microcosms with two natural waters and an anthropogenically contaminated urban wetland soil from the Mid-Atlantic region of the U.S.

3.2 Materials and Methods

3.2.1 Study Site

Soil samples were collected from a historic wetland in an urban area along the Christina River in Wilmington, Delaware, USA, within the state of Delaware's 1.0 m SLR scenario. The soil is characteristic of the area, with a history of tannery, chemical

production, and/or ore processing contamination. At the request of the property owners, exact locations are withheld. The study sites flood periodically from the Christina River and urban runoff. Access to sites was granted in collaboration with Delaware's Department of Natural Resources and Environmental Control (DNREC), who served as a mediator between the research team and the responsible parties and property owners.

3.2.2 Bulk Soil Sampling and Characterization

Over the course of the past century, a historic wetland was filled with contaminated soils, slag, and miscellaneous other soil-like materials. Because of this, the soil heterogeneity found at this site is extreme. Using the extensive soil sampling data previously collected by DNREC, U.S. Environmental Protection Agency (EPA), and their affiliates, sample locations were selected with elevated As, within DNREC's 1.0 m SLR scenario, and were representative of the respective site.

The soil was sampled from 0-20 cm from 10 random locations at the site and combined into one composite sample.[11] The composited sample was homogenized, air-dried, ground to pass through a 2 mm sieve, and stored at 4°C in the dark until experiments were conducted. Soil pH_{water}, texture, and organic matter were measured using standard methods. Particle size was determined by laser diffraction (Beckman Coulter LS 13 320). Total metal content of the homogenized soil samples was determined by microwave-acid digestion (US EPA 1995 Method 3051), followed by analysis via inductively coupled plasma atomic emission spectrometry (ICP-AES, Thermo Elemental Intrepid II XSP Duo View).[12] Total ("free") iron oxide content was determined using the citrate-bicarbonate-dithionite method.[13] Poorly crystalline ("active") iron oxide content was determined using the acid ammonium oxalate in darkness method.[13] Soil mineralogy was determined via X-ray diffraction (Bruker D8 Discover).

3.2.3 Microcosm Experimental Setup

An advanced automated biogeochemical microcosm (MC) system was used to simulate oxidizing and reducing conditions. This system has been used successfully by others; a detailed description can be found therein.[14–16] Soils were mixed, in triplicate, with water from the Christina River in Wilmington, DE, USA or seawater from the Atlantic Ocean collected at Cape Henlopen State Park in Sussex County, DE, USA. A soil:solution ratio of 1:8 was used for optimum slurry mixing conditions in each MC, with a total volume of 4 L.[15,16] The rate of mixing was set to minimize sedimentation on the bottom of the vessel, while avoiding over-mixing which could change the behavior of the soil particles, particularly surface area.[17] Mixing of the MC ensured a homogenous system so that the soil/solution ratio remained constant for the extent of the experiment.

At the initiation of each MC trial, an additional 10 g of "fresh" (moist) soil collected from the field site was added to each MC as a microbial inoculant. Additionally, 10 g of dried and ground reed (*Phragmites australis*) collected at the site was used as a slow-release C source for microorganisms. Two 10 g doses of glucose were also added to each MC to prime the system for reaching low redox potentials by ensuring a C-limited system did not exist. Minimum Eh levels were obtained through microbial reduction and flushing the MC with N_2 gas.

After reaching a stable Eh minimum, the Eh was sequentially raised in 100-200 +/- 20 mV increments by injecting O_2 gas into the reactor then regulating at the target Eh using O_2 (to increase Eh) or N_2 (to decrease Eh). Each targeted Eh window was maintained for 24 h and then a slurry sample was taken. A total of 4-5 distinct Eh levels (-300 to +200 mV) were set and sampled for each replicate.

Measurements of Eh, pH, and temperature of the microcosms were logged every 10 minutes for the entirety of the incubation. Mean Eh values during the 6h prior to sampling was previously determined to give the best correlation coefficients between

Eh/pH and metal(loid)s in solution within the MC system and therefore will be presented in this study.[16]

Slurry samples were sealed at sampling and immediately centrifuged at 2400 rpm for 10 min. Once centrifuged, samples were moved into an anaerobic glove box and the supernatant was filtered through a 0.45um Millipore nylon membrane (Whatman, Inc). While under the 95% O_2/5% H_2 atmosphere, aqueous subsamples were prepared for total elemental analyses. Subsamples analyzed via ICP mass spectrometry (ICP-MS) for total metal content in solution were acidified to 2% trace metal grade HNO_3 (Agilent Technologies, 7700 ICP-MS). To determine As speciation in supernatant solution, samples were stored at -20 C in the dark until immediately before analysis by high performance liquid chromatography ICP-MS (HPLC-ICP-MS) using a 10mM NH_4NO_3 and 10 mM $(NH_4)_3PO_4$, pH 9.4 eluent solution and a Hamilton PRP-X100 column. Total organic carbon (TOC) was determined by high temperature catalytic oxidation (Vario TOC cube, Elementar Americas, Mt. Laurel, NJ)

3.2.4 3.2.4. Synchrotron-based solid phase analysis.

Solid samples from each defined redox window from both the river water and seawater trials were air dried under a 95%N2/5%H2 atmosphere and the dried soils were mounted between layers of 25 μm thick Kapton tape for synchrotron analysis. Samples were stored and transported under anaerobic conditions until analysis. Micro X-ray fluorescence (μ-XRF) analyses were performed at beamlines X26a and X27a of the National Synchrotron Light Source at Brookhaven National Laboratory to determine elemental hot spots and colocation patterns. The monochromator was calibrated to the As(V) white line position (11874 eV) with a known standard (As-bearing topaz). The μ-XRF maps were generated with the beam energy set to 12.5 keV, above the As K-edge but below the Pb K-edge due to potential signal interference. Maps were up to 9 mm2 using a 0.01 mm step size and 0.1 sec dwell time. Hotspots of high concentration were

identified with the μ-XRF maps and then micro X-ray absorption near edge structure (μ-XANES) spectroscopy was performed to determine speciation at selected points of interest. At least five μ-XANES spectra were collected for each sample analyzed. Spectra were normalized and merged for each sample, setting Eo to the peak of the first derivative for each scan and merged spectrum. The merged spectra for the hot spots analyzed were then merged to form an average spectrum for each sample. Linear combination fitting (LCF) was performed on these average spectra using Athena on normalized XANES regions of the spectra with peak fitting. Standards used for μ-XANES LCF analysis were NaHAsO4 [As(V)], $NaAsO_2$ [As(III)], and arsenopyrite (FeAsS). Standard spectra were collected in transmission mode at 25 K at Beamline 11-2 at the Stanford Synchrotron Radiation Laboratory that was calibrated by assigning the whiteline position of a Na_3AsO_4 standard to 11.874 keV.

3.3 Results and Discussion

3.3.1 Characterization of the soil and natural waters.

The wetland soil used in the MC was a loam with a mean particle size of 801 μm (s.d. 641.6 μm) and pH = 6.4. Prior to MC trials, the total As concentration in the soil was 23 mg kg^{-1}, twice the background level of 11 mg kg^{-1} As in Delaware soils (Table 1). This level of soil As is common in the urban soils of Wilmington, DE, USA, due to anthropogenic input of As through industrial activities. More extensive sampling of the wetland by regulatory agencies showed As concentrations in excess of 100 mg kg^{-1}, but the lower As concentrations were selected for this study as they are representative of the area. The total Fe concentration was 2.1 wt %, 15% of which were “free” Fe oxides (Table 1). Arsenic speciation in the soil collected and preserved for bulk XANES analysis was primarily As^V (data not shown). The river water had a pH of 7.2 and an EC of 0.7 mmhos cm^{-1}. Total Fe and As in the natural river water were below detection (< 0.1 mg

L^{-1}). The DOC was 4.4 mg L^{-1} and the S was 7.8 mg L^{-1}. The seawater had a pH of 7.8 and an EC of 45.6 mmhos cm^{-1}. Total Fe and As in the natural seawater were < 0.1 mg L^{-1}. The DOC was 5.5 mg L^{-1} and the S was 788.7 mg L^{-1}.

The elemental colocation μ-SRXF maps show that the As was heterogeneously distributed in the wetland soil. According to the colocation linear correlation, it is evident that while not all As in the soil is associated with Fe, a large proportion is. This suggests that the As has been sorbed by soil Fe (hydr)oxides. There is a less significant correlation between As and Mn, another important mineral element in soil.

3.3.2 Aqueous Desorption and Speciation.

The general trend across both river and seawater is that low Eh led to increased As in solution, which corroborates with earlier studies (Fig. 3).[15,18,19] The maximum concentrations of As released when inundated with river or sea water were observed with negative Eh values. The maximum desorbed As measured in river water trials was 195 μg L^{-1}, with a redox potential of -198 mV (Fig. 4). Only the two most oxic river water samples in both had arsenic in solution below the U.S. EPA drinking water standard of 10 μg L^{-1}. When the Eh was above 200 mV, total As concentrations in solution from all river water trials were below 20 μg L^{-1}, suggesting that under oxidizing conditions, innocuous or nearly innocuous levels of As are released when inundated with river water.

By comparison, when inundated with seawater, significantly more As was released across all measured redox potentials. At no point was the measured As in solution with seawater below the U.S. EPA drinking water standard. The maximum desorbed As measured in seawater trials was 492 μg L^{-1}, with a redox potential of -126 mV (Fig. 4). Arsenic in solution was the most similar between river and seawater trials when Eh levels were above 200 mV (average 10.2 and 53.6 μg L^{-1}, respectively). Although these levels were relatively close, the seawater trials averaged concentrations 5 times the drinking water standard. The most drastic differences of As concentrations in

solution were observed when the Eh was below 0 mV, with seawater and river water trials averaging 89.0 and 314.7 μg L^{-1}, respectively.

In one replicate for both the seawater and river water, the maximum As in solution was not measured at the Eh minimum, but rather the second lowest redox potential sampling point (Figure 4). This delay in total As in solution may be a result of arsenic-iron-sulfur mineral precipitation/pedogenesis under reducing conditions.[6] Arsenic speciation in solution is not reported due to analytical interferences with the LC-ICP-MS due to the high salt matrix in the seawater trials.

Reductive dissolution of Fe minerals followed a similar pattern to that of As (Figure 6). Reducing conditions led to more Fe in solution, and as the Eh increased the Fe in solution decreased in both inundation scenarios (river and sea water). A linear correlation regression of total As and total Fe in solution show stronger correlation between Fe and As seawater inundation scenarios than in river water scenarios (Figure 7). It is widely known that under reducing conditions, reductive dissolution of Fe^{3+} leads to release of Fe into solution as Fe^{2+} and this is likely the mechanism for Fe entering solution in this system. Similar to As, the maximum Fe in solution was not measured at the lowest Eh level, but usually at the next lowest Eh level. This delay of total Fe in solution gives more evidence to the hypothesis that S reduction is occurring and leading to precipitation of As-Fe-S minerals. Sea water inundation led to significantly more Fe entering into solution than river water inundation, which may be a product of ionic competition (or proton-promoted dissolution of ferric oxides due to lower pH of seawater).

Another important factor in Fe and As sorption in soil is pH. Although the pH of the seawater was initially higher than the river water, during all of the trials, the pH of the slurry for these trials was significantly lower than the river water trials (averages of 4.5 and 6.7, respectively). This pH difference likely impacted the Fe sorption behavior in these systems and can be attributed to competitive ionic exchange and hydrolysis of

desorbed trace metals such as Al^{3+}, Fe^{2+}, and Mn.[10] The behavior of these and other trace metal(loids) varied widely. A common behavior was increased desorption with sea water with relation to river water. However, for some metals, such as Pb, an inverse trend to that of As and Fe was noted and higher Eh values corresponded with increased Pb in solution (Figure 8).

3.3.3 Solid Phase Speciation

Speciation was determined by μ-XANES on inundated with river and seawater at various redox potentials (Figures 9 and 10). Arsenite and arsenate accounted for 87% of the unreacted soil A, with arsenic sulfide as the balance.

When inundated with river water, As(V) decreased by proportion over time, as Eh increased (Table 3). At the lowest measured Eh level, (-307 mV) As was comprised of As(V) and arsenic sulfide (67.4 and 32.6%, respectively). This solid phase data corroborates with the solution data that demonstrated a lag of As(III) entering solution and suggested the possible formation of As-Fe-S minerals. As the system progressed and increased Eh, arsenic sulfide levels returned to those found in the unreacted soil and remained steady. The proportion of As(III) on the solid was 0% under the most reducing conditions when the contribution of arsenic sulfide was high. After this, As(III) increased steadily on the soil for the duration of the trial as the Eh increased, eventually accounting for over 50% of the total speciation. These results suggest an unexpected pattern of As oxidation state shift on the soil surface. A more detailed analysis of the μ-XANES was necessarily to understand if these results are real or an artifact of data analysis (Fig. 10). The individual normalized μ-XANES spectra show in more detail the heterogeneity of the As speciation, with no noticeable trend across Eh. Only after averaging the spectra are the above trends discovered for the river water. The same lack of a clear trend is present for seawater. Future work should be performed with bulk XAS to better understand how the average As speciation is shifting on soil surface.

The relatively low concentrations of As in this soil inhibited bulk XAS in this study, but implementation of more sensitive detectors at beamlines could help overcome this.

Also similar to when inundated with river water, inundation of soil A with sea water showed a large proportion of the total speciation as arsenic sulfide at the most reducing conditions measured (46.4% at -118 mV). While similar in that arsenic sulfide was present, it was more pronounced with sea water and both As (V) and As(III) were present on the soil surface with sea water, whereas only As(V) complimented the arsenic sulfide in the river water systems (Table 3). Sea water trials displayed a similar trend of As(V) decrease and As(III) increase on the soil surface as Eh increased. However, the extent of these shifts from arsenic sulfide to As(V) to As(III) on the surface was more dramatic with sea water than with river water.

The energy region at higher energy to the white line can provide information as to the crystallinity of the mineral phase of As. Because these samples show no significant features in this region, it is likely that the As is associated with more amorphous phased minerals.[20]

3.4 Conclusion

The compounding issues of SLR and its impacts on the cycling of contaminants in coastal soils is of merit and calls for field- and lab-based observations to understand the risks posed to these soils and surrounding communities. Climate change induced seawater inundation, short and/or long term flooding, and salinification will alter the biogeochemistry of these sensitive sites. Newly flooded areas will see formerly oxic zones turn more reducing and thereby change the ability of the soils and sediments to sequester contaminants. Our findings show that introducing reducing conditions can lead to As release from soils through reductive dissolution of As-bearing mineral oxides in both river water and seawater inundations scenarios. Additionally, short-term inundation with seawater can lead to decreased pH and increased As release compared to river water

inundation. Accordingly, the threat of SLR stands to impact release of As from contaminated coastal wetland soils primarily by changing the pH, redox conditions and subsurface mineralogy. Future work should include abiotic controls to further understand the mechanisms of As release, a microbial inoculant from a brackish or seawater soil or sediment to determine how similar experimental conditions impact As cycling with a microbial community adept to salinity. Additionally, it is important to understand how different soils around the world will be impacted by impending SLR and thus this work should be replicated with other similarly contaminated but mineralogically and chemically distinct soils.

3.5 References Cited

(1) Church, J. a.; White, N. J.; Aarup, T.; Wilson, W. S.; Woodworth, P. L.; Domingues, C. M.; Hunter, J. R.; Lambeck, K. Understanding global sea levels: Past, present and future. *Sustain. Sci.* **2008**, *3*, 9–22.

(2) Church, J. a.; Clark, P. U.; Cazenave, a.; Gregory, J. M.; Jevrejeva, S.; Levermann, a.; Merrifield, M. a.; Milne, G. a.; Nerem, R. .; Nunn, P. D.; et al. Sea level change. *Clim. Chang. 2013 Phys. Sci. Basis. Contrib. Work. Gr. I to Fifth Assess. Rep. Intergov. Panel Clim. Chang.* **2013**, 1137–1216.

(3) Sallenger, A. H.; Doran, K. S.; Howd, P. a. Hotspot of accelerated sea-level rise on the Atlantic coast of North America. *Nat. Clim. Chang.* **2012**, *2*, 1–5.

(4) Titus, J. G. (Coordinating lead author); Anderson, K. E.; Cahoon, D. R.; Gesch, D. B.; Gill, S. K.; Gutierrez, B. T.; Thieler, E. R.; Williams, S. J. (lead authors). *Coastal Cycle Sensitivity to Sea-Level Rise : Focus on Mid-Atlantic Region*; Washington, D.C., USA, 2009.

(5) Mandal, B. K.; Suzuki, K. T. Arsenic round the world: A review. *Talanta* **2002**, *58*, 201–235.

(6) Johnston, S. G.; Keene, A. F.; Bush, R. T.; Burton, E. D.; Sullivan, L. a.; Smith, D.; McElnea, A. E.; Martens, M. a.; Wilbraham, S. Contemporary pedogenesis of severely degraded tropical acid sulfate soils after introduction of regular tidal inundation. *Geoderma* **2009**, *149*, 335–346.

(7) Johnston, S. G.; Keene, A. F.; Burton, E. D.; Bush, R. T.; Sullivan, L. a; McElnea, A.; Ahern, C. R.; Smith, C. D.; Powell, B.; Hocking, R. K. Arsenic mobilization in a seawater inundated acid sulfate soil. *Environ. Sci. Technol.* **2010**, *44*, 1968–1973.

(8) Borch, T.; Kretzschmar, R.; Kappler, A.; Cappellen, P. Van; Ginder-Vogel, M.;

Voegelin, A.; Campbell, K. Biogeochemical redox processes and their impact on contaminant dynamics. *Environ. Sci. Technol.* **2010**, *44*, 15–23.

(9) Burton, E. D.; Johnston, S. G.; Kocar, B. D. Arsenic Mobility during Flooding of Contaminated Soil: The Effect of Microbial Sulfate Reduction. *Environ. Sci. Technol.* **2014**, *48*, 13660–13667.

(10) Wong, V. N. L.; Johnston, S. G.; Burton, E. D.; Bush, R. T.; Sullivan, L. a.; Slavich, P. G. Seawater causes rapid trace metal mobilisation in coastal lowland acid sulfate soils: Implications of sea level rise for water quality. *Geoderma* **2010**, *160*, 252–263.

(11) Tan, K. H. *Soil Sampling, Preparation, and Analysis*; Second.; Taylor & Francis Group: New York, 2005.

(12) Agency, U. S. E. P. *Method 3051a: Microwave Assisted Acid Digestion of Sediments, Sludges, Soils, and Oils*; Washington, D.C., USA, 1998.

(13) Loeppart, R. H.; Inskeep, W. P. Iron. In *Methods of Soil Analysis. Part 3. Chemical Methods*; Sparks, D. L., Ed.; Soil Science Society of America: Madison, WI, 1996; pp. 384–411.

(14) Yu, K.; Rinklebe, J. Advancement in soil microcosm apparatus for biogeochemical research. *Ecol. Eng.* **2011**, *37*, 2071–2075.

(15) Frohne, T.; Rinklebe, J.; Diaz-Bone, R. A.; Du Laing, G. Controlled variation of redox conditions in a floodplain soil: Impact on metal mobilization and biomethylation of arsenic and antimony. *Geoderma* **2011**, *160*, 414–424.

(16) Frohne, T.; Diaz-Bone, R. a.; Du Laing, G.; Rinklebe, J. Impact of systematic change of redox potential on the leaching of Ba, Cr, Sr, and V from a riverine soil into water. *J. Soils Sediments* **2015**, *15*, 623–633.

(17) Sparks, D. L. *Environmental Soil Chemistry*; Second.; Academic Press: New York, 2003.

(18) Frohne, T.; Rinklebe, J.; Diaz-Bone, R. a. Contamination of Floodplain Soils along the Wupper River, Germany, with As, Co, Cu, Ni, Sb, and Zn and the Impact of Pre-definite Redox Variations on the Mobility of These Elements. *Soil Sediment Contam. An Int. J.* **2014**, *23*, 779–799.

(19) Shaheen, S. M.; Rinklebe, J.; Frohne, T.; White, J. R.; DeLaune, R. D. Redox effects on release kinetics of arsenic, cadmium, cobalt, and vanadium in Wax Lake Deltaic freshwater marsh soils. *Chemosphere* **2015**, 1–9.

(20) Landrot, G.; Tappero, R.; Webb, S. M.; Sparks, D. L. Arsenic and chromium speciation in an urban contaminated soil. *Chemosphere* **2012**, *88*, 1196–1201.

3.6 Tables and Figures

Table 3.1: Soil and water characterization

Soil Name	Depth (cm)	Texture	Mean Particle Size (um)	pH	Free Fe Oxides	As	Cr	Pb	Total Fe	Mn	S	Al
					mg kg^{-1}							
Ditch Sediment	0-20	Loam	801	6.4	3,205	23	108	2232	22,239	1,792	1,578	10,160

Water Type	pH	EC	DOC	Ca	Mg	Na	As	Cr	Pb	Total Fe	Mn	S	Al
		(mmhos/cm)	mg kg^{-1}										
River	7.2	0.7	4157	16,265	1091	7153	bd*	bd	bd	bd	bd	789	bd
Sea	7.8	45.6	5.5	24	9.4	42.4	bd	bd	bd	bd	bd	7.8	bd

*bd indicates values that were below the detection limit of 0.1 mg kg^{-1}

Table 3.2: Automated Geochemical Microcosm Data

Trial No.	Soil	Water	Eh_{min}	Eh_{max} mV	Eh_{avg}	pH_{min}	pH_{max}	pH_{avg}	$Temp_{min}$	$Temp_{max}$ °C	$Temp_{avg}$
1	A	River	-284	315	178	3.97	6.07	4.65	22.2	23.0	22.6
2	A	River	-135	330	203	1.70	6.33	5.08	15.5	22.5	22.0
3	A	River	-125	320	169	4.68	6.72	5.76	15.4	23.1	22.5
4	A	River	-417	383	178	6.13	7.14	6.53	21.4	23.1	22.6
5	A	River	-431	471	204	4.85	7.05	6.53	21.3	22.8	22.3
6	A	Sea	--*	--	--	4.32	6.41	5.01	21.6	23.8	22.0
7	A	Sea	-253	251	14	4.71	6.55	5.77	20.9	23.6	22.4
8	A	Sea	-290	263	-29	5.33	6.64	6.28	20.8	23.5	22.3

*Trial 6 incurred a data logger error such that Eh values were not recorded. At each sampling point the Eh was recorded manually and this is the Eh reported in figures for this trial in lieu of the Eh_{6hr} values.

Table 3.3: Micro-XANES Linear Combination Fitting Results.

Trial	Soil	Water	Eh_{6hr}	pH_{6hr}	R factor	As2S3	As(III)	As(V)
			(mV)			----------%----------		
--	A	Air-dried	--	--	0.009	12.9	44.5	42.5
4	A	River	-307	7.1	0.036	32.6	0.0	67.4
4	A	River	-110	6.8	0.019	3.8	36.3	59.9
4	A	River	101	6.7	0.015	12.0	37.2	50.7
4	A	River	320	6.5	0.012	13.9	42.0	44.1
4	A	River	367	6.2	0.006	8.2	50.5	41.3
6	A	Sea	-118	4.7	0.019	46.4	31.3	22.3
6	A	Sea	-12	4.4	0.024	0.0	19.8	80.2
6	A	Sea	137	4.4	0.009	26.9	21.9	51.2
6	A	Sea	230	4.5	0.012	10.9	53.6	35.5

Figure 3.1: Advanced automated biogeochemical microcosm (MC) system used in experimental set up. A 4L borosilicate glass vessel with an air-tight seal and stir paddle has Eh, pH, and temperature sensors permanently installed from the lid to take measurements every 10 minutes. Measurements are taken and Eh, pH, and T can all be regulated automatically with the corresponding control unit.

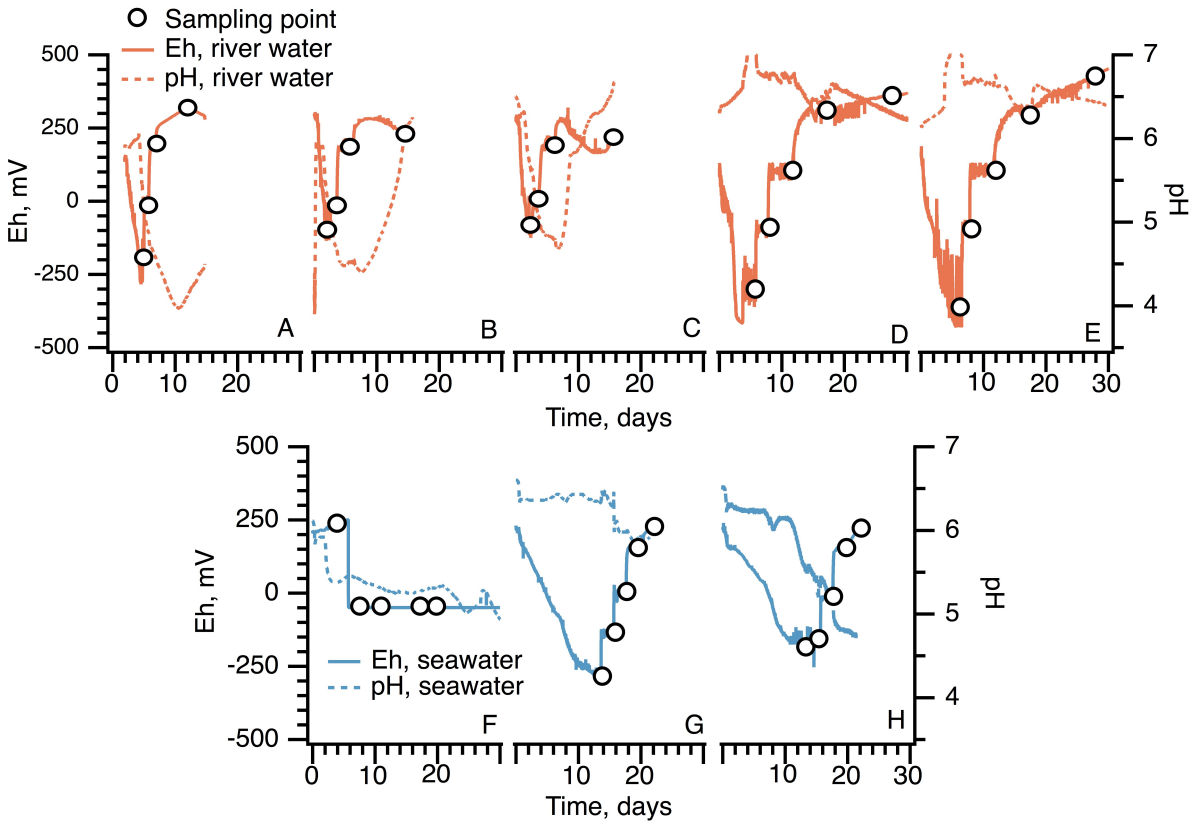

Figure 3.2: Detailed rendering of redox potential (Eh) and pH relationship for the duration of the trial, including all replicates. River water and seawater are represented by subfigures A-E and F-H, respectively.

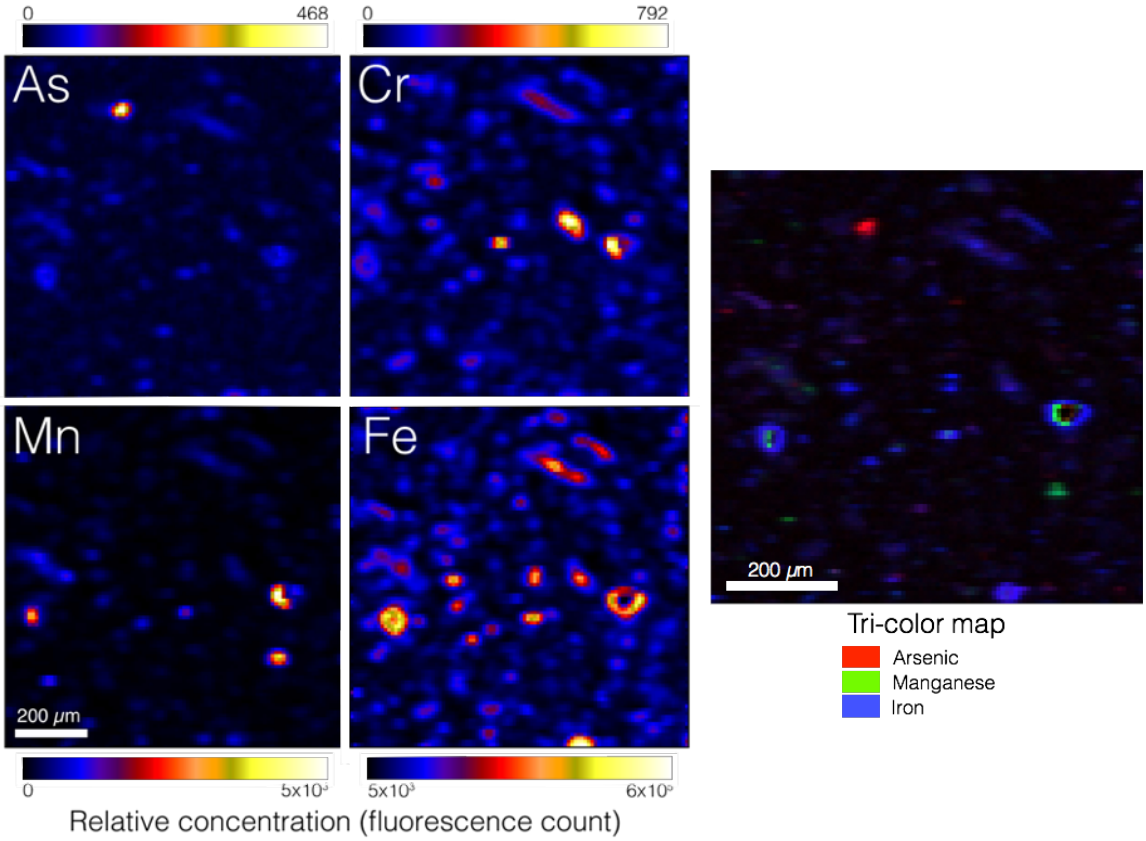

Figure 3.3: μ-SXRF Map of As-contaminated wetland soil before treatment and tri-color map showing elemental colocation of As, Cr, Fe, and Mn.

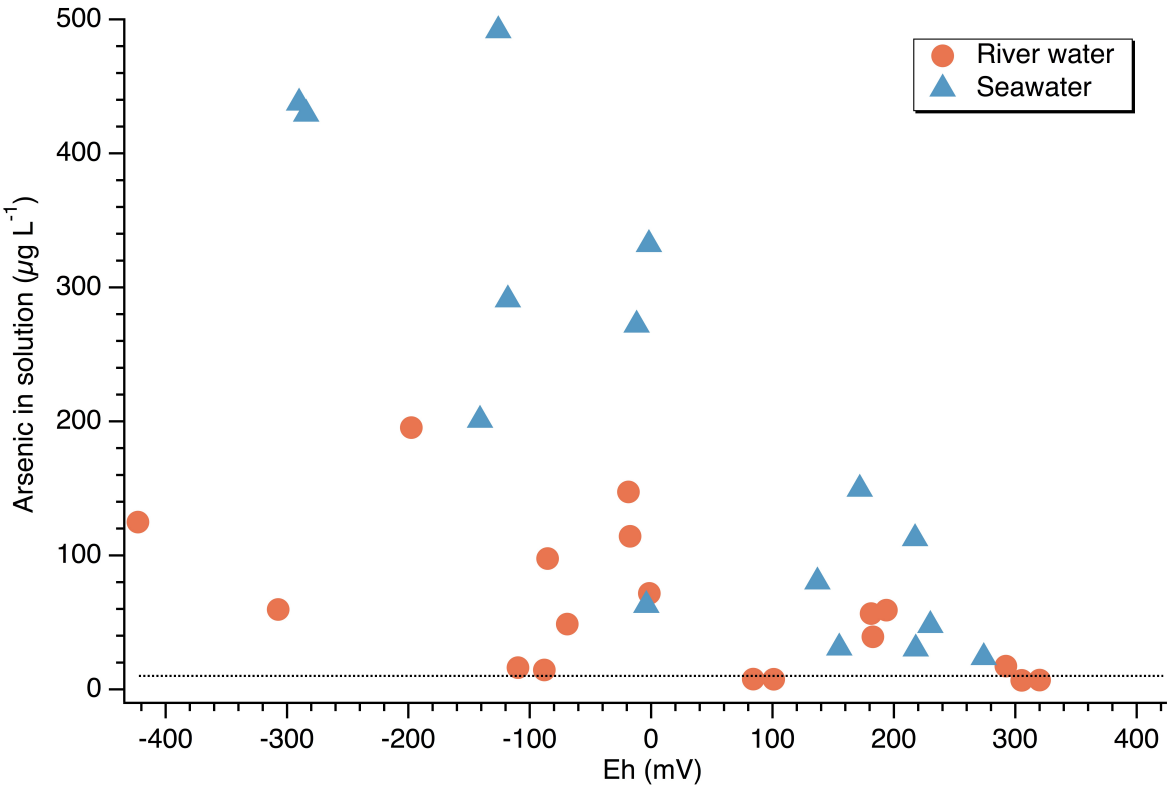

Figure 3.4: Total arsenic in solution following desorption from soil A with sea water and river water across a range of defined redox windows. Blue triangles indicate data points from seawater trials and orange circles indicate river water trials. The dotted line indicates the USEPA drinking water standard (10 μg L^{-1}).

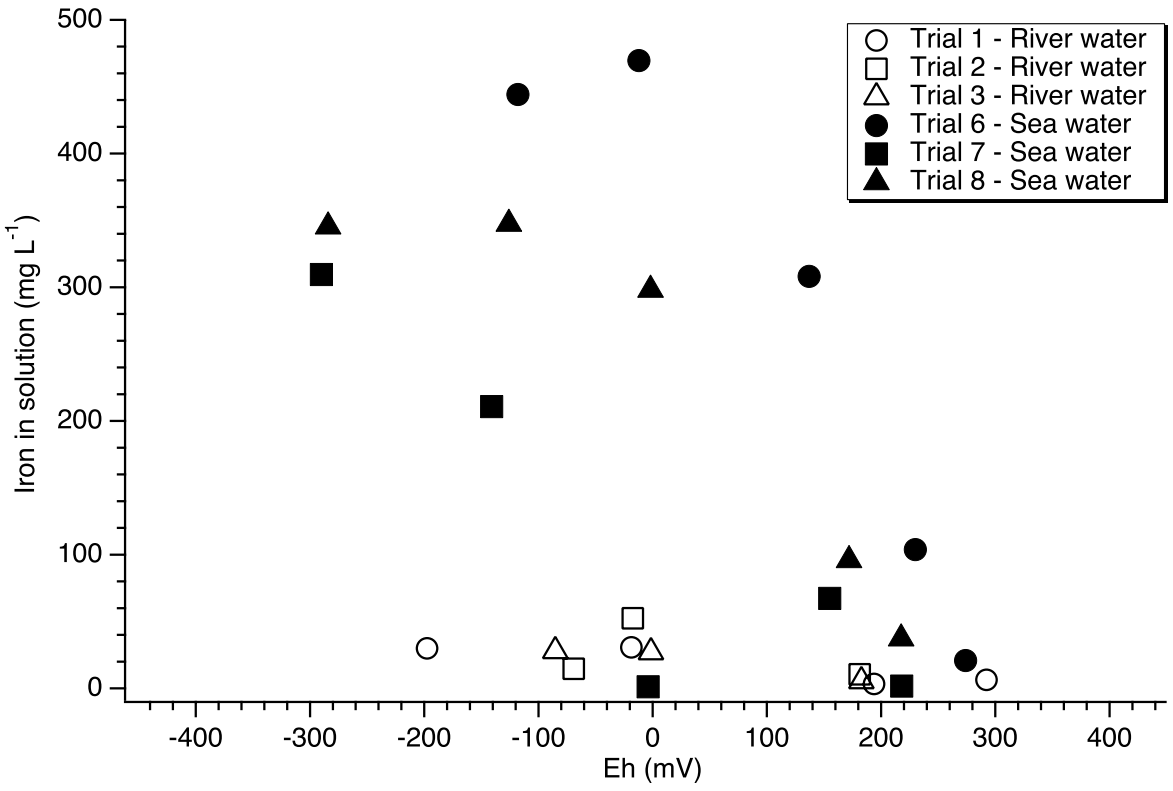

Figure 3.5: Total Fe in solution following desorption from soil A with sea water and river water across a range of defined redox windows. For both river and sea water trials Fe in solution increased as Eh decreased. The filled markers indicate sea water trials and show a marked increased in total Fe in solution in these trials compared to trials with river water.

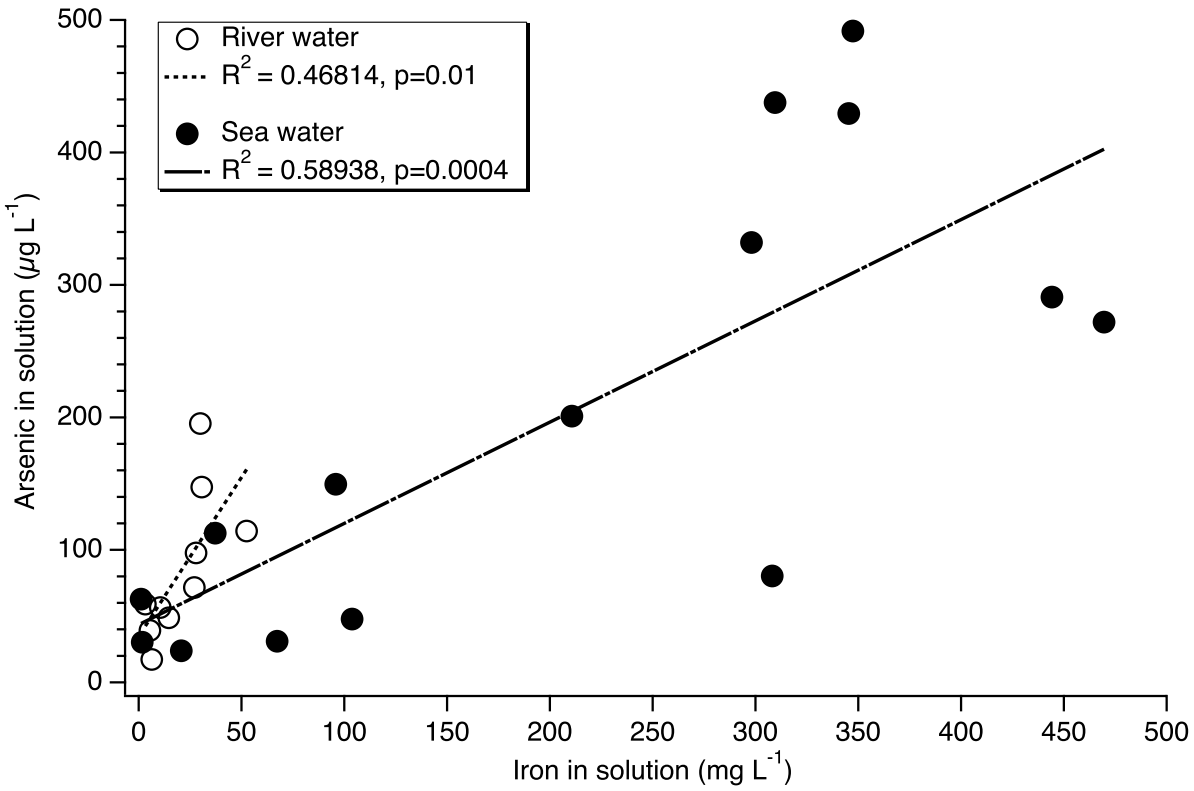

Figure 3.6: Linear regression analysis of As and Fe in solution when inundated with river water or sea water across a wide range of defined redox potentials (-400 mV to 350 mV). Arsenic and Fe in solution were well correlated for both sea water and river water trials.

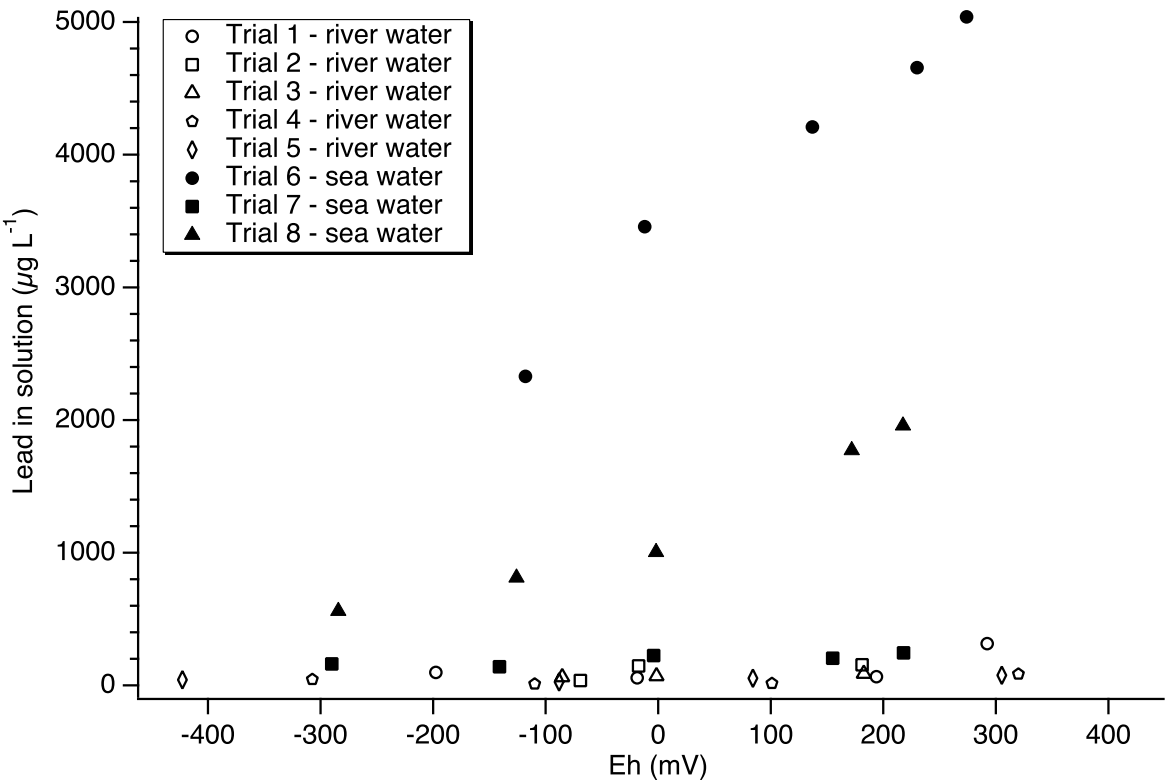

Figure 3.7: Total Pb in solution following desorption from soil A with sea water and river water across a range of defined redox windows. Increasing Eh with sea water corresponded to increasing Pb in solution.

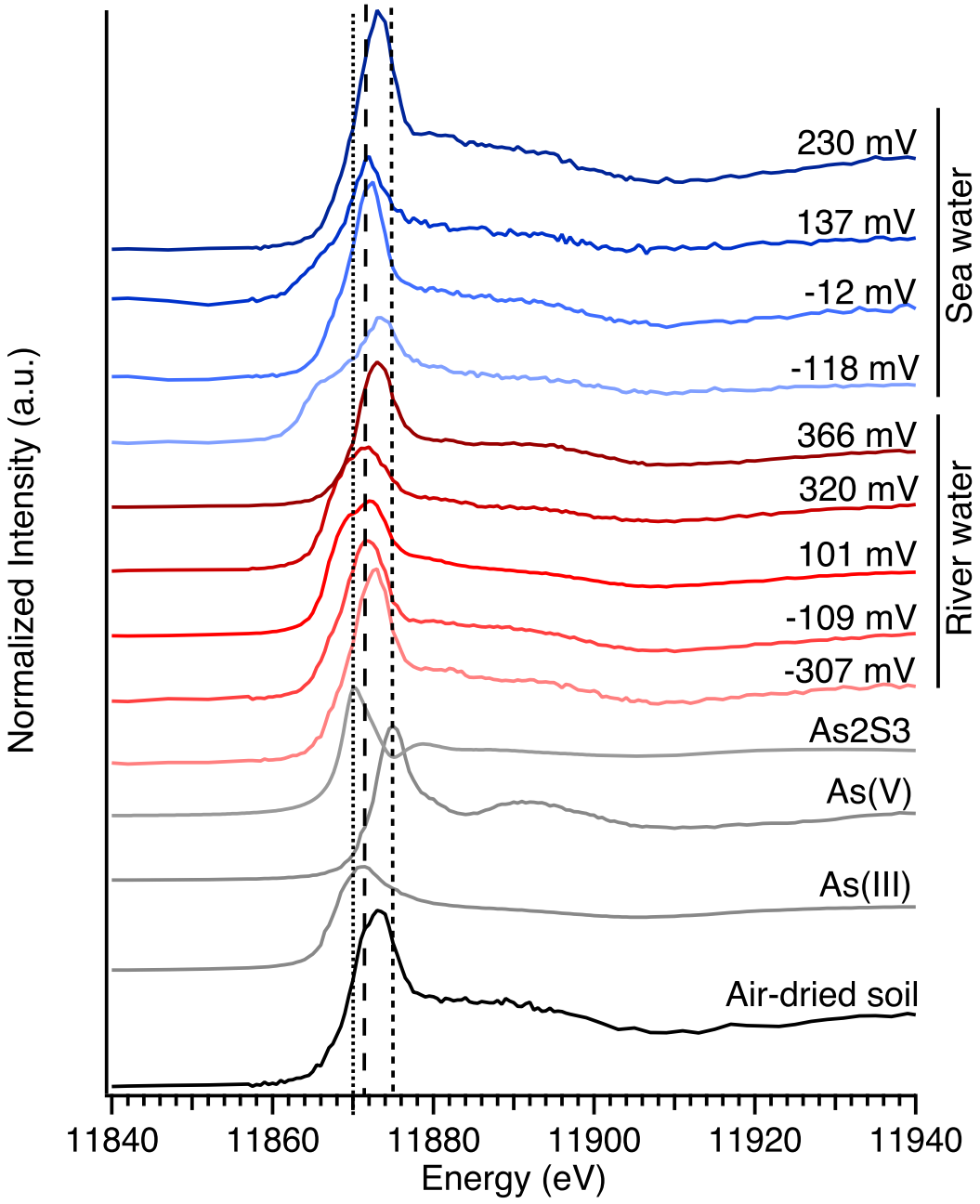

Figure 3.8: Normalized As K-edge μ-XANES of wetland soil with river and sea water inundation across controlled redox potentials. Multiple hotspots (3-10) were analyzed and averaged for each sample taken at the defined redox potentials. The dotted line indicates the orpiment (As_2S_3) white line (11870 eV), the large dashed line indicates the As(III) white line (11872 eV), and the small dashed line indicates the As(V) white line (11874 eV).

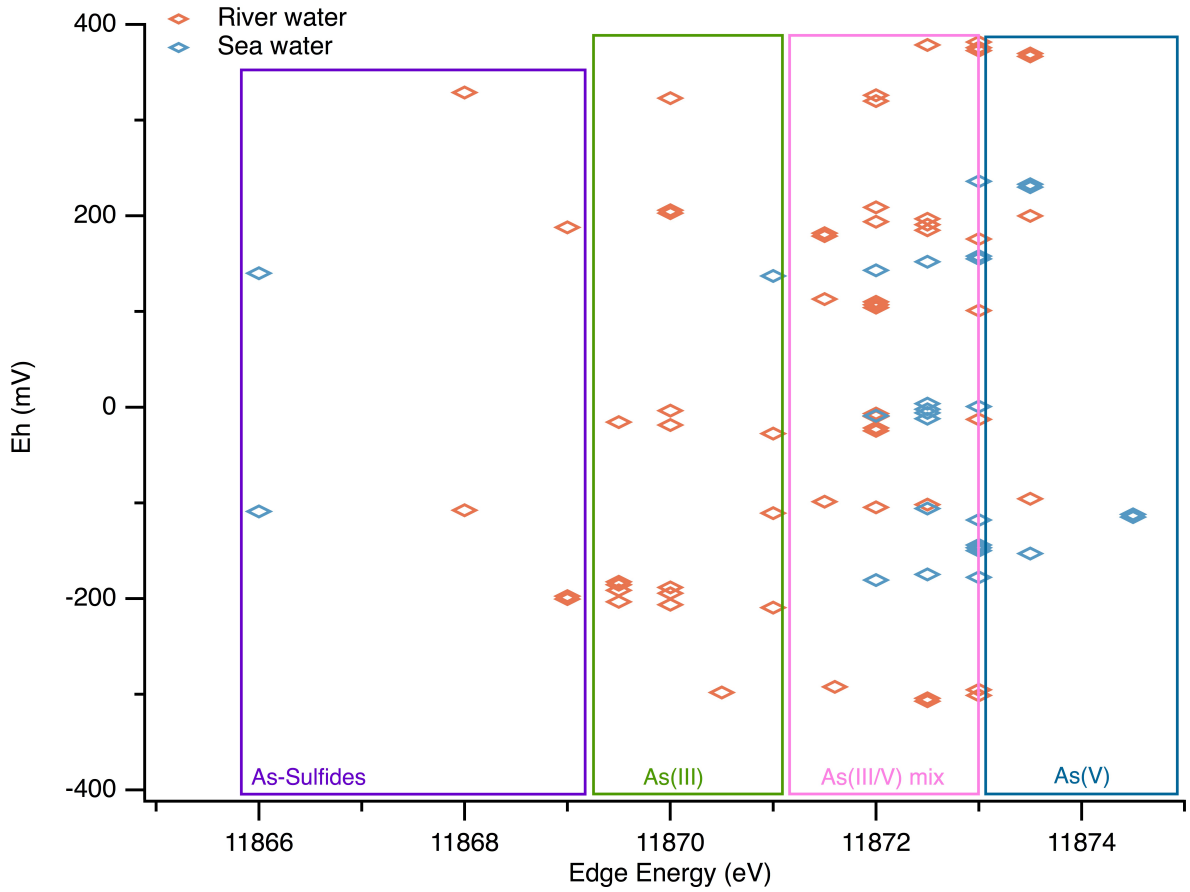

Figure 3.9: Whiteline positions of all normalized As K-edge μ-XANES of wetland soil with river and sea water inundation across controlled redox potentials.

Chapter 4

ARSENIC MOBILITY AND SPECIATION AS DETERMINED BY X-RAY ABSORPTION SPECTROSCOPY AND BULK METHODS FOR A DELAWARE HIGHWAY DRAINAGE DITCH SITE

Joshua J. LeMonte*[1], Xuan Yu[1], John Cargill[2], Holly A. Michael[1], and Donald L. Sparks[1]

[1]Delaware Environmental Institute, University of Delaware, Newark, DE
[2]Delaware Department of Natural Resources and Environmental Control, Division of Waste and Hazardous Substances, SIRS, New Castle, DE

Submitted as a report to DNREC and US EPA on 21 March, 2016

4.1 Introduction

In the U.S. there are thousands of contaminated sites that pose potential risks to the neighboring populations and environments. The largest and most hazardous sites are regulated at a federal level, with many others regulated at the state or local levels. In the state of Delaware, USA, nearly 4% of the state's total acreage is contaminated. Among this expanse of contaminated land are over 150 certified brownfields. Brownfields are sites that have been contaminated or have the stigma that they were contaminated and thereby redevelopment and reuse of that land is complicated. These sites have either been remediated or remedial actions are in the works. However, the remedial actions do not always guarantee that a given site no longer poses a threat. Indeed, if environmental conditions are altered, remediated brownfield sites may pose new threats of contamination.

One such instance recently occurred in the state of Delaware. As part of the remedial action plan for a federal Superfund site, a drainage ditch was constructed leading into a nearby river in 2003. Less than ten years after the construction of the ditch, extremely high As levels (30,000 mg kg^{-1}) were located in sediments that had accumulated along the sides of the basin. Arsenic occurs naturally in the environment in low concentrations, commonly associated with soil minerals such as Al, Mn, or Fe (hydr)oxides.[1] The background level of As in Delaware soils has been set at 11 ppm by the Delaware Department of Natural Resources and Environmental Control (DNREC). Arsenic is a carcinogenic toxin associated with skin, lung, bladder, and other internal organ cancers[2], and was a contaminant of concern for two clean-up efforts on contaminated sites adjacent to the drainage ditch. Toxicity and mobility of As in soils are primarily functions of oxidation state and sorption behavior.[1] The two major redox states of As in the environment are trivalent arsenite and pentavalent arsenate, arsenite being the more toxic and mobile form.[1,3]

Sorption (adsorption + desorption) of As strongly influences As mobility in the environment and is determined by concentration, sorption complexation, microbial activity, S chemistry, pH, reductive potential (Eh or redox), and ionic competition. [4–6] While sorption of arsenate onto soil minerals generally decreases with increasing pH, oxidation state is the primary driver of As sorption within the pH range of 5.5 – 7.5.[4] Above this range a significant reduction in arsenite and arsenate sorption occurs as the pH exceeds the pK_a of the prevalent As species onto Fe oxides (pK_a H_3AsO_4 = 6.9; pK_a $H_3AsO_3^0$ = 9.2).[4] Additionally, when the pH exceeds the soil's point of zero charge the soil and mineral constituents will then be negatively charged and repel the As oxyanions, exacerbating release.

Flooding and saturated conditions can lead to the formation of anaerobic zones through microbially mediated oxidation of dissolved organic C (DOC) and subsequent consumption of O_2. It has been shown that As concentration increases in solution of these anaerobic zones. Under these conditions, some anaerobic microbes are able to directly reduce the sorbed As^{V} to As^{III}. Otherwise, the reductive dissolution of As-bearing Fe (hydr)oxide minerals drives As desorption from the soil surface. Following the dissolution of Fe^{III} to Fe^{II}, the associated As^{V} is released and subsequently reduced to As^{III} in solution. These reductive processes utilize buried natural organic matter for fuel, and thus release of As from sediments may be linked to availability of DOC.[7,8]

Delaware's Department of Natural Resources and Environmental Control performed a thermal imaging survey of the drainage ditch to determine locations of groundwater discharge. The groundwater discharge locations correspond with the areas of high sediment As and Fe oxides. This provided insight that the As may be moving through groundwater via preferential flow from contaminated sites upgradient and entering the drainage ditch. Upgradient are two potential As source sites for this contamination. The first, a federal Superfund site, was formerly a chemical production plant that used arsenic trioxide as a raw ingredient to manufacture a corrosion inhibiting and descaling agent. Approximately 170 tons of this material were produced on site. The second potential source, a Delaware Hazardous Substance Cleanup Act (HSCA) site, was formerly an ore processing facility that performed roasting activities for several decades on As-containing ores (i.e. pyrite). The typical As content of the pyrite cinder was 0.134%, adding up to 225-352 tons of As per year that were managed at this facility. This site falls immediately adjacent to the constructed ditch and was used as cinder storage, wastewater lagoons, and a dump area. The cumulative

amounts of As handled by each site were approximately 129 tons for the Superfund site and 6,903 tons for the HSCA site. However, it should be noted that the As handled at the Superfund site was in a mobile form (As_2O_3), while the HSCA site handled primarily less mobile mineral forms of As (As-bearing pyrite).

The drainage ditch where the elevated levels of As exist is located along the south bank of a tidal river. The added influence of tides makes this site susceptible to shifting hydrologic and redox regimes on daily, monthly, and seasonal scales. Dynamic redox scenarios affect As redox state and subsequent mobility and toxicity in groundwater.

Our research team has joined forces with DNREC in an effort to understand the driving forces behind the As accumulation in the ditch. We were tasked with the following questions: 1) Can the As at each potential source site be differentiated from the other site, 2) Can we determine which source the As in the ditch originated from, and 3) What is the role of C input in the As mobilization and concentration at the ditch? This reports seeks to answer the above questions by combining field monitoring, laboratory experiments, hydrologic modeling, and advanced analytical techniques.

4.2 MATERIALS AND METHODS

4.2.1 Site Selection

This site, a Delaware highway drainage ditch, feeds directly into the tidally impacted river. The ditch is approximately 150 m x 10 m, with its base just over 1 m below sea level, and its bank reaching 5 m above sea level (Fig. 1 and 2). Extremely

high levels of As at this site have been reported previously with levels up to 30,000 mg kg^{-1} in the sediments and 5,000 ug L^{-1} in the groundwater. However, the highest levels found in this investigation were 13,296 mg kg^{-1} in the sediment and 8,994 ug L^{-1} in the groundwater (Table 1). The Superfund site and the HSCA site were both identified by the state as potential sources of As for the drainage ditch and are located upgradient to the southwest and south of the ditch, respectively.

4.2.2 Soil Sampling and Analysis

For the purpose of geochemical characterization, soil cores from each site were obtained using a Geoprobe direct push drill. A single location was used at each site to collect the cores. Cores were taken and logged from the surface to 3.7 m below the surface. Once recovered, cores were immediately capped and wrapped in polyethlyene film to inhibit oxidation of the core, and stored in a dark, cool location for transport to the lab. Samples were stored in the dark at 4°C for 24 h or less before being subsampled for analysis. Subsamples were taken from each core based on visually observed changes in the soil profile (approximately every 15-30 cm). Subsamples were air-dried, lightly ground to pass through a 2 mm sieve, and stored in the dark at 4°C until analyses were conducted. Soil pH, organic matter, exchangeable cations, and total C and N were performed using standard methods. Total metal content of the homogenized soil samples was determined by microwave-acid digestion (US EPA 1995 Method 3051), followed by analysis via inductively coupled plasma atomic emission spectrometry (ICP-AES). Total ("free") iron oxide content was determined using the citrate-bicarbonate-dithionite method.[9]

Additionally, separate cores from each site were subsampled in 120 cm increments for synchrotron-based analysis. These cores were subsampled with N_2 passing over the core into vials that were then flushed with N_2 and immediately placed into an anaerobic glove bag to preserve the oxidation state. Once in the glove bag, samples were air dried under anaerobic (95% N_2/5% H_2) atmosphere and homogenized to a fine powder, and stored in the inert atmosphere until synchrotron analyses.

X-ray absorption near-edge spectroscopy (XANES) is a synchrotron based technique that utilizes unique spectra from known standards to serve as a geochemically distinct fingerprint or signature. As and Fe K-edge XANES were collected at both the Brazilian Synchrotron Light Laboratory (LNLS) and the Canadian Light Source (CLS). At LNLS, samples were analyzed on the XAFS2 beamline in transmission mode at ambient conditions. The XAFS2 is a bulk-XAFS beamline (spot size 450 x 250 μm^2) and delivers a photon flux of 1 x 10^{10} photons sec^{-1} at 100 mA, equipped with a monochromator consisting of a double crystal Si (111). The electron storage ring was operated at 1.37 GeV with a current range of about 110 – 260 mA. Energy calibration was performed on the XAFS2 beamline by assigning the intersect point of the second derivative to 11868.0 eV to a NaH_2AsO_4 standard. Samples were analyzed on the Hard X-ray Micro-Analysis (HXMA) beamline of CLS in fluorescence mode with a 32-element solid-state Ge detector at ambient conditions. The HXMA is also a bulk-XAFS beamline (spot size 0.8 mm x 1.5 mm^2) and delivers a photon flux of 1 x 10^{12} photons sec^{-1} at 100 mA, equipped with a liquid nitrogen cooled double crystal Si (111). Energy calibration was performed on the HXMA beamline by using an in-line Au foil set to 11919.0 eV. Samples were sealed between

two layers of Kapton tape on the sample holder and scanned from 11667—12511 eV. The step size was decreased to 0.3 eV and dwell time increased to 3 s over the XANES region (11850 to 11900 eV) for increased spectral resolution. XANES spectra were background subtracted, normalized, and averaged using the program Athena.[10] Least squares linear combination fitting of XANES spectra was optimized at ± 20 eV from E0, using six standards including sodium arsenite, sodium arsenate, orpiment, realgar, arsenopyrite, and arsenic trioxide. No more than three standards were allowed when fitting the data to avoid over-fitting and the creation of artifacts.

4.2.3 Field Monitoring

Pressure transducers were installed in five shallow wells (12 ft depth) alongside the ditch to monitor groundwater level and tidal influence (Fig. 4). Transducers were also installed in the drainage ditch and a nearby collecting pond to monitor hydraulic head and temperature fluctuations, with data recorded in 10 min intervals.

To monitor reductive potential flux at the site, multilevel in situ redox sensors (Paleo Terra, Amsterdam, Netherlands) were installed immediately adjacent to well #3 and parallel to where a groundwater seep was identified in the ditch. The sensors contained redox sensing platinum electrodes at 15 cm intervals from the surface to 3.6 m. The sensors were constructed of fiberglass epoxy tubing with an external diameter of 20 mm and installed vertically within 2 m of the well. Data was logged every 15 min using a Campbell data logger CR1000.

Pore water samplers were installed within 2 m of the redox sensors at depths of 175, 259, and 307 cm to monitor geochemical changes in pore water. Pore water samples were collected monthly at high and low tide during spring and neap tides.

Upon collection, pore water samples were immediately analyzed in the field for pH, dissolved oxygen, Eh, salinity, and temperature via a YSI Professional Plus handheld multiparameter meter (Yellow Springs, Ohio, USA). Following these analyses, samples were immediately filtered using a 0.2 um nylon filter. Once filtered, samples were analyzed for ferrous iron (Fe^{2+}) via the phenanthroline method using field colorimetric analysis (CHEMetrics V-2000, Washington, D.C., USA). A subsample aliquot was acidified to 2% trace metal grade HNO_3 and stored at 4°C for total metal analysis via ICP-MS. A second filtered aliquot for dissolved organic carbon (DOC) analyses was stored under cool, dark conditions for transport back to the lab where it was stored frozen (-20°C) until analysis via high temperature catalytic oxidation (Vario TOC Cube, Elementar Americas, Mt. Laurel, NJ, USA). In addition to pore water samples, surface water from the ditch was collected as a grab sample at high and low tides during spring and neap tides. These samples were analyzed and subsampled in the same manner as the pore water samples.

4.3 RESULTS AND DISCUSSION

4.3.1 Bulk Soil Characterization

The sediment found in the drainage ditch contained authigenic As reaching 13,296 mg kg^{-1}. Bulk soil characteristics show large differences in total metal composition between the Superfund and HSCA sites and throughout each soil profile (Fig. 5). Drastic increases in total soil As are observed below the water table (1.75 m) at both sites. Both sites have been remediated, with approximately the top meter of soil being fresh fill introduced as a replacement for the more contaminated pre-remediation soil. Therefore, it is expected that this area of fill will have significantly

less total As than soil lower in the profile that was not remediated. Although these elevated As levels are far below the surface (2 m for the Superfund site and 2.6 m for the HSCA site), the concentrations are extremely high (the Superfund site over 2000 mg kg^{-1} and the HSCA site over 1000 mg kg^{-1}), and in the saturated zone. Therefore, they should not be deemed innocuous. Concentrations of Fe and S remain relatively constant for the Superfund site throughout the soil profile. The HSCA site has an elevated S zone from 1.3 m to 2.2 m below the surface, and an elevated Fe zone below 1.5 m. Maximum measured S occurs at 1.5 m and maximum measured Fe occurs at 2.5 m below the surface at the HSCA site (Fig. 5). When looking at all three sites composited into 1.2 m increments, there is a common zone of increased As concentration from 1.2 – 2.4 m below the surface (Fig. 6).

Sorption of As is affected by pH, and the pH between the ditch and both potential sources varies greatly. The pH at the HSCA site follows a general decreasing trend as depth increases, with a maximum value of 7.9 at 0.5 m below the surface, and minimum of 3.7 at 3.1 m below the surface (Fig. 7). These low pH values occur at the same depth of the increased soil As, which is in agreement with what others have found previously to show that As sorbs more readily and stronger at lower pH levels.[4] In contrast, the Superfund site had pH levels up to 9.9, which is rarely seen in soils and can be attributed to the legacy of contamination at this site. The pH did decrease through the soil profile, but only at 1.5 m below the surface and the minimum value was a circumneutral 6.7 at 1.9 m below the surface. The zone in which the pH was at or above 9.0 is above the point of zero charge for many soil minerals and therefore the soil has a net negative charge and thus contributes to low

levels of sorption and subsequent high levels of anionic As release from the Superfund site.[11]

4.3.2 Solid-phase arsenic speciation via XANES

To gain a greater understanding of the chemical form and oxidation state of the As in the ditch sediments and the potential source sites, XANES analyses were performed. A qualitative visual inspection of the spectra indicates distinct differences between the ditch sediment and soils at both sites (Fig. 8). The white lines of the collected standard spectra were located at 11875 eV for As^{V}, 11871 eV for As^{III}, and 11868 eV for As-S. The white line position of the ditch sediment resembles that of the As^{III} white line, while the white line positions of the ditch bank and potential source sites correspond to that of the more stable As^{V}, with a shoulder present on the spectra of lower depth samples, indicative of mixed oxidation state for these samples.

Least squares linear combination fitting of the bulk XANES spectra provides a more quantitative interpretation of the data. The data show that the As in the ditch sediment is nearly completely As^{III} (90%), with the balance comprised of As^{v}. (Table 2). At the ditch bank As was roughly 90% As^{V} at depths above 2.4 m. Below this depth, a considerable shift occurred, with As^{III} increasing to 18%, and the appearance of As-S species (realgar, α-As_4S_4, was used in the linear combination fit) making up 16%. The As oxidation state at the HSCA property was also primarily As^{V} above the depth of 2.4 m (80-90%, with the balance as As^{III}). Below 2.4 m the oxidation state shifted toward the more reduced As^{III} and it comprised 27%, while the majority of the As was still in the As^{V} oxidation state. Sampling at the Superfund site prohibited retrieval of samples below 2.4 m because the samples were saturated as this was below the water table. The Superfund site showed similar As speciation to both the ditch

bank and the HSCA site above 1.2 m. Below this point, however, there was considerably more As^{III} (40%) than any of the other samples, aside from the ditch sediment. In addition to the elevated As^{III} below 1.2 m at the Superfund site, there was also increased As-S formation (15%) that occurred at the lower depth. The balance of the As speciation below 1.2 m at the Superfund site was As^{V} (45%). Because the water table is located below 2.4 m, it is assumed that reducing conditions would also exist below this depth at the Superfund site and produce an environment conductive to As-reducing processes.

The As speciation above 1.2 m depth for the ditch bank, and at both sites was consistent and this is to be expected as above this depth each site has been remediated. Continuing down the soil profile is where differences between the sites occur. The ditch bank and HSCA site maintained similar As speciation from the surface to 2.4 m below the surface. These two sites only displayed evidence of As reduction below 2.4 m. The Superfund site, however, showed a significant shift to more reduced As speciation below 1.2 m, and the reduction occurred to a greater extent at this location and depth than at either of the other sites.

Soil minerals have the ability to attenuate As, but As^{III} is generally more mobile, and therefore toxic, than As^{V} in soil environments because of increased mineral sorption capacity for As^{V} compared to As^{III}. Arsenic can be reduced directly through enzymatic processes or indirectly through reductive dissolution of Fe and/or Mn oxides. Reduction of As^{V} on the solid surface, as is the case in the lower depths, especially at the Superfund site, can correspond to increased release of As into solution, which in this case is the surrounding groundwater.[12] It is therefore reasonable

to assume that the zones with increased levels of As^{III} on the surface are more susceptible to As release than zones comprised almost completely of As^{V}.

The As speciation at the HSCA site is primarily As^{V}, ranging from 73-90%. This stable form of As, paired with low levels of the more mobile As^{III} suggest that the As from this site is not substantially migrating to the drainage ditch. The XANES data show considerable contribution (40%) of As^{III} at the Superfund site. As mentioned previously, it is well documented that As^{III} is more mobile and toxic than its counterpart As^{V} in the environment.[1,4,13,3] The As found at the Superfund site is considerably more mobile, based on this solid phase spectroscopic evidence, than either the HSCA site or on the ditch bank.

It has also been shown that under prolonged reducing conditions with sufficient S concentrations, As can be removed from solution via incorporation into authigenic sulfide minerals, such as orpiment or realgar.[14,15] Arsenic-sulfide species formed at both the ditch bank (2.4 – 3.6 m depth) and the Superfund site (1.2 – 2.4 m depth; Table 2). These species are relatively more stable than As^{III}, but a shift in redox conditions from reducing to oxidizing may lead to oxidative dissolution of the authigenic arsenic sulfides.

4.3.3 Water table and redox potential

The ditch surface water elevation is strongly influenced by tides, ranging from 0 cm at low tide to more than 1.2 m at high tide. The water table level measured in the groundwater wells fluctuates from 1.75 to 2.7 m below the soil surface, is dependent on the tides, and is seasonally impacted (Fig. 9).

Redox potential as measured by the multilevel in situ redox sensors demonstrated a wide range of Eh values present at the ditch bank, from -450 mV to

600 mV (Fig. 10). The unsaturated zone nearest the surface is oxidizing down to 50 cm below the surface. From 50-115 cm below the surface there is a reducing zone. This zonation may be a result of installation of a clay liner during remediation of the site or construction of the drainage ditch. Below this distinct zone of low Eh values, the Eh drastically increases to oxidizing once again. The capillary fringe zone is indicated by Eh values that shift between reducing and oxidizing or vice versa and is 150 – 250 cm below the surface (Fig. 6). Both above and below this zone the amount of change in measured redox potential for each depth is limited, with the smallest variance occurring immediately below the surface (0 – 45 cm) and at the lowest depth (360 cm). The soil redox potential from 2 to 3.5m has decreased by 40 mV (from -130 mV to -170 mV), on average, since installation of the sensors. Tidal influence on redox potential is the greatest at depths within +/- 1.0 m of the water table (Fig. 7). It is of note that these are also the same depths where the highest amount of As was identified in the soil. Reducing conditions lead to reduction of As-bearing Fe minerals and their subsequent mobilization, or direct reduction of As(V) to As(III).[16,17] The dynamic redox potential is likely influencing As behavior and merits further research to determine how a fluctuating redox potential influences As in soils.

4.3.4 Pore water chemistry

The pore water chemistry indicates that the reducing conditions are leading to the reductive dissolution of Fe oxides and the subsequent reduction of As, as there is a strong correlation between As and Fe in solution across all sampling locations and dates (Fig. 12). The porewater concentration of As increased by depth, with the samples obtained from 3.07 m always having the highest amount of As in solution (Fig. 13). This is expected as the Eh decreases with increased depth. More As was in

the groundwater during summer months than winter months, but sampling must be continued to determine if this is an anomaly or pattern.

Monthly samples were collected to determine if there is a seasonal shift in groundwater chemistry. Results are still preliminary in this vein as a larger data set is needed to draw any conclusions. Observations to this point indicate that dissolved oxygen content decreases with depth in the soil profile and at low tide. During neap tides, Eh is oxidizing at 1.75 m below the surface and shifts to reducing at lower depths. During spring tides Eh is below zero for all measured depths, including the surface water. Depth does not significantly impact pore water pH.

All trace metals measured (As, Cr, Ni, Zn, Mn, Fe) in pore water samples increased with depth and had their highest concentrations at 3.07 m depth (Fig. 8). This can likely be attributed to the fact that this site was remediated at more shallow depths and historic contamination is still present at lower depths. The surface water trace metal content varied significantly with the tides. Low tides generally resulted in the highest amount of all trace metals. During low tides the surface water is much less diluted by the influx of river water and thus more powerfully impacted by the metal content of sediments in the ditch and groundwater seeping into the ditch.

The dissolved organic carbon in pore water samples collected at the ditch bank were similar at both 1.75 and 2.59 m depths. A two- to three-fold increase was found between DOC concentrations at the 3.07 m depth and the more shallow depths, with concentrations reaching more than 15 mg L^{-1} (Fig. 14). The high concentrations of DOC correspond to the depth where the highest As was found in the pore water, and where reducing conditions exist. This is suggestive that there is a large pool of DOC available for microbially driven redox processes which drive As release. More

research must be conducted to determine critical points of DOC for As reduction and release at the ditch site.

4.4 CONCLUSION

This Delaware highway drainage ditch site is a geochemically interesting and complex site with many variables influencing the contaminant behavior. This report utilizes spectroscopic "finger printing" techniques to show that the As oxidation states at both sites were distinctively different at depths below 1.2 m. The findings herein present evidence suggestive of a relatively mobile form of As (As^{III}) in conditions that promote desorption (high pH) at the Superfund site. Although the specific form of As likely changes as it undergoes sorption and/or redox shifts, the data suggest that the As found at the HSCA site is more stable and less likely to undergo changes to allow hydrologic transport to the drainage ditch. The As in the drainage ditch is accumulating as the relatively unstable As^{III} on the sediment surface. The arsenic release from the surrounding sites to the drainage ditch is a microbially mediated process and therefore is dependent on available C to fuel the redox processes. Early data suggest that ample DOC has been supplied to the aquifer for dissimilatory reductive dissolution of Fe/Mn oxides and subsequent release of As to occur, but more research must be done to fully understand how the availability of C has and/or will influence the release of As at the ditch and the extent to which the mineral oxides are undergoing reductive dissolution.

4.5 REFERENCES CITED

(1) Smith, E.; Naidu, R.; Alston, A. M. Arsenic in the soil environment: A review. *Adv. Agron.* **1998**, *64*, 149–195.
(2) Mandal, B. K.; Suzuki, K. T. Arsenic round the world: A review. *Talanta* **2002**,

58, 201–235.
(3) Smedley, P. L.; Kinniburgh, D. G. A review of the source, behaviour and distribution of arsenic in natural waters. *Appl. Geochemistry* **2002**, *17*, 517–568.
(4) Raven, K. P.; Jain, A.; Loeppert, R. H. Arsenite and arsenate adsorption on ferrihydrite: Kinetics, equilibrium, and adsorption envelopes. *Environ. Sci. Technol.* **1998**, *32*, 344–349.
(5) Manning, B. a.; Fendorf, S. E.; Goldberg, S. Surface structures and stability of arsenic(III) on goethite: Spectroscopic evidence for inner-sphere complexes. *Environ. Sci. Technol.* **1998**, *32*, 2383–2388.
(6) Fendorf, S.; Eick, M. J.; Grossl, P.; Sparks, D. L. Arsenate and Chromate Retention Mechanisms on Goethite. 1. Surface Structure. *Environ. Sci. Technol.* **1997**, *31*, 315–320.
(7) Stuckey, J. W.; Schaefer, M. V.; Kocar, B. D.; Dittmar, J.; Pacheco, J. L.; Benner, S. G.; Fendorf, S. Peat formation concentrates arsenic within sediment deposits of the Mekong Delta. *Geochim. Cosmochim. Acta* **2015**, *149*, 190–205.
(8) McArthur, J. M.; Ravenscroft, P.; Banerjee, D. M.; Milsom, J.; Hudson-Edwards, K. A.; Sengupta, S.; Bristow, C.; Sarkar, A.; Tonkin, S.; Purohit, R. How paleosols influence groundwater flow and arsenic pollution: A model from the Bengal Basin and its worldwide implication. *Water Resour. Res.* **2008**, *44*, 1–30.
(9) Loeppart, R. H.; Inskeep, W. P. Iron. In *Methods of Soil Analysis. Part 3. Chemical Methods*; Sparks, D. L., Ed.; Soil Science Society of America: Madison, WI, 1996; pp. 384–411.
(10) Ravel, B. A THENA U ser ' s G uide. **2009**.
(11) Sparks, D. L. *Environmental Soil Chemistry*; Second.; Academic Press: New York, 2003.
(12) Burton, E. D.; Johnston, S. G.; Kraal, P.; Bush, R. T.; Claff, S. Sulfate availability drives divergent evolution of arsenic speciation during microbially mediated reductive transformation of schwertmannite. *Environ. Sci. Technol.* **2013**, *47*, 2221–2229.
(13) Manning, B. a; Fendorf, S. E.; Bostick, B.; Suarez, D. L. Arsenic(III) oxidation and arsenic(V) adsorption reactions on synthetic birnessite. *Environ. Sci. Technol.* **2002**, *36*, 976–981.
(14) O'Day, P. a; Vlassopoulos, D.; Root, R.; Rivera, N. The influence of sulfur and iron on dissolved arsenic concentrations in the shallow subsurface under changing redox conditions. *Proc. Natl. Acad. Sci. U. S. A.* **2004**, *101*, 13703–13708.
(15) Burton, E. D.; Johnston, S. G.; Kocar, B. D. Arsenic Mobility during Flooding of Contaminated Soil: The Effect of Microbial Sulfate Reduction. *Environ. Sci. Technol.* **2014**, *48*, 13660–13667.
(16) Johnston, S. G.; Keene, A. F.; Burton, E. D.; Bush, R. T.; Sullivan, L. a; McElnea, A.; Ahern, C. R.; Smith, C. D.; Powell, B.; Hocking, R. K. Arsenic mobilization in a seawater inundated acid sulfate soil. *Environ. Sci. Technol.*

2010, *44*, 1968–1973.
(17) Borch, T.; Kretzschmar, R.; Kappler, A.; Cappellen, P. Van; Ginder-Vogel, M.; Voegelin, A.; Campbell, K. Biogeochemical redox processes and their impact on contaminant dynamics. *Environ. Sci. Technol.* **2010**, *44*, 15–23.

4.6 TABLES AND FIGURES

Table 4.1: Soil and water characteristics.

Soil Name	Depth (cm)	pH	N, %	C, %	OM, %	Free Fe Oxides, %	As	Cr	Pb	Total Fe	Mn	S	Al
							mg kg^{-1}						
Ditch Sediment	0-20	5.9	737	7.1	8.8	16.5	13,296	62	360	97,057	558	4157	13,296
Ditch Bank	0-120	8.0	0.07	2.8	2.0	--	89	33	525	19301	217	649	10602
Ditch Bank	120-240	7.7	0.12	7.1	0.9	--	2573	30	11250	53070	197	3049	3656
Ditch Bank	240-360	7.2	0.04	4.5	1.9	--	1261	17	13210	49040	67	4121	2407
Superfund *	0-120	9.5	0.04	2.8	2.7	0.3	444	119	1210	35050	577	2978	13013
Superfund	120-240	9.9	0.07	2.9	1.8	0.5	894	53	384	23700	310	11300	12676
HSCA site	0-120	8.6	0.05	3.0	1.8	0.4	17	35	133	18413	425	1597	13771
HSCA site	120-240	7.6	0.08	5.2	4.3	1.4	412	164	4311	159800	550	7774	4622
HSCA site	240-360	7.5	0.09	6.0	1.0	3.2	185	13	1770	105600	143	8150	2709

*Superfund 240-360 not included as no retrieval was able to be made during sampling due to saturated nature of sample.

Table 4.2: Least squares linear combination fitting of bulk XANES data.

Sample	Depth (m)	Arsenic-Sulfide*	Arsenite	Arsenate	R-factor	Reduced chi-square
		%				
Ditch sediment	0 – 0.2	0	90	10	.007	.005
Ditch bank	0 – 1.2	0	11	89	.010	.007
Ditch bank	1.2 – 2.4	0	12	88	.010	.007
Ditch bank	2.4 – 3.6	16	18	66	.026	.012
HSCA site	0 – 1.2	0	17	83	.026	.019
HSCA site	1.2 – 2.4	0	10	90	.014	.010
HSCA site	2.4 – 3.6	0	27	73	.013	.009
Superfund	0 – 1.2	0	18	82	.011	.008
Superfund	1.2 – 2.4	15	40	45	.004	.002

*Arsenic sulfide standard used was realgar as these provided the best fits.

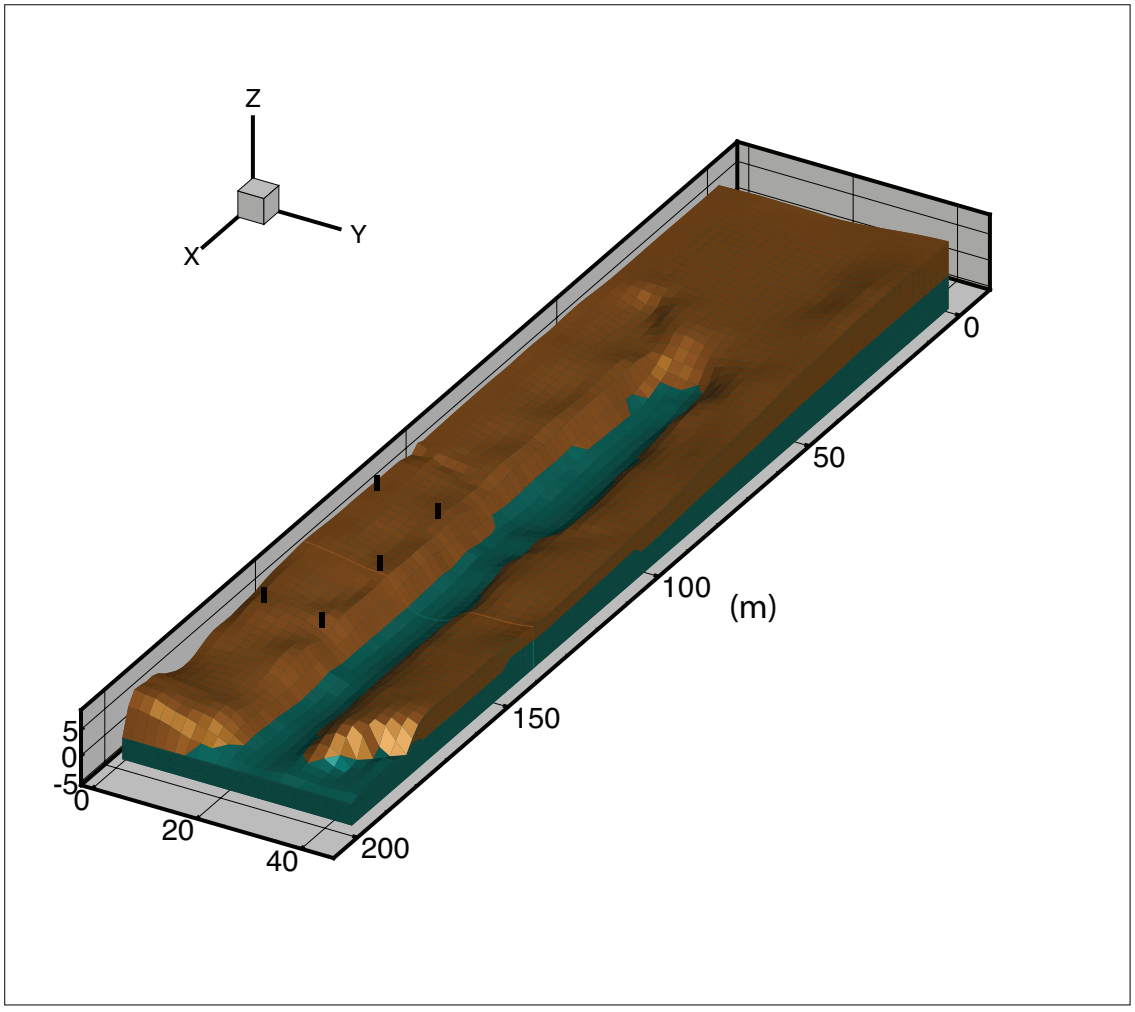

Figure 4.1: 3D view of the site topography. Black rectangles represent the groundwater wells (MW-1 to MW-5). Blue represents the saturated soil, while brown represents the unsaturated soil.

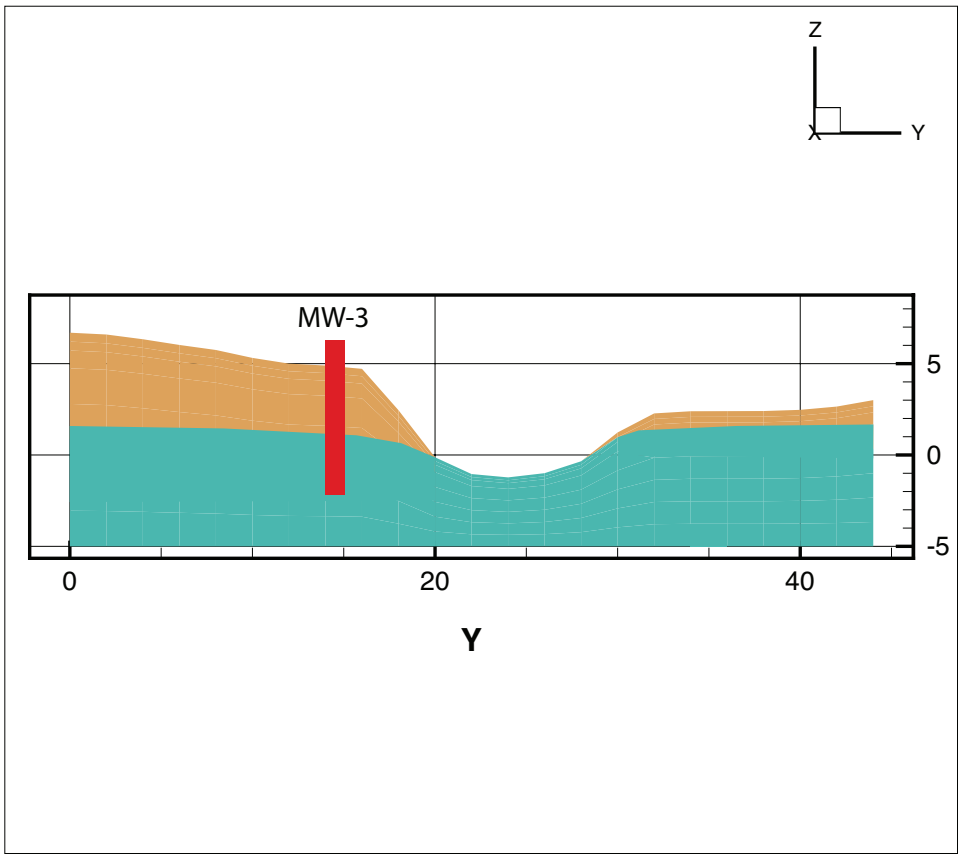

Figure 4.2: Transect of the ditch. Blue represents the saturated soil, while brown represents the unsaturated soil. The red rectangle represents a groundwater well.

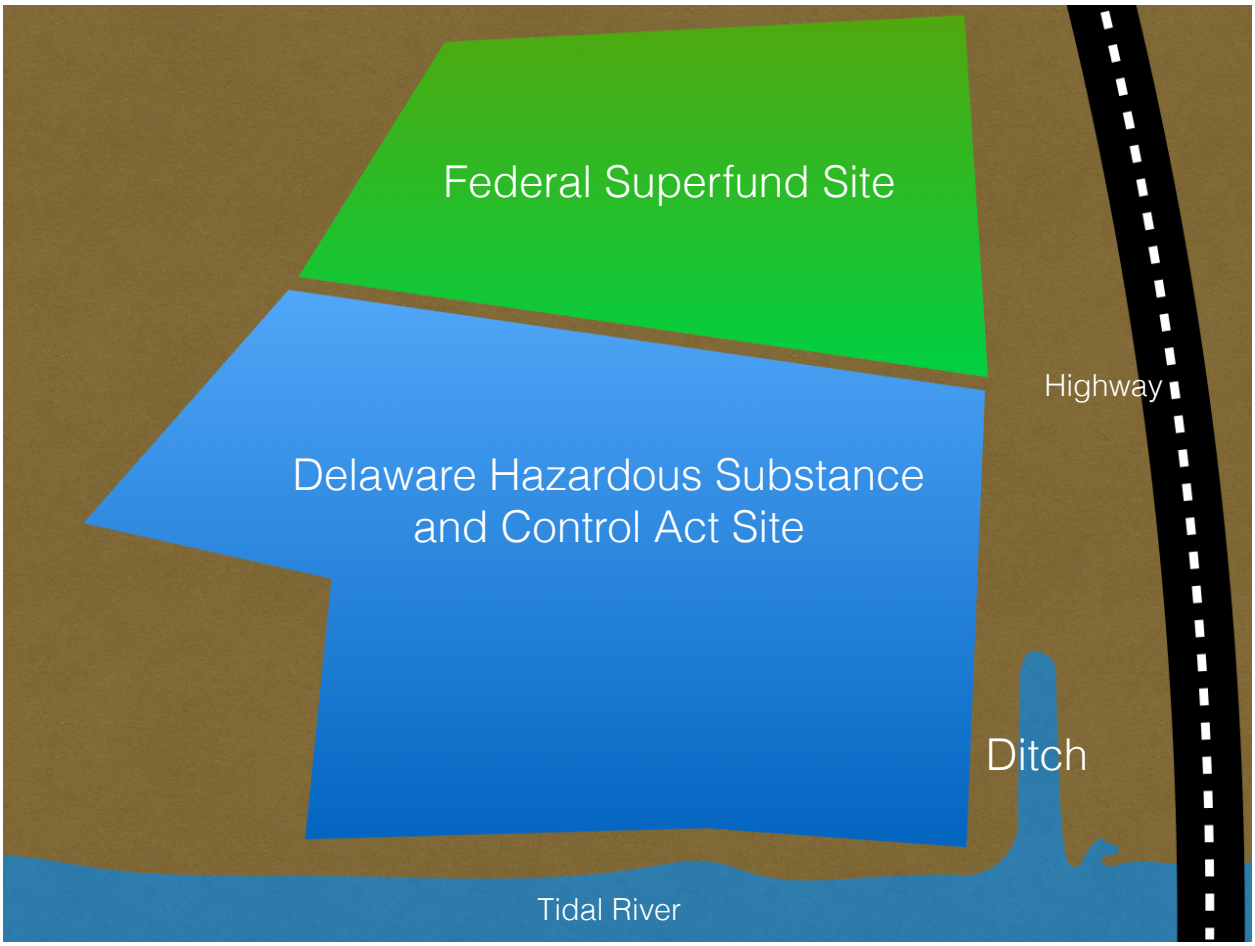

Figure 4.3: Schematic showing proximity of sampling sites in south Wilmington, DE.

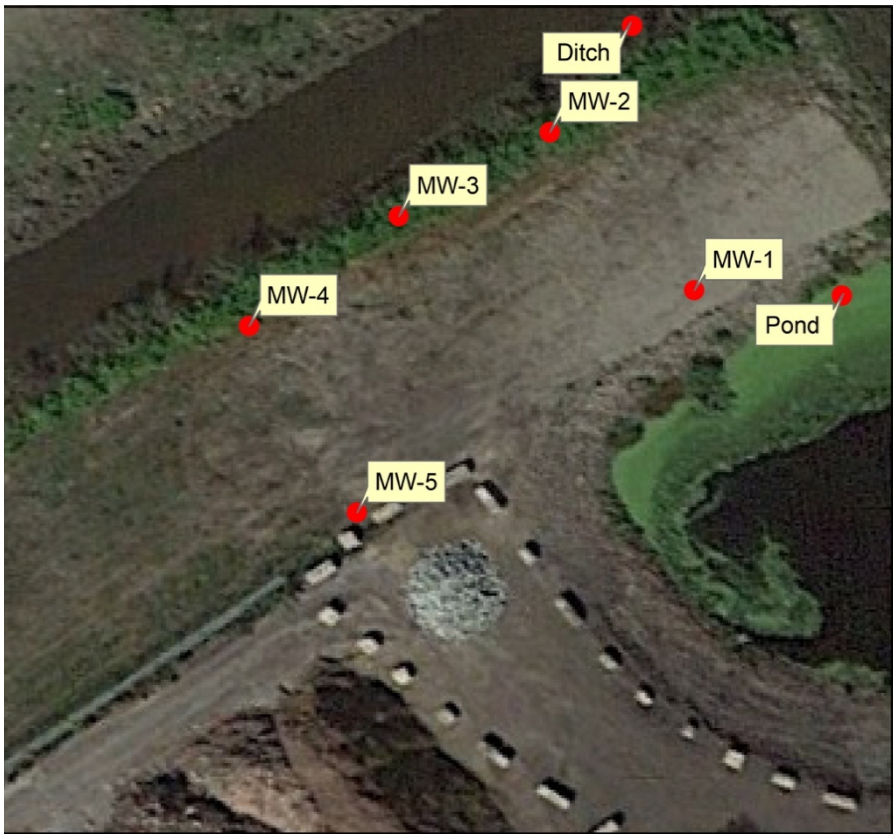

Figure 4.4: Location of groundwater wells installed by a consultant and used with their permission. Pressure transducers were installed in each of the indicated wells, as well as the ditch and collecting pond.

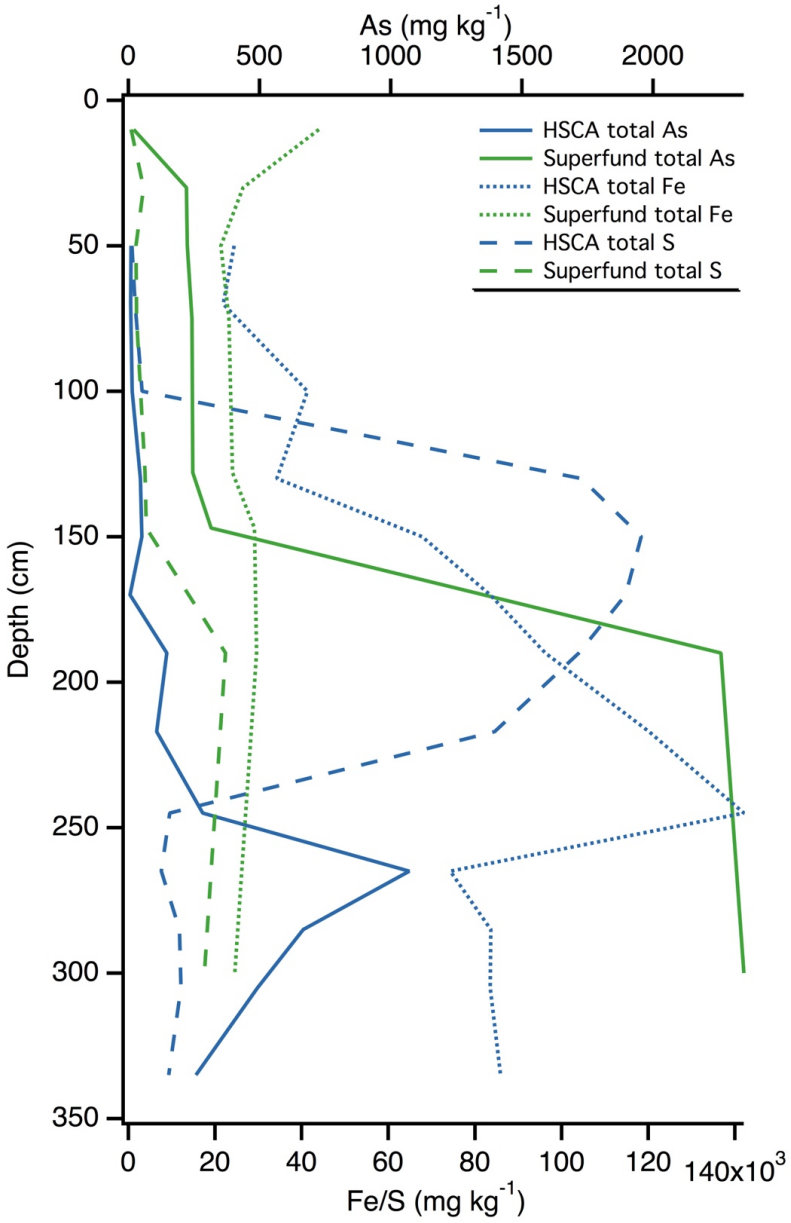

Figure 4.5: Bulk soil As, Fe, and S for both sites in 15-30 cm increments. The HSCA site is indicated by the green lines and the Superfund site by the blue. Despite their relative proximity to one another, there are large difference in the displayed elements. Arsenic at both sites increased dramatically below the water table (1.75-2.5 m).

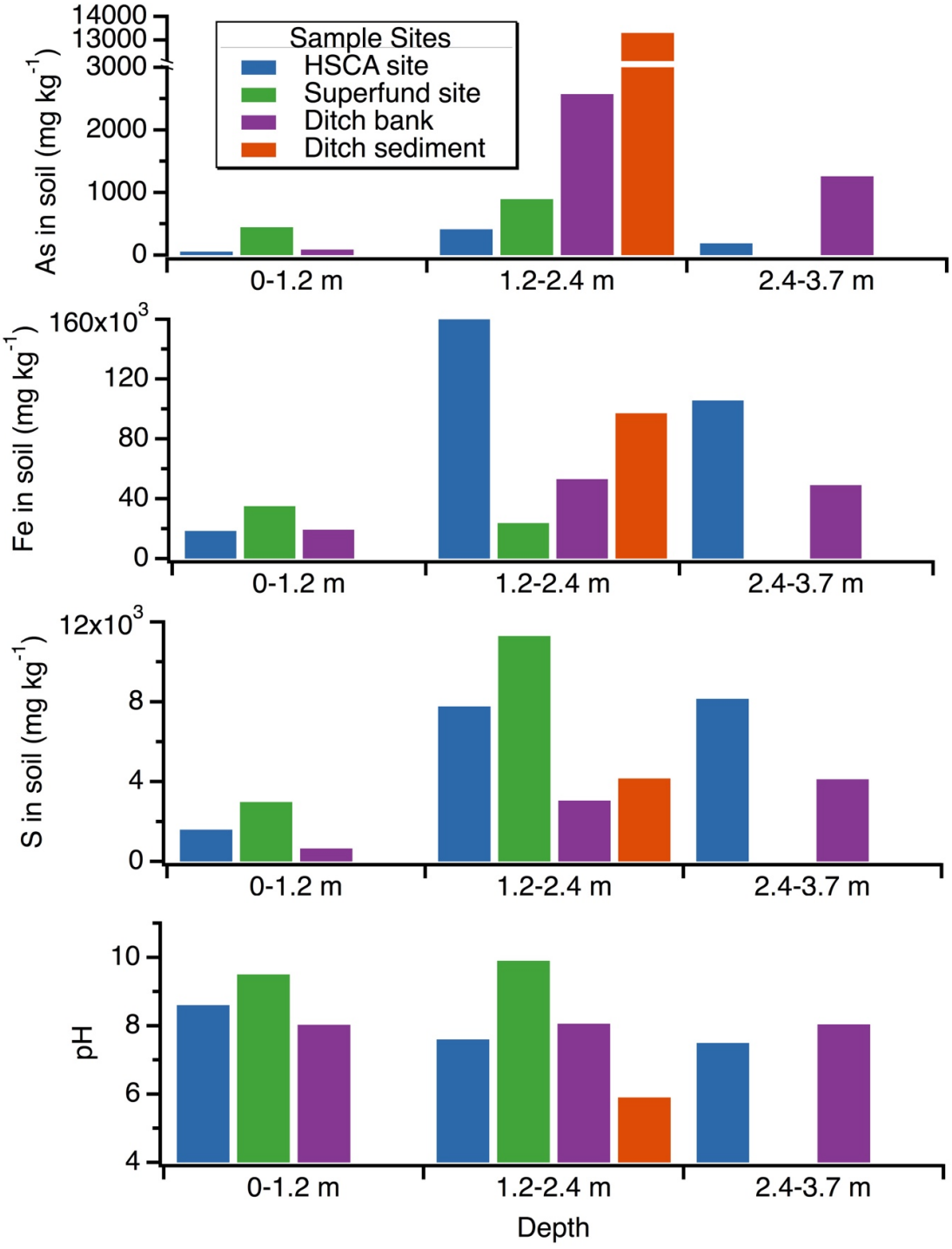

Figure 4.6: Bulk soil As, Fe, S, and pH for the HSCA and Superfund sites in 120 cm increments.

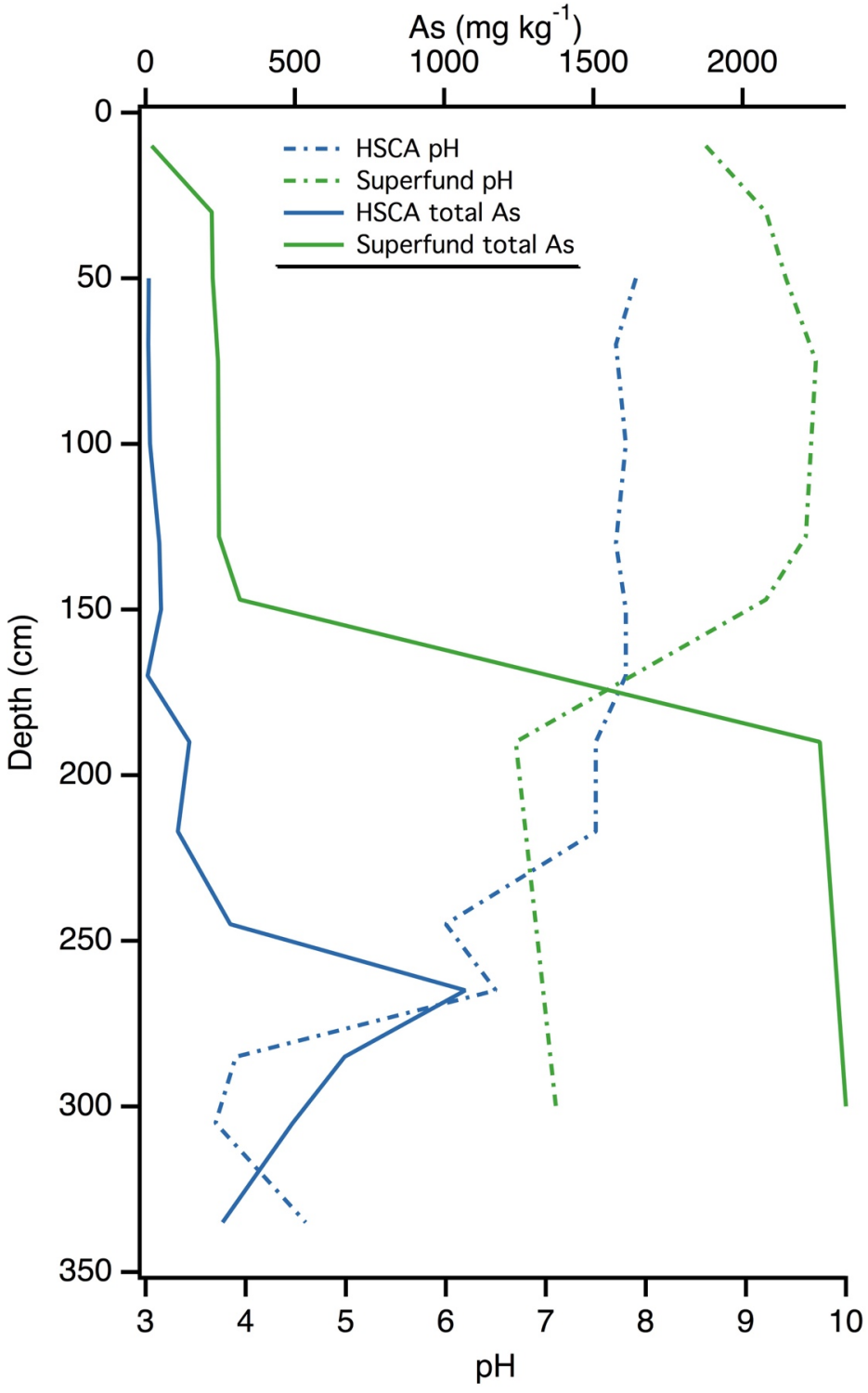

Figure 4.7: Bulk soil As and pH levels at the HSCA and Superfund sites in 15-30 cm intervals. HSCA is indicated by the blue lines and Superfund in green.

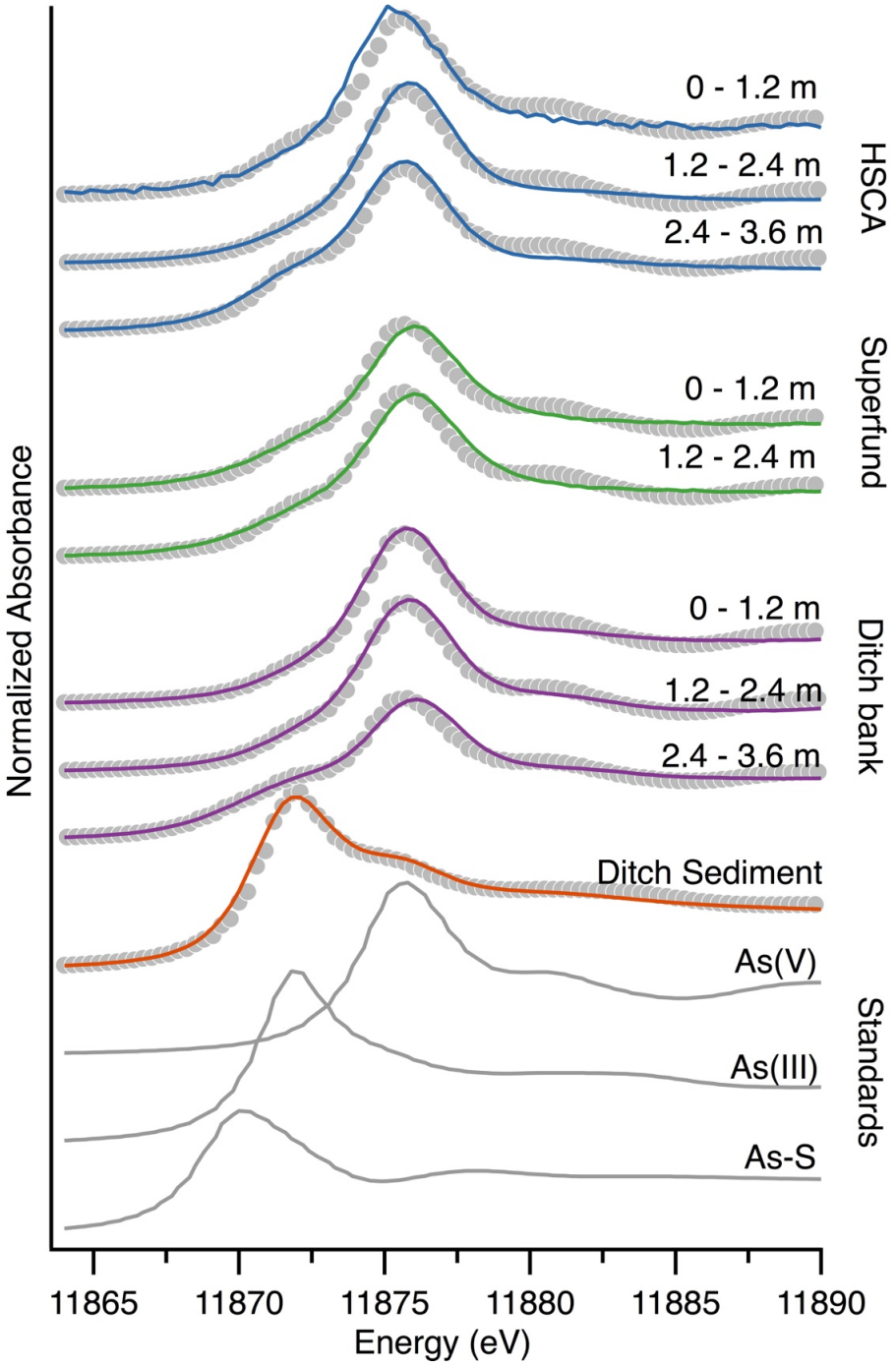

Figure 4.8: Least squares linear combination fitting of XANES analysis for the ditch sediment, ditch bank, HSCA and Superfund sites across depths from 0 – 3.2 meters below the surface. The collected data are solid colored lines and the gray dotted lines represent the fits.

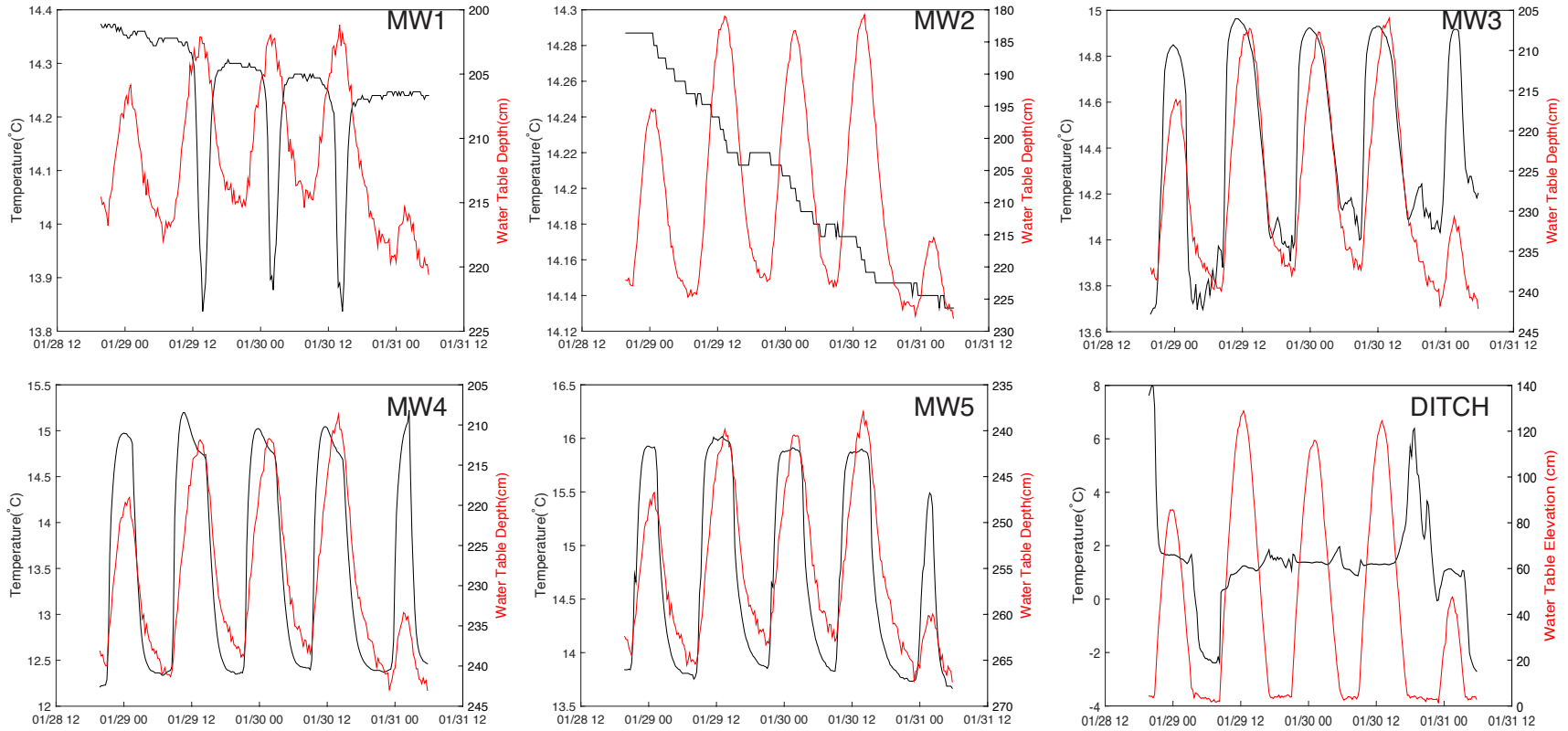

Figure 4.9: The water table elevation and temperature for groundwater wells MW1-MW5 and the Ditch during a representative time period. The red lines show the water table elevation and the black lines show the water temperature. The water table was strongly influenced by tides at all wells and the ditch. The only instances where tide was not influential was the temperature at MW2 and the ditch.

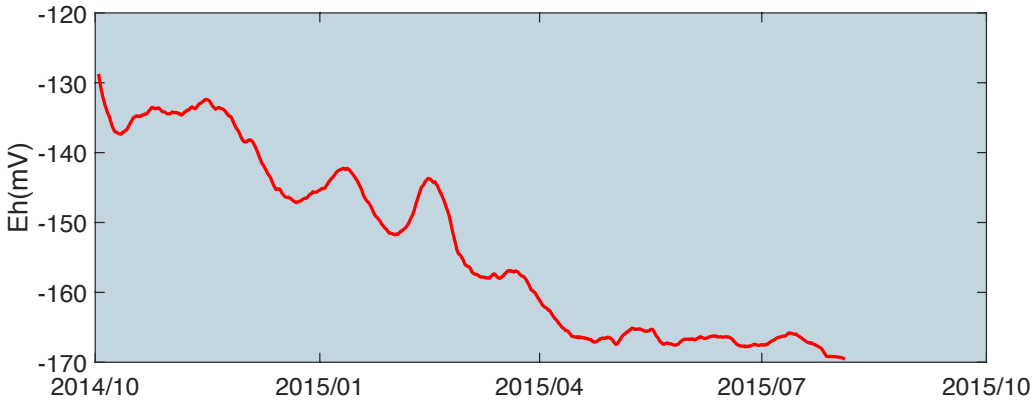

Figure 4.10: Average soil redox potential between 2 to 3.5m during the time (approx. 1 year) since the redox sensors were installed at the ditch field site along the ditch bank.

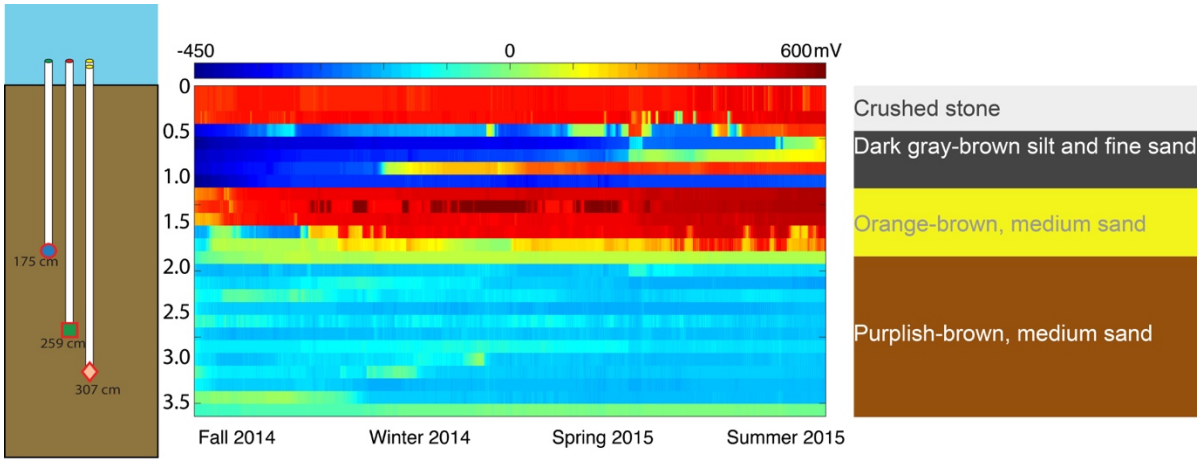

Figure 4.11: Soil redox potential variation along depth (from surface to 3.5 m deep) and time (from Fall 2014 to Summer 2015). The left sub figure suggested the porewater sampling locations, and the right sub figure shows the soil layer.

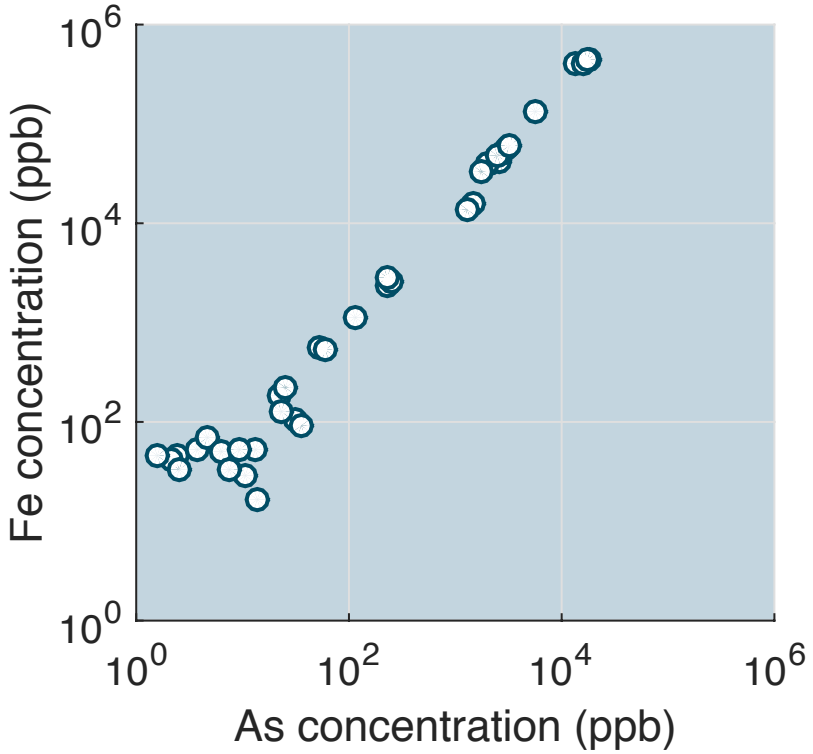

Figure 4.12: Porewater concentration of As and Fe. The pore water samples were collected from different depths (1.75m 2.59m, and 3.07m) and different times including spring/neap, high/ low tide cycles) at the ditch bank.

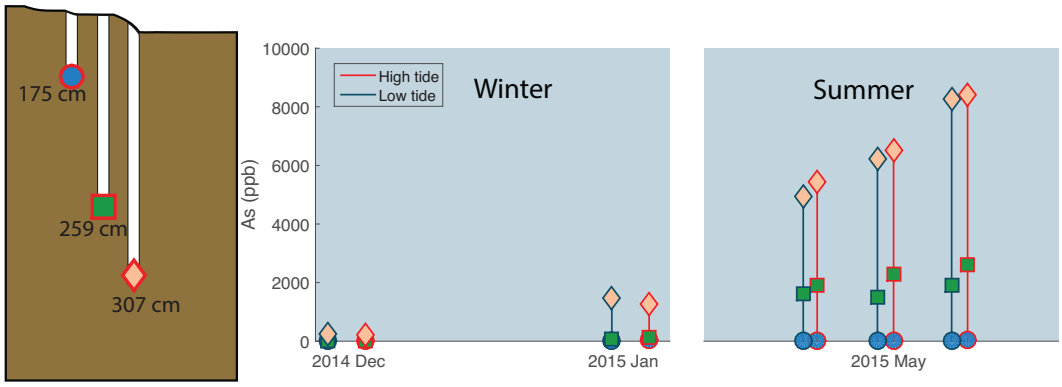

Figure 4.13: Porewater Arsenic concentration variation along depth and time at the ditch bank.

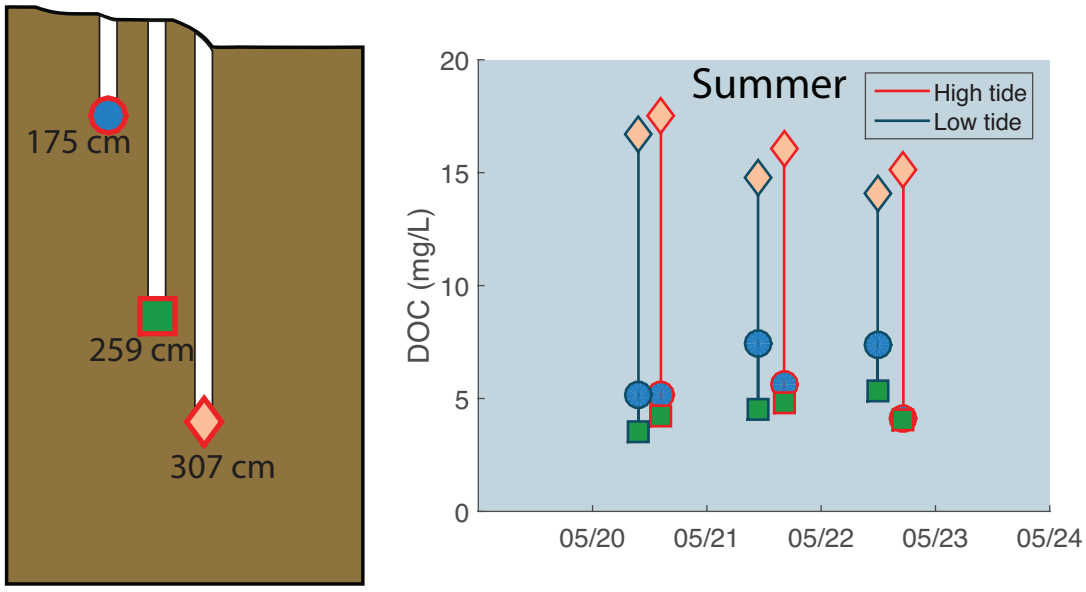

Figure 4.14: Pore water dissolved organic carbon concentrations across depth and time at the ditch bank.